Curriculum vitae

INFORMAZIONI PERSONALI Lema Fernandez Anair Graciela

Skype

Sesso | Data di nascita | Nazionalità

OCCUPAZIONE DESIDERATA Ricerca in Ambito Biomedico

ISTRUZIONE E FORMAZIONE

15 Gen. 18–14 Gen. 19 **Assegno per la Collaborazione ad attività di Ricerca**

Dipartimento di Medicina, Università degli Studi di Perugia. Laboratorio di Citogenetica e Genetica Molecolare, Prof.ssa Cristina Mecucci

Progetto da titolo: "Uso delle tecnologie avanzate per la determinazione dell'assetto genomico delle Sindromi Mielodisplastiche (MDS)"

1 Gen. 17–31 Dic. 17 **Assegno per la Collaborazione ad attività di Ricerca**

Dipartimento di Medicina, Università degli Studi di Perugia. Laboratorio di Citogenetica e Genetica Molecolare, Prof.ssa Cristina Mecucci, Perugia (Italia)

Progetto dal titolo: "Diagnosi personalizzata nelle leucemie acute linfoblastiche del bambino e dell'adulto: un ponte indispensabile verso nuove terapie."

12 Dic. 12–7 Mar. 17 **Dottorato di Ricerca in "Biotecnologie nel trapianto di Midollo Osseo Umano, MED15"**

Università degli Studi di Perugia, Perugia (Italia)

Titolo Tesi: "No-gene DNA in Leukemia: Personal Contributions"

Tecniche: colture cellulari, Harvesting, Lisi dei globuli rossi, estrazione acidi nucleici (RNA e DNA), Polymerase ChainReaction (PCR), Elettroforesi, Denaturing high-performance liquid chromatography (DHPLC), Sequenziamento automatizzato capillare con metodo Sanger (Applied Biosystem 3500), Clonaggio, 5' Race, 3' Race, Methylation Specific PCR, Affymetrix array, Hamilton Robotics, Luciferase Assay, Whole Genome Bisulfite Sequencing (WGBS), Enhanced Reduced Representation Bisulfite Seqencing (ERRBS), multiplex ERRBS, RNAseq, Exome Sequencing, Bioinformatica.

Apr. 16–Ago. 16 **Visiting Student presso: "University of Michigan, Department of Pathology" , Prof.ssa Maria E. Figueroa**

Ann Arbor, Michigan (Stati Uniti d'America)

-Analisi bioinformatica di dati di Next Generation Sequencing (NGS): ERRBS, mERRBS, RNAseq, Exome
-Allineamento di dati di NGS (BWA-MEM, Bistmark, Botwie, STAR, TopHat, HTseq) ed utilizzo dei programmi Phyton, R e dei pacchetti bioconductor (MethylKit, Methylsig, EdgeR, DESeq, DexSeq, made4)
- Analisi dei pathway e dei siti di legame per fattori di trascrizione mediante l'utilizzo di DAVID , Hypergeometric Optimization of Motif EnRichment (HOMER), RNA-Enrich e ChipEnrich .

Documenti collegati FigueroaME_Letter.pdf

1 Ott. 14–31 Mar. 15 **Visiting Student presso: "University of Michigan, Department of Pathology" , Prof.ssa Maria E. Figueroa**

Ann Arbor, Michigan (Stati Uniti d'America)

Studio della deregolazione della metilazione del DNA nelle Emopatie Maligne (Leucemie Acute e Sindromi Mielodisplastiche).Tecniche:

-Whole Genome Bisulfite Sequencing (WGBS)
-Enhanced Reduced Representation Bisulfite Seqencing (ERRBS)
-Multiplex ERRBS

-RNA-seq

-HydroxymethylatedDNAImmunoprecipitation(hMeDip)

10–17 Ott. 12 **Laurea Magistrale in scienze Biomolecolari Applicate (LM-6)**

Università degli Studi di Perugia, Perugia (Italia)

Titolo Tesi Sperimentale: "GNAS gene: genomic insights in human leukemia", Relatore: Prof.ssa Cristina Mecucci, Prof.ssa Maria Rita Micheli.
Voto Finale: 110/110 cum laude

Tecniche: analisi mutazione, PCR, DHPLC, Sequenziamento Sanger, q-RTPCR

05–28 Mag. 10 **Laurea Triennale in Scienze Biologiche (Curriculum Biomedico)**

Università degli Studi di Perugia, Perugia (Italia)

Titolo Tesi : "Glycosilated Hemoglobins" , Relatore: Prof. ssa Carla Saccardi

Voto Finale: 101/110

ESPERIENZA PROFESSIONALE

28 Mar. 19 **Pubblicazione su rivista scientifica**

Fernandez AGL, Crescenzi B, Pierini V, Di Battista V, Barba G, Pellanera F, Di Giacomo D, Roti G, Piazza R, Adelman ER, Figueroa ME, Mecucci C. “A distinct epigenetic program underlies the 1;7 translocation in myelodysplastic syndromes.” Leukemia 2019. doi: 10.1038/s41375-019-0433-9. PMID:30923319

Documenti collegati A distinct epigenetic program.pdf

Nov. 17 **Pubblicazione su rivista scientifica**

Di Giacomo D, Pierini V, La Starza R, Borlenghi E, Pellanera F, Lema Fernandez AG, Bellotti D, Lamorgese C, Rossi G, Mecucci C. "Involvement of a member of the histone cluster 1 at 6p21 in NUP98-positive MDS/AML." Leuk Lymphoma. 2017 Nov; 58(11):2765-2767. PMID: 28482724

Documenti collegati Involvement of a member of the histone cluster 1 at 6p21 in NUP98-positive MDS:AML.pdf

14 Set. 17–15 Set. 17 **Relatrice al "Corso avanzato di citogenetica costituzionale e acquisita. VIII edizione". Responsabili Scientifici: Paola Grammatico, Orsetta Zuffardi**

Roma (Italia)

Documenti collegati Corso di Citogenetica.pdf

12 Giu. 17–14 Giu. 17 **Abilitazione allla sperimentazione animale**

Università degli Studi di Perugia, Perugia (Italia)

Documenti collegati Sperimentazione_Animale.PDF

23 Apr. 17–28 Apr. 17 **Presentazione Poster al "Cancer Genetics & Epigenetics " Gordon Research conference**

Lucca (Italia)

Titolo Poster: " Genetic and Epigenetic Landscape of dic(1;7)(q10;p10) in AML/MDS "

Documenti collegati Poster dic(1;7)PDF.pdf, GRC_Certificate.pdf

12 Dic. 12–7 Mar. 17 **Vincitrice della borsa di Dottorato di Ricerca in: "Biotecnologie nel trapianto di midollo osseo umano"**
Università degli Studi di Perugia, Perugia (Italia)

22 Ago. 16 **Pubblicazione su rivista scientifica**
Pierini T, Di Giacomo D, Pierini V, Gorello P, Barba G,Lema Fernandez AG, Pellanera F, Iannotti T, Falzetti F, La Starza R, Mecucci C.
MYB deregulation from a EWSR1-MYB fusion at leukemic evolution of a JAK2 (V617F) positive primary myelofibrosis.
Mol Cytogenet. 2016. PMID:27594918
Documenti collegati MYB deregulation from a EWSR1-MYB fusion at leukemic evolution of a JAK2 (V617F) positive primary myelofibrosis .pdf

12 Apr. 16–14 Apr. 16 **Partecipazione all corso "RNA-seq Workshop, An introductory course to RNA-seq"**
MBC Via Nizza 52, Torino (Italia)

Workshop organizzato da specialisti Illumina e dal Prof. Raffaele Calogero, esperto di high-throughput technology.
Argomenti:
- Utilizzo di BaseSpace
- Analisi dell'espressione di geni/isoforme/miRNA/non-coding RNA
- Utilizzo di applicazioni online per l'analisi di RNAseq
- Analisi funzionale dei dati di espressione
- Workflow per l'identificazione dei trascritti di fusione e di circular-RNA

18 Mar. 16 **Partecipazione al training: MiSeq System, Illumina**

Documenti collegati MiSeq_Certificate.pdf

24 Feb. 16–24 Feb. 16 **Partecipazione al training Hamilton (Life Science Robotics)**

Documenti collegati Hamilton_Certificate.pdf

4 Dic. 14 **Pubblicazione su rivista scientifica**
La Starza R, Borga C, Barba G, Pierini V, Schwab C, Matteucci C, Lema Fernandez AG, Leszl A, Cazzaniga G, Chiaretti S, Basso G, Harrison CJ, Te Kronnie G, Mecucci C.
Genetic Profile of T-cell Acute lymphoblastic leukemias with MYC translocations.
Blood. 2014. PMID:25270907
Documenti collegati Genetic profile of T-cell acute lymphoblastic leukemias with MYC translocations.pdf

Ott. 14 **Vincitrice della borsa di studio per soggiorno all'estero "CONSORZIO INTERUNIVERSITARIO PER LE BIOTECNOLOGIE (CIB)**

Documenti collegati CIB.pdf

Giu. 14 **Pubblicazione su rivista scientifica**
Di Giacomo D, Lema Fernandez AG, Pierini T, Crescenzi B, Brandimarte L, Matteucci C, Testoni N, Mecucci C."The GNAS1 gene in myelodysplastic syndromes (MDS)"

Leuk Res. 2014 Jul;38(7):804-7. PMID:24795070

Documenti collegati The GNAS1 gene in myelodysplastic syndromes (MDS).pdf

12 Giu. 14–15 Giu. 14 **Presentazione Poster al "19th Congress of the European Hematology Association (EHA14)"**
Milano (Italia)

La StarzaR, Borga C, Barba G, Schwab C , Pierini V , Lema Fernandez A, Leszl A, Sammarelli G, Rossetti E, Cazzaniga G, Chiaretti S, Morerio C, Matteucci C, Harrison C, te Kronnie G, Mecucci C ."CMYC-TRANSLOCATIONS IN T-CELL ACUTE LYMPHOBLASTIC LEUKEMIA". Haematologica 2014

Documenti collegati EHA14(2).pdf

19 Mag. 14 **Partecipazione al meeting "Giornate Umbre di Medicina Molecolare: il globulo rosso e il metabolismo del ferro"**
Prof.ssa Cristina Mecucci, Onco-ematologia Università degli Studi di Perugia, Perugia (Italia)

13 Nov. 13–14 Nov. 13 **Partecipazione al meeting "The Bioinformatic Roadshow"**
Prof. Claudio Brancolini, Prof. Federico Fogolari and Prof.ssa Laura Emery, Università di Udine, Udine (Italia)

Risorse dati e tools EMBL-EBI.

EBI training :

- Trascrittomica ed EBI Tools: ArrayExpress, Gene Expression Atlas
- Interazioni & Pathways: IntAct, Reactome
- Enzimi: ChEBI, The Enzyme Portal,ChEMBL

16 Set. 13–17 Set. 13 **Partecipazione al meeting "MicroRNA: from basic research to therapeutic applications"**
Prof.ssa Roberta Piva (Università di Ferrara), Prof. Roberto Gambari (Università di Ferrara), Prof. Roberto Corradini (Università di Parma), Ferrara (Italia)

microRNAs:

-Biogenesi e target molecolari
-Metodi per la loro identificazione
-microRNAs e patologie umane
-microRNA e terapie

12 Giu. 13 **Partecipazione al meeting: Life Technologies " Digital PCR & miRNA"**
Università degli Studi di Perugia, Perugia (Italia)

24 Mag. 13 **Partecipazione al meeting: " Giornate Umbre di Medicina Molecolare 2013 - Telomeropatie"**
Prof.ssa Cristina Mecucci, Onco-ematologia, Università degli Studi di Perugia, Perugia (Italia)

8 Mag. 13–11 Mag. 13 **Presentazione poster al "The 12th International Symposium on Myelodysplastic Syndromes"**
Berlino (Germania)

Documenti collegati Abstract.pdf, Poster.pdf

1 Nov. 11–30 Ott. 12

Tirocinio di Laurea specialistica in Scienze Biomolecolari Applicate

Laboratorio di Citogenetica e Genetica Molecolare Prof. ssa Cristina Mecucci (Ospedale S.M. della misericordia, Ematologia di Perugia), Perugia (Italia)

Genetica delle Emopatie Maligne ed analisi mutazionale dei principali geni leucemogeni. Durata: 900 ore

Tecniche: Lisi dei globuli rossi, Estrazione di Acidi nucleici (RNA e DNA), Polymerase Chain Reaction (PCR), Elettroforesi, Denaturing high-performance liquid chromatography (DHPLC)-Sequenziamento capillare automatizzato con metodo Sanger (Applied Biosystem 3500)

29 Gen. 12–31 Gen. 12

Partecipazione al meeting: " Genomics in Hematology

Prof. Franco Aversa,Prof.ssa Cristina Mecucci, Prof. Brunangelo Falini, Prof. ssa Luigina Romani, Perugia (Italia)

22 Feb. 10–18 Mar. 10

Tirocinio di Laurea Triennale in Scienze Biologiche

Prof.ssa Sabata Martino Università degli Studi di Perugia (Medicina Sperimentale e Biochimica), Perugia (Italia)

Identificazione di markers molecolari in Patologie Neurodegenerative (Alzheimer, Sclerosi multipla).Cross correzione ed applicazioni terapeutiche nelle malattie da accumulo lisosomiale. Durata: 80 ore

Tecniche: Comatografia a scambio ionico, Elettroforesi, Saggio di Bradford-
Analisi spettrofotometriche.

COMPETENZE PERSONALI

Lingua madre: Spagnolo, Italiano

Lingue straniere

	COMPRENSIONE		PARLATO		PRODUZIONE SCRITTA
	Ascolto	Lettura	Interazione	Produzione orale	
inglese	B2	B2	B2	B2	B2
francese	A2	A2	A2	A2	A2

Livelli: A1 e A2: Utente base - B1 e B2: Utente autonomo - C1 e C2: Utente avanzato
Quadro Comune Europeo di Riferimento delle Lingue

Competenze comunicative: Buone capacità interpersonali in attività che richiedono la collaborazione di gruppo. Durante le mie esperienze lavorative all'estero ho rafforzato il mio interesse a lavorare in ambienti multiculturali che possano incoraggiare nuove idee.

Competenze organizzative e gestionali: Buone competenze organizzative nella gestione di progetti di breve e lunga durata. Buone competenze nel tenere lezioni di teoria e laboratorio didattico a studenti di Biotecnologie e Medicina acquisite durante la mia esperienza come tutor agli studenti durante il loro tirocinio di Laurea.

Competenze professionali: Buona conoscenza delle principali tecniche di analisi in Biologia molecolare applicate in ambito della Ricerca in area Biomedica. Buone capacità nell'analisi bioinformatica di dati di Next Generation Sequencing (NGS) e del linguaggio di programmazione R.

Competenze digitali

AUTOVALUTAZIONE				
Elaborazione delle informazioni	Comunicazione	Creazione di Contenuti	Sicurezza	Risoluzione di problemi
Utente avanzato	Utente avanzato	Utente autonomo	Utente avanzato	Utente avanzato

Competenze digitali - Scheda per l'autovalutazione

- Buona conoscenza dei programmi per analisi di sequenziamento Sanger
- Buona conoscenza dell'utilizzo di EBI Tools
- Hamilton Robotics
- Buona conoscenza di sistemi OSX e Windows
- Capacità di lavorare su linea di comando, preferibilmente linux.
- Buona conoscenza di R programming
- Buona conoscenza dei linguaggi di base per gli script (Perl / python)
- Analisi bioninformatica di dati di Next Generation Sequencing: ERRBS, RNAseq, Exome
- Uilizzo di BaseSpace
- Bioconductor software e relativi pacchetti
- Analisi di Pathways biologici e di siti di legame per fattori di trascrizione

Patente di guida B

ALLEGATI

- Abstract.pdf
- Poster.pdf
- The GNAS1 gene in myelodysplastic syndromes (MDS).pdf
- EHA14(2).pdf
- MYB deregulation from a EWSR1-MYB fusion at leukemic evolution of a JAK2 (V617F) positive primary myelofibrosis .pdf
- Genetic profile of T-cell acute lymphoblastic leukemias with MYC translocations.pdf
- Poster dic(1;7)PDF.pdf
- Involvement of a member of the histone cluster 1 at 6p21 in NUP98-positive MDS:AML.pdf
- Hamilton_Certificate.pdf
- MiSeq_Certificate.pdf
- GRC_Certificate.pdf
- Corso di Citogenetica.pdf
- Sperimentazione_Animale.PDF
- CIB.pdf
- FigueroaME_Letter.pdf
- A distinct epigenetic program.pdf

Abstract.pdf

Insights on *GNAS1* gene involvement in MDS

Danika Di Giacomo, Tiziana Pierini, Anair Graciela Lema Fernandez, Lucia Brandimarte, Valentina Pierini, Caterina Matteucci, Barba Gianluca, Barbara Crescenzi, Cristina Mecucci.

Background. Patients with myelodysplastic syndrome (MDS) are currently stratified according to conventional cytogenetics. Recently recurrent gene mutations have been associated with specific clinical features (Bejar R. et al NEJM 2011). Mapping at 20q13.32, *GNAS1* gene, has been reported to undergo activating mutations at amino acid R201 in solid tumors (Kalfa et al.The journal of Urology 2006). Bejar R. and co-workers(Bejar et al NEJM 2011) found the *GNAS1* R201 mutation in 3/439 (0.7%) cases of MDS.

Aim. To investigate mutations, deletions, and haploinsufficiency of *GNAS1* gene in MDS.

Methods and Patients. *GNAS1* was analyzed in 38 MDS with 20q- (25 samples with isolated and 13 with not-isolated 20q-) and in 52 MDS with a complex karyotype but without involvement of chromosome 20. FISH was performed with fosmids G248P80239D1 and G248P80321H8 spanning the gene.

Mutational analysis was carried out in 15/38 MDS with 20q- (12 with isolated and 3 with not-isolated 20q-) and 100 MDS with normal or complex karyotypes without involvement of chromosome 20. DHPLC and sequencing analysed exons 11-12 (referred to NC_000020.10).

Expression was investigated by RT-qPCR in 11/38 MDS (7 with isolated and 4 not-isolated 20q-) and in 8 control samples (TaqMan assay probe Hs00255603_m1, Applied Biosystems). Reference controls were endogenous *ABL1* (Hs00245445_m1, Applied Biosystems) and Universal Human Reference RNA (Stratagene, Cedar Creek, TX, USA).

Results. 20q monoallelic deletions encompassing *GNAS1*/20q13.32 were found in 10/38 (26.3%) cases and were significantly associated with complex karyotypes (7/10 vs 3/28; Fisher exact test, P=0,002). Interestingly, all complex karyotypes showed del(5q)/-5. Mutations were not detected in 4 patients with deletion. FISH was normal in MDS with a complex karyotype but without involvement of chromosome 20, suggesting the absence of cryptic *GNAS1* deletions. No mutations were identified in *GNAS1* coding region but in 2 cases sequence variations were detected at intron 1. In one patient the substitution at nucleotide 69914 was found in both bone marrow and saliva. Substitution g.69904G>A in the second case was not found in 200 DNA samples from healthy donors suggesting g.69904G>A may be a new mutation or a very rare polymorphism. Haploinsufficiency was significantly related to non-isolated 20q-/-20 with *GNAS1* deletion (median value: 0.51 P=0.012).

Conclusions. *GNAS1* might behave as an oncogene (gain-of-function mutations) and as a tumor suppressor (deletions). Mutations were very rare and involved the noncoding region. Monoallelic loss/haploinsufficiency appeared more relevant, particularly in MDS with 20q deletion plus other karyotypic aberrations.

Poster.pdf

Insights on *GNAS1* gene involvement in MDS

[1]Di Giacomo D, [1]Pierini T, [1]Lema Fernandez A.G, [1]Brandimarte L, [1]Pierini V, [1] Matteucci C, [1]Barba G, [1]Crescenzi B, [1]Mecucci C
[1]Haematology and Bone Marrow Transplantation Unit, University of Perugia, Italy

Introduction

Recurrent gene mutations have been associated with specific clinical features in MDS [(1)]. Mapping at 20q13.32, *GNAS1* gene has been reported to undergo activating mutations at amino acid R201 in solid tumors [(2)]. Bejar R. and co-workers [(1)] found the *GNAS1* R201 mutation in 3/439 (0.7%) cases of MDS.

Objectives

To investigate mutations, deletions, and haploinsufficiency of *GNAS1* gene in MDS.

Patients

171 cases were investigated. Forty of them (23%) had a del(20q) at karyotype.

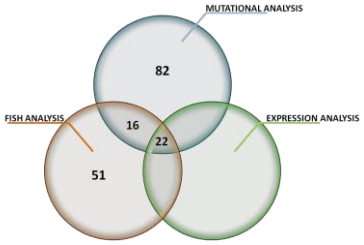

Fig.1 Figure shows the analysis performed in 120 MDS patients. All three analyses in 22 cases. Both mutational analysis and FISH in 16 cases. Only mutational analysis in 82 cases. Only FISH in 51 cases.

Methods

FISH

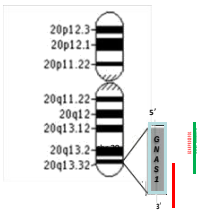

Fig.2 Fosmids spanning *GNAS1* used for FISH analysis.

Mutational analysis

PCR was performed with primers:

• *GNAS_CF: 5'-GCTTTGGTGAGATCCATTGAC-3'* and *GNAS_BR: 5'-ACCACGAAGATGATGGCAGT-3'* to investigate the known exon 11 R201 mutation[(1)].

• *GNAS_1849FW: 5'-GCCAGACGCAAGATCCAT-3'* and *GNAS_2036RW: 5'-CCATCGTCGGACTCGTCTC-3'* to investigate exon 2.

PCR products were analysed with DHPLC (Wavemaker software, Wave System, MD Transgenomic Inc) and abnormal chromatograms sequenced by Sanger method (3500 Genetic Analyzer, Applied Biosystems)

Expression analysis

Real time PCR was performed using TaqMan assay probe Hs00255603_m1 (Applied Biosystems) for *GNAS1*; endogenous *ABL1* (Hs00244545_m1, Applied Biosystems) was used as control. Eight non neoplastic bone marrows were used as wild type.

Results

FISH

20q- deletions encompassed *GNAS1*/20q13.32 in 10/89 (11.2%) cases. All these cases showed del(20q) at karyotype (Tab. A). *GNAS1* gain was found in 3/89 (3.4%) cases (Tab. B).

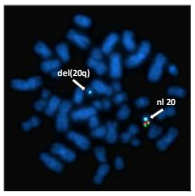

Fig.3 Example of *GNAS1* deletion (patient 2)

PATIENT	(Y) SEX/AGE	DIAGNOSIS	KARYOTYPE *	STATUS *GNAS1*
1	M/49	RAEB-2	45,XY,del(12p),del(13q),del(20q),-5,-7,+mar [14 cell. /46,XY [1 cell.]	DEL
2	M/86	MDS-U	46,XY,del(20)(q11q13)[20]	DEL
3	M/63	RARS	46,XY [2 cell]/40-48,XY,t(1;3)(p32;p21),-5,-7,-13,-18,-20,-22,+markers	DEL
4	M/52	MDS	46,XY,del(5)(q),-7,del(12)(p),-18,-20,+mar1,+mar2	DEL
5	M/91	RCMD	46,XY,del(20q)(q11q13)[4]/46,XY[11]	DEL
6	M/51	RAEB-1	45,XY [2 cell.]/45,XY,del(5q),-7,del(20q) [8 cell.] / 46,XY ,idem,-22,+marker[1 cell.]	DEL
7	M/87	MDS (RA)	46-50,XY,del(5)(q11)?O-5,der(7),+8,add(12)(p13),del(13)(q14q32),del(20)(q11) [20/20 cell.]	DEL
8	M/64	MDS (RA)	46,XY,del(20)(q11q13) [19]/46XY [1]	DEL
9	M/73	MDS	44,XY,del(5q),del(9q),del(21q),-4,-20[7]	DEL
10	M/46	t-MDS	46,XY,del(4)(q21q26),del(5)(q33q34),add(6)(p21),add(10)(q25),add(17p)(13)[8]/46,idem,del(20q)	DEL

Tab. A. 20q- cases with *GNAS1* deletion

PATIENT	SEX/AGE (Y)	DIAGNOSIS	KARYOTYPE *	*GNAS1* STATUS
11	F/54	RAEB-1	47,XX,del(20)(q11q13),+del(20)(q11q13) [10]	GAIN
12	M/87	MDS (RA)	47,XY,del(20)(q11q13),+del(20)(q11q13) [10]/46XY[10]	GAIN
13	M/64	MDS	46,XY,idel(20)(q11q13) [24]/46XY[1]	GAIN

Tab. B. 20q- cases with *GNAS1* gain

Abbreviations: M, male; F, female; (y) age in years; *Karyotype obtained from bone marrow culture at diagnosis; MDS, Myelodysplastic Syndrome; RAEB, Refractory Anaemia with Excess Blasts (type 1 or type 2); RCMD, Refractory Cytopenia with Multilineage Dysplasia; MDS-U, Myelodysplastic Syndrome Unclassifiable; RARS, Refractory Anaemia with Ring Sideroblasts; DEL, deletion; NL, normal.

Mutational analysis

PATIENT	SEX/AGE (Y)	DIAGNOSIS	KARYOTYPE *	GNAS1 MUTATIONS
14	F/68	RAEB-1	46,XX,add(11)(q?)/46,idem,del(5)(q13q31)/46,XX	g.69904G>A
15	M/78	RCMD	46,XY	g.69914A>T (germline ?)

Tab. C. *GNAS1* mutations were found in two MDS patients

Abbreviations: M, male; F, female; (Y) age in years; *Karyotype obtained from bone marrow culture at diagnosis; RAEB-1, Refractory Anaemia with Excess Blasts type 1; RCMD, Refractory Cytopenia with Multilineage Dysplasia.

Sequence variation were found at intron 11 in two patients. In one of them DNA from saliva was positive. 200 DNA samples from healthy donors were investigated to define the germline or somatic origin of the g.69904G>A substitution found in patient 14: none had the variation, suggesting it may be a new *GNAS1* mutation in MDS.

Expression analysis

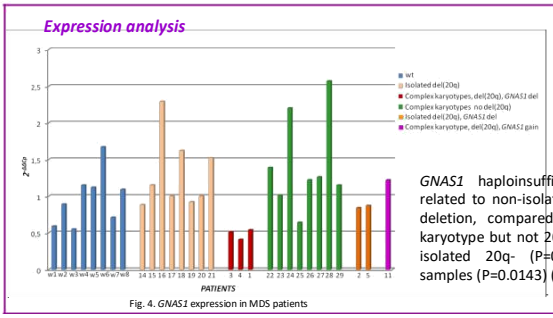

Fig. 4. *GNAS1* expression in MDS patients

GNAS1 haploinsufficiency was significantly related to non-isolated 20q-/-20 with *GNAS1* deletion, compared to MDS with complex karyotype but not 20q- (P=0.0143), MDS with isolated 20q- (P=0.0141) and wild type samples (P=0.0143) (Mann Whitney test).

Discussion

- The known gain of function (R201) mutation[(1)] did not emerge in our 120 cases. An intronic putative new mutation was found;
- monoallelic loss was present in 10/40 cases with a karyotypic 20q deletion (25%);
- significant haploinsufficiency seems to be more relevant in complex karyotypes with del(20q).

References: [1] Bejar R. et al NEJM 2011. [2] Kalfa et al.The journal of Urology 2006.

The GNAS1 gene in myelodysplastic syndromes (MDS).pdf

Leukemia Research 38 (2014) 804–807

Contents lists available at ScienceDirect

Leukemia Research

journal homepage: www.elsevier.com/locate/leukres

The GNAS1 gene in myelodysplastic syndromes (MDS)

Danika Di Giacomo [a], Anair Graciela Lema Fernandez [a], Tiziana Pierini [a], Barbara Crescenzi [a], Lucia Brandimarte [a], Caterina Matteucci [a], Nicoletta Testoni [b], Cristina Mecucci [a,*]

[a] Hematology and Bone Marrow Transplantation Unit, University of Perugia, Perugia, Italy
[b] Institute of Hematology and Medical Oncology "Seràgnoli", University of Bologna, Bologna, Italy

article info

Article history:
Received 20 January 2014
Received in revised form 19 March 2014
Accepted 21 March 2014 Available online 29 March 2014

Keywords:
MDS
del(20q)/20q−
GNAS1
Haplo-insufficiency

abstract

GNAS1 gene is located at the long arm of chromosome 20 (q13.32). GNAS1 gene deletion has never been investigated in MDS. A GNAS1 activating mutation (R201) was recently found in MDS. We applied FISH and DHPLC plus sequencing to investigate GNAS1 gene in MDS cases with and without del(20q) at karyotype.

1. Introduction

GNAS1 is an imprinted gene involved in G signaling encoding for the -subunit of protein Gs (Gs) [1]. Loss of function and acti-vating gene mutations were reported in a variety of solid tumors [2,3](COSMIC database, http://www.sanger.ac.uk/cosmic). Specific amino acid substitutions, such as R201 and Q227, confer a gain-of-function to the -subunit of protein Gs in endocrine tumors [3–5]. Activating mutations at codon R201 lead to a condition known as McCune Albright syndrome (MAS; OMIM #174800) [6]. Haplo-insufficiency due either to heterozygous loss of function mutations distributed throughout the gene or to complete GNAS1 gene dele-tion underlie the Albright hereditary osteodystrophy (AHO; OMIM #103580) phenotype [1,7]. Putative inactivating mutations have been described also in tumors (COSMIC database). In MDS the GNAS1 R201 activating mutation was first detected in 3/439 (0.7%) cases [8]. GNAS1 gene maps at 20q13.32, which is telomeric to a common deleted region in MDS, at q12 [9]. These 20q deletions may or may not be isolated, but only as a sole aberration, 20q− is associ-ated with a favorable outcome [10,11]. Focusing on the GNAS1 gene we performed mutational analysis, FISH and expression investiga-tions to assess its involvement in MDS with or without 20q−.

2. Materials and methods

2.1. Samples

This study was performed using archival samples from 170 MDS cases collected from the Laboratories of Cytogenetics at the Hematology Departments of the Uni-versity of Perugia and Bologna (Italy) (Supplementary Table 1). According to recent cytogenetic stratification (IPSS-R) [12], these cases were grouped into risk cate-gories as follows: 5/170 very good, 88/170 good, 12/170 intermediate, 11/170 poor and 54/170 very poor. Informed consent was available in all cases.

Supplementary Table 1 can be found, in the online version, at http://dx.doi.org/10.1016/j.leukres.2014.03.017.

2.2. FISH (fluorescence in situ hybridization)

Bone marrow or peripheral blood cells from 88 MDS cases (Supplementary Table 1) were investigated. Cytogenetically, 40/88 MDS cases had del(20q)/-20 at karyotyping (27 had isolated del(20q)/-20, 3 one additional chromosome abnor-mality and 10 had del(20q)/-20 in complex karyotypes); 48 cases had complex karyotypes without chromosome 20 involvement. Interphase FISH (I-FISH) was performed with fosmids G248P80239D1 and G248P80321H8 (BACPAC Resources Center, Oakland, California), spanning GNAS1. Other probes: LSI-D20S108 for the 20q CDR (Vysis Abbott, Milan, Italy), RP11-358N2 for ASXL1 as additional locus on 20q and RP1-81F12 for sub-telomeric sequences (kindly provided by Dr. Mariano Rocchi, University of Bari, Italy). Fluorescence microscopy analyzed 200 nuclei using an Olympus BX61 (Olympus, Milan, Italy) equipped with a highly sensitive camera JAI (Copenhagen, Denmark) and CytoVision 4.5.4 software (Genetix, New Milton, Hampshire, UK).

* Corresponding author at: Hematology and Bone Marrow Transplantation Unit, University of Perugia, Polo Unico S. Maria della Misericordia, Perugia, Italy.
Tel.: +39 0755783808; fax: +39 0755783691.
E-mail address: cristina.mecucci@unipg.it (C. Mecucci).

http://dx.doi.org/10.1016/j.leukres.2014.03.017 0145-2126/

Table 1
Mutational analysis results.

Case	Sex/age (y)	Diagnosis	Karyotype	GNAS1 mutations
89	F/68	RAEB-1	46,XX,add(11)(q?)/46,XX,add(11)(q?),del(5)(q13q31)/46,XX	g.69904G > A
90	M/78	RCMD	46,XY	g.69899A > T

Two new sequence variations were identified at intron 12 of the GNAS1 gene. Sequence numbers refer to GenBank accession NC 000020.10. RAEB: refractory anemia with excess blasts; RCMD: refractory cytopenia with multilineage dysplasia.

2.3. Mutational analysis

Bone marrow or peripheral blood cells from 120 cases (Supplementary Table 1) with MDS were analyzed using PCR-based denaturing HPLC (Wave-maker software, Wave System, MD Transgenomic Inc., Omaha, Nevraska, USA) for GNAS1 mutations. Coding exons 11–12 were amplified using primers GNAS1 in10CF: 5 -GCTTTGGTGAGATCCATTGAC-3 and GNAS1 ex13BR: 5 -ACCACGAAGATGATGGCAGT-3 (sequence numbers refer to GenBank accession NC 000020.10); abnormal chromatograms were sequenced by Sanger's method (3500 Genetic Analyzer,Applied Biosystems). 200 DNA samples from peripheral blood of healthy donors (wt) were analyzed to investigate new variations.

2.4. qRT-PCR

GNAS1 expression was analyzed in 21 MDS cases (Supplementary Table 1). 10 cases had isolated 20q- and 2/10 had GNAS1 gene deletion; 3 had complex kar-yotype with 20q- and GNAS1 deletion; 8 had complex karyotype without 20q- or GNAS1 deletion. Controls were eight non-malignant disease samples. Total RNA was extracted by Trizol reagent (Invitrogen, Carlsbad, CA, USA), according to the manufacturer's protocol. 1 g was retrotranscribed using 100U of SuperscriptII and esa-random primers (Invitrogen, Carlsbad, CA, USA). Quantitative PCR was performed using TaqMan assay probe Hs00255603 m1 (Applied Biosystems, Life Technologies, Carlsbad, USA) for GNAS1. Reference controls were endogenous ABL1 (Hs00245445 m1, Applied Biosystems, Life Technologies, Carlsbad, USA) and Uni-versal Human Reference RNA (Stratagene, Cedar Creek, TX, USA). All samples were tested in triplicate. Real-time reactions were performed in 96-well plates using the Roche Light Cycler 480 (LC480); fluorescence data were analyzed with the soft-ware version 1.5 and second derivative maximum method; gene expression was expressed as Cp (Crossing point) values. Statistic significance for GNAS1 expression was tested by Mann–Whitney test (*p < 0.05/4).

3. Results

In 2/120 MDS cases sequence variations, i.e., g.69904G > A and g.69899A > T, were identified at intron 12 (Table 1). Neither varia-tion was detected from our screening on 200 normal samples.

FISH analysis showed GNAS1/20q13.32 was deleted in 10/88 MDS cases (11.4%), all with isolated or non-isolated del(20q)/-20 at karyotyping (Table 2). Cryptic deletions were excluded in all other cases. The three cases (nos. 7, 16 and 22 in Table 2) with signal gain for the GNAS1 probe corresponded to duplication of a 20q- at karyo-type. Notably, among 40 cases with involvement of chromosome 20 at karyotype, FISH revealed that the 4 cases classified as -20 in com-plex karyotypes (cases nos. 20, 33, 34 and 35 in Table 2) retained 20q probe signals, including subtelomeric sequences. One of these cases (no.35) also retained the GNAS1 gene. Interestingly, GNAS1 deletion was significantly ($p \leq 0.005$) associated with del(20q) in MDS with complex karyotypes and poor/very poor cytogenetic risk (7/10; 70% of cases in Table 2) rather than in MDS with isolated del(20q) and good cytogenetic risk (3/10; 30%, cases nos. 11, 27, 36 in Table 2). Moreover in complex 20q- GNAS1 deletion corre-sponded significantly (*$p < 0.05/4$) to haploinsufficiency, compared with complex karyotypes without chromosome 20 involvement and with non-malignant samples (Fig. 1a and b).

4. Discussion

Our results from mutational analysis confirmed that GNAS1 mutations are rare in MDS (1.7% of cases in this study). In this study we focused on substitutions R201 and Q227, as they are the hotspots in GNAS1 [1,3]. However, other exonic variations may have a clinical–biological impact in MDS and remain to be deter-mined. Neither the published activating mutations [3,8] nor other coding sequence variations were found in our cohort. However, in two cases (Table 1) heterozygous mutations emerged at intron 12. Chromosome 20 was not involved in the karyotype of these cases. In silico analysis of these new intronic sequence variations using Human Splice Finder (HSF, version 2.4.1, http://www.umd.be/HSF/)

[13] predicted cryptic splice acceptor site activation in patient 89 (accuracy 75.56%) and splice donor site activation in patient 90 (accuracy 68.06%). Moreover, as both intronic substitutions were absent in our series of 200 healthy controls, we assume that they played a role in disease pathogenesis. Notably, in solid tumors [14–16] and in chronic lymphocytic leukemia (CLL) [17] a T393C polymorphism was associated with increased Gs mRNA expres-sion, of which a prognostic role is debated [17,18].

Our results from FISH investigations documented mono-allelic GNAS1 gene deletion and low expression of its transcript as a con-sequence of del(20q) at karyotype, particularly when associated with complex changes (70% of cases in this study). Further stud-ies should be performed to understand the specific role, if any, of GNAS1 haplo-insufficiency in high-risk MDS.

Interestingly, FISH investigations in the four cases with −20 at cytogenetics (Table 2) showed that chromosome 20 was only partially missing, suggesting that monosomy 20 is rare in MDS

Table 2
FISH analysis results.

Case n.		1	2	3	4	5	6	7	8	9	10	11	12	13	14	15	16	17	18	19	20	21	22	23	24	25	26	27	28	29	30	31	32	33	34	35	36	37	38	39	40
del(20q)/-20		I	I	I	I	I	C	I	I	I	C	I	I	I	I	C	I	I	I	I	C*	C	I	I	I	I	I	I	I	I	C	I	I	C*	C*	C*	I	I	C	I	I
RP11-358N2 (*ASXL1*)	20q11.21																																								
LSI-D20S108 (CDR Vysis)	20q12																																								
F.39D1 + F.21H8 (*GNAS1*)	20q13.32																																								
RP1-81F12 (subtel.)	subtel. 20q																																								

GNAS1/20q13.32 was deleted in 10/40 (25%) MDS with karyotypic del(20q)/−20. Black: complete loss of signal; blue: partial loss of signal; green: gain of signal; dots: normal signal; *: −20 at karyotype not confirmed by FISH; F: Fosmid; subtel: subtelomeric; I: isolated; C: complex.

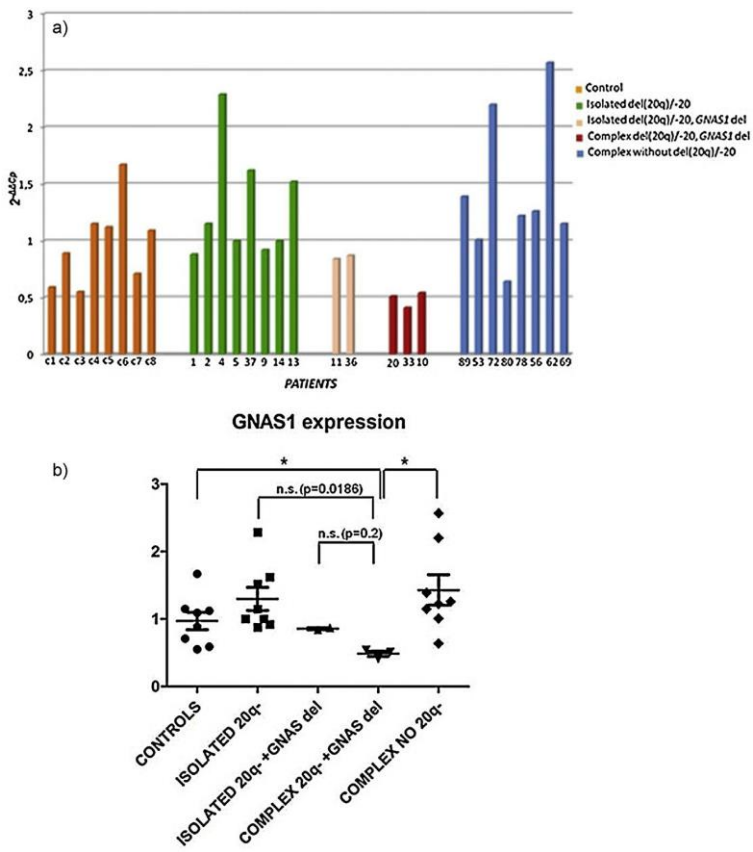

Fig. 1. GNAS1 expression analysis. (a) RT-qPCR showed significant GNAS1 haploinsufficiency in complex 20q−/−20 with gene deletion (case nos. 20, 33, 10). (b) Significance for GNAS1 expression was tested by Mann–Whitney test (*p < 0.0125); values are expressed as means ± SEM. c: control samples.

karyotypes, if indeed it ever occurs. Thus, in cases with −20 FISH investigations are recommended to refine the karyotype and to cor-rectly identify genomic unbalances. Similar results were obtained from FISH studies on monosomy 5 in complex karyotypes, which demonstrated chromosome 5 material persisted [19].

In conclusion in this study we found new rare putatively acti-vating GNAS1 mutations. Moreover, for the first time GNAS1 gene deletion/haplo-insufficiency was found in MDS, particularly in poor/very poor risk cases with complex karyotypes.

Role of the funding source

This work was funded by Associazione Italiana per la Ricerca sul Cancro (AIRC IG-11512), PRIN 2010–2011, Fondo per gli Inves-timenti della Ricerca di Base (FIRB 2011 RBAP11TF7Z 005).

Conflict of interest statement

The authors have no conflicts of interest.

Acknowledgements

Mutation data were obtained from the Sanger Institute Catalog Of Somatic Mutations in Cancer web site, http://www.sanger.ac.uk/ cosmic. DDG performed mutational and expression analysis, analyzed the data and wrote the paper, AGLF, LB and CaMa performed mutational analysis, TP and BC performed FISH exper-iments, NT provided some MDS samples, CM supervised the study, analyzed the data and reviewed the manuscript. All authors approved the final manuscript.

References

[1] Aldred MA, Trembath RC. Activating and inactivating mutations in the human GNAS1 gene. Hum Mutat 2000;16:183–9.
[2] Weinstein LS, Liu J, Sakamoto A, Xie T, Chen M. Minireview: GNAS: normal and abnormal functions. Endocrinology 2004;145:5459–64.
[3] Lania A, Mantovani G, Spada A. G protein mutations in endocrine disease. Eur J Endocrinol 2001;154:543–59.
[4] Landis CA, Masters SB, Spada A, Pace AM, Bourne HR, Vallar L. GTPase inhibiting mutations activate the chain of G_s and stimulate adenylyl cyclase in human pituitary tumors. Nature 1989;340:692–6.
[5] Clementi E, Malgaretti N, Meldolesi J, Taramelli R. A new constitutively activat-ing mutation of the Gs protein alpha subunit-gsp oncogene is found in human pituitary tumours. Oncogene 1990;5:1059–61.
[6] Weinstein LS, Shenker A, Gejman PV, Merino MJ, Friedman E, Spiegel AM. Activating mutations of the stimulatory G protein in the McCune–Albright syndrome. N Engl J Med 1991;325:1688–95.
[7] Aldred MA, Aftimos S, Hall C, Waters KS, Thakker RV, Trembath RC, et al. Con-stitutional deletion of chromosome 20q in two patients affected with albright hereditary osteodystrophy. Am J Med Genet 2002;113:167–72.
[8] Bejar R, Stevenson K, Abdel-Wahab O, Galili N, Nilsson B, Garcia-Manero G, et al. Clinical effect of point mutations in myelodysplastic syndromes. N Engl J Med 2011;364(26):2496–506.
[9] Kanagal-Shamanna R, Yin CC, Miranda RN, Bueso-Ramos CE, Wang XI, Mud-dasani R, et al. Therapy-related myeloid neoplasms with isolated del (20q): comparison with cases of de novo myelodysplastic syndrome with del(20q). Cancer Genet 2013;206(1–2):42–6.

[10] Brezinova J, Zemanova Z, Ransdorfova S, Sindelarova L, Siskova M, Neuwirtova R, et al. Prognostic significante of del(20q) in patients with hematological malignancies. Cancer Genet Cytogenet 2005;160:188–92.
[11] Bacher U, Haferlach T, Schnittger S, Zenger M, Meggendorfer M, Jeromin S, et al. Investigation of 305 patients with myelodysplastic syndromes and 20q deletion for associated cytogenetic and molecular genetic lesions and their prognostic impact. Br J Haematol 2013, http://dx.doi.org/10.1111/bjh.12710.
[12] Greenberg PL, Tuechler H, Schanz J, Sanz G, Garcia-Manero G, Solé F, et al. Revised international prognostic scoring system for myelodysplastic syn-dromes. Blood 2012;120:2454–65.
[13] Desmet FO, Hamroun D, Lalande M, Collod-Beroud G, Claustres M, Beroud C. Human splicing finder: an online bioinformatics tool to predict splicing signals. Nucleic Acids Res 2009;37(9):e67.
[14] Frey UH, Eisenhardt A, Lummen G, Rubben H, Jockel KH, Schmid KW, et al. The T393 Cpolymorphism of the G a s gene (GNAS1) is a novel prognostic marker in bladder cancer. Cancer Epidemiol Biomarkers Prev 2005;14:871–7.
[15] Frey UH, Alakus H, Wohlschlaeger J, Schmitz KJ, Winde G, van Calker HG, et al. GNAS1 T393C polymorphism and survival in patients with sporadic colorectal cancer. Clin Cancer Res 2005;11:5071–7.
[16] Frey UH, Lummen G, Jager T, Jockel KH, Schmid KW, Rubben H, et al. The GNAS1 T393C polymorphism predicts survival in patients with clear cell renal cell carcinoma. Clin Cancer Res 2006;12:759–63.
[17] Frey UH, Nu H, Sellmann L, Siemer D, Kuppers R, Durig J, et al. The GNAS1 T393C polymorphism is associated with disease progression and survival in chronic lymphocytic leukemia. Clin Cancer Res 2006;12:5686–92.
[18] Kaderi MA, Murray F, Jansson M, Merup M, Karlsson K, Roos G, et al. The GNAS1 T393C polymorphism and lack of clinical prognostic value in chronic lymphocytic leukemia. Leuk Res 2008;32:984–7.
[19] Pitchford CW, Hettinga AC, Reichard KK. Fluorescence In Situ Hybridization Testing for–5/5q,–7/7q, +8, and del(20q) in Primary Myelodysplastic Syndrome Correlates With Conventional Cytogenetics in the Setting of an Adequate Study. Am J Clin Pathol 2010;133:260–4.

EHA14(2).pdf

multiple testing). Using the top 50 most differentially expressed lncRNAs for each subgroup, individual patients could be assigned to their appropriate molecular genetic T-ALL subtype (Pearson clustering). Given their proposed association with poor clinical outcome, we further focused on the early immature T-ALL subtype and looked for putative functionally relevant lncRNAs in this genetic subgroup. To this end, a guilt-by-association was performed for the top 10 most differentially expressed known lncRNAs derived from the Agilent platform and an additional top 10 expressed previously unannotated lncRNAs identified through RNA-seq analysis. Of further interest, several immature T-ALL specific lncRNAs were located in the immediate vicinity of important protein coding genes implicated in early haematopoiesis and leukemia such as *MYB*, *RUNX2* and *MEF2C*. Further analyses of selected immature T-ALL associated lncRNAs also showed strong differential expression between $CD34^+CD4^-CD8^-$ *versus* $CD4^+CD8^+$ double positive thymocytes, pointing at important roles for these lncRNAs in normal differentiation. Finally, we selected several top candidate ETP-ALL specific lncRNAs for further functional analyses in order to unravel their exact role in early haematopoiesis and malignant T cell transformation as a prelude for possible lncRNA oriented molecular therapy in immature T-ALL.
Summary and Conclusions: This is the first comprehensive analysis of lncRNA expression in primary T-ALL samples and their normal thymic counterparts. Our finding that lncRNA expression patterns follow the previously established genetic classification is of importance as it marks functional relevance for lncRNAs in T-ALL development.

P105

PTEN MICRO-DELETIONS IN T-CELL ACUTE LYMPHOBLASTIC LEUKEMIA ARE CAUSED BY ILLEGITIMATE RAG-MEDIATED RECOMBINATION EVENTS

R Mendes[1,*] L Sarmento[2], K Canté-Barrett[1], J Buijs-Gladdines[1], V Povoa[2], W Smits[1], A Yunes[3], R Pieters[1,4], J Barata[2], J Meijerink[1]
[1]Department of Pediatric Oncology/Hematology, Erasmus MC Rotterdam-Sophia Children's Hospital, Rotterdam, Netherlands, [2]Instituto de Medicina Molecular, Faculdade de Medicina da Universidade de Lisboa, Lisboa, Portugal, [3]Centro Infantil Boldrini, Sao Paulo, Brazil, [4]Prinses Maxima Center, Utrecht, Netherlands

Background: T-cell acute lymphoblastic leukemia (T-ALL) is characterized by distinct chromosomal abnormalities and mutations. The Phosphatidylinositol 3-kinase (PI3K) signal transduction pathway is often aberrantly activated in various cancers. The main negative regulator of PI3K activity is the phosphatase and tensin homolog (PTEN) tumor suppressor gene. In T-ALL, *PTEN* is inactivated by point-, frameshift insertion/deletion mutations and entire locus deletions. For some seemingly *PTEN* wild-type or monoallelic mutated T-ALL patients that lack total PTEN protein, the mutational mechanisms remain unclear.
Aims: Our goal is therefore to investigate copy-number variations among *PTEN* exons and to detect potential additional *PTEN* deletions.
Results: Here, we show that *PTEN* can be inactivated by micro-deletions spanning introns 1-3 or introns 3-5 in 8% of pediatric T-ALL patients. These micro-deletions were clonal in 5 out of 146 patients, whereas in 8 patients they were present at the sub-clonal level and only detected through PCR techniques. Specific sequences flanking these deletions together with insertion of random nucleotides between the breakpoints pointed to illegitimate RAG-mediated activity. The cryptic RAG recombination signal sequences (cRSS) that flanked the breakpoints drive RAG-dependent recombination in an *in vitro* reporter system as efficiently as established RSSs from TCR gene segments. Similar to other PTEN-inactivating events, *PTEN* micro-deletions are strongly associated with the TALLMO T-ALL cluster, characterized by TAL1 or LMO2 chromosomal rearrangements. As these leukemias frequently display rearranged αβ T-cell receptors at a maturation stage with ongoing RAG activity, our results imply that the TALLMO subgroup has an increased chance of acquiring *PTEN* micro-deletions. Notably, primary and secondary xenotransplants of human *TAL1*-rearranged T-ALL cells in NSG-mice displayed sub-clonal *PTEN* micro-deletions, and we identified equivalent micro-deletions in thymocytes of healthy individuals.
Summary and Conclusions: We propose that *PTEN* micro-deletions result from ongoing RAG activity that is perpetuated during the leukemogenic process, thereby contributing to clonal diversification and disease progression.

P106

CMYC-TRANSLOCATIONS IN T-CELL ACUTE LYMPHOBLASTIC LEUKEMIA

R La Starza[1,*] C Borga[2], G Barba[1], C Schwab[3], V Pierini[1], A Lema Fernandez[1], A Leszl[2], G Sammarelli[4], E Rossetti[4], G Cazzaniga[5], S Chiaretti[6], C Morerio[7], C Matteucci[1], C Harrison[3], G te Kronnie[2], C Mecucci[1]
[1]Hematology and Bone Marrow Transplantation Unit, University of Perugia, Perugia, [2]Oncohematology, Department of Women's and Children's Health, University of Padova, Padova, Italy, [3]Leukaemia Research Cytogenetics Group, Northern Institute for Cancer Research, Newcastle University, Newcastle-upon-Tyne, United Kingdom, [4]Hematology and Bone Marrow Transplantation Unit, University of Parma, Parma, [5]Centro Ricerca Tettamanti, Pediatric Clinic, University of Milano-Bicocca, Monza, [6]Hematology, Department of Cellular Biotechnologies and Hematology, Sapienza University, Roma, [7]Laboratorio di Citogenetica Ematoncologica, Istituto di Ricovero e Cura a Carattere Scientifico Istituto G Gaslini, Genova, Italy

Background: *CMYC* is a transcription factor which regulates critical cell functions such as metabolism, proliferation, and survival. In T-ALL high *CMYC* expression is mainly caused by activation of *NOTCH1* and post-transcriptional mechanisms mediated by *PTEN*.
Aims: To delineate the genetic profile and clinical-hematological features of human T-ALL with *CMYC*-translocations.
Methods: We investigated 62 adults and 132 children belonging to the AIEOP, GIMEMA, and UK clinical trials. *CMYC* was studied by LSI MYC Dual Color, Break Apart Rearrangement Probe (Vysis-Abbott) and homegrown G248P8135G5, RP11-367L7 and RP11-26E5 clones. Affymetrix HU133 Plus 2.0 arrays were used for whole transcriptome profiling (GEP) and Cytoscan HD Platform for SNPa. CI-FISH was performed as described (La Starza R, Leuk Res 2013). *NOTCH1*, *FBW7*, and *PTEN* were analysed by DHPLC (Transgenomic) and sequencing (AB3500 Genetic Analyzer).
Results: CI-FISH and/or predictive analysis by microarray classified 155 cases into 5 distinct molecular subtypes, *i.e. TAL/LMO* (56), *HOXA* (48), *TLX3* (31), *TLX1* (15), and *NKX2-1* (5). *CMYC* reciprocal translocations were detected in 12 cases and involved *TCR* loci in 6 cases while remained undetermined in the other 6. FISH showed that the 8q24 breakpoints clustered at the telomeric region of *CMYC* in all cases with *TCR* translocations, while in 3/6 non-*TCR* translocations breakpoints fell upstream (1 case) or within (2 cases) fosmid G248P8135G5. As type B abnormalities, *CMYC*-translocations occurred in all cases in association with other changes (range: 1-10 additional abnormalities). Association with the TAL/LMO subgroup was significant (Pearson Chi-square, P=0,018). Frequent concurrent rearrangements were *CDKN2A/B* deletions (58,3%) and *PTEN* deletion and/or mutation (41,6%). *NOTCH1* and *FBXW7* mutations were found in a single case. In accordance with their secondary nature, *CMYC*-translocations were found in variable sized subclones (range: 8-62%) in 6 cases, suggesting a contribution to disease progression rather than to disease initiation. Notably, *CMYC*-positive clones appeared to be treatment-resistant. In one case, paired diagnosis/relapse samples showed an increase in size of the CMYC clone from 8% to 100%, whereas other abnormalities $ETV6^{del}$, $BCL1B^{del}$, and $WT1^{del}$ disappeared. In a second case, backtracking to initial diagnosis did not show the *CMYC*-translocation that at relapse was present in 60% of cells. Within the *TAL/LMO* subgroup, 7 translocated *CMYC* specimens with available material for GEP showed high *CMYC* expression in the fourth quartile. Interestingly, in the same quartile, *CMYC* translocated cases showed significantly upregulated *CD44* expression and absence of activated *NOTCH1* signaling compared to cases without these translocations.
Summary and Conclusions: *CMYC*-translocations occurred in about 6% of *NOTCH1* independent T-ALL with marked leukocytosis (>50.000/mmc in 90%; >100.000/mmc in 60% of cases) and a cortical/mature differentiation arrest (60% of cases). *CMYC*-translocations clustered in *TAL/LMO* positive T-ALL with co-occurrence of poor prognostic markers, such as high *CD44* expression and *PTEN* inactivation. Our findings recapitulate murine models in which c-Myc had a crucial role on maintenance and self-renewal of leukemia-initiating cells resulting into resistance to chemotherapy and disease relapse. Early identification (and eradication) of small *CMYC*-positive subclones not only at diagnosis but also during treatment might be helpful to prevent disease progression.

P107

REVEALING EXPRESSION, POST-TRANSLATIONAL MODIFICATIONS AND PROTEOLYSIS IN CHILDHOOD ACUTE LEUKEMIA USING A NOVEL FLOW CYTOMETRY-BASED METHOD OF AFFINITY PROTEOMICS

D Kuzilkova[1,*] V Kanderova[1], J Stuchly[1], K Fiser[1], W Wu[2], A Holm[2], O Hrusak[1], F Lund-Johansen[2], T Kalina[1]
[1]CLIP-Cytometry, Dpt. of Pediatric Haematology and Oncology, 2nd School of Medicine, Charles University and University Hospital Motol, Prague, Czech Republic, [2]Dpt. of Immunology, Rikshospitalet University Hospital, Oslo, Norway

Background: Acute leukemia (AL) is the most common childhood malignancy. It is driven by a number of aberrations detectable at the DNA and mRNA level, but the functional consequences of these alterations at the cellular level are not fully understood. Proteins are the entities that form connection between gene expression and cellular response. Therefore, more effective and sensitive approaches to detect changes in proteome are needed. In the present study we develop and validate new affinity proteomics based tool for analysis of clinical samples.
Aims: Using Size-exclusion Chromatography - Microsphere-based Affinity Proteomics (SEC-MAP) we are able to resolve expression and activation (*e.g.* phosphorylation) of proteins in AL cells.
Methods: SEC-MAP array is a set of 1728 populations of fluorescently-labeled latex microbeads each carrying an antibody against a human protein. We isolate the cellular proteins from membranes, nuclei and cytoplasm using detergents, label them with biotin and separate them using gel chromatography into 24 fractions. These fractions are incubated with SEC-MAP microbeads and the

MYB deregulation from a EWSR1-MYB fusion at leukemic evolution of a JAK2 (V617F) positive primary myelofibrosis .pdf

Pierini et al. Molecular Cytogenetics (2016) 9:68
DOI 10.1186/s13039-016-0277-1

Molecular Cytogenetics

CASEREPORT Open Access

MYB deregulation from a EWSR1-MYB fusion at leukemic evolution of a JAK2^{V617F} positive primary myelofibrosis

Tiziana Pierini†, Danika Di Giacomo†, Valentina Pierini, Paolo Gorello, Gianluca Barba, Anair Graciela Lema Fernandez, Fabrizia Pellanera, Tamara Iannotti, Franca Falzetti, Roberta La Starza and Cristina Mecucci*

Abstract

Background: Although Philadelphia-negative myeloproliferative neoplasms (Ph-MPN) are usually not aggressive, the type and the number of molecular lesions impact greatly on leukemic transformation. Indeed, the molecular background underlying progression is still largely unexplored even though ASXL1, IDH1/2, SRSF2, and TP53 mutations, together with adverse karyotypic changes, place the patient at high risk of leukemic transformation.

Case presentation: Our patient, a 64-year old man with a diagnosis of JAK2^{V617F} primary myelofibrosis (PMF) had an unusually rapid leukemic transformation. Genomic profiling showed that TET2 and SRSF2 mutations were also present. At leukemic transformation, the patient developed a complex chromosome rearrangement producing a EWSR1-MYB fusion. Remarkably, the expression of MYB and of its target BCL2 was, respectively, ≥4.7 and ≥2.8 fold higher at leukemic transformation than after chemotherapy, when the patient obtained the hematological remission. At this time point, the EWSR1-MYB fusion disappeared while JAK2^{V617F}, TET2, and SRSF2 mutations, as well as PMF morphological features persisted.

Conclusions: Rapid leukemic transformation of JAK2^{V617F} PMF was closely linked to a previously undescribed putative EWSR1-MYB transcription factor which was detected only at disease evolution. We hypothesize that the EWSR1-MYB contributed to leukemia transformation through at least two mechanisms: 1) it sustained MYB expression, and consequently deregulated its target BCL2, a putative onco-suppressor gene; and 2) ectopic EWSR1-MYB expression probably fulfilled its own oncogenic potential as demonstrated for other MYB-fusions. As our study confirmed that MYB is recurrently involved in chronic as well as leukemic transformation of PMF, it appears to be a valid molecular marker for tailored treatments.

Keywords: PMF, Leukemic transformation, MYB

Abbreviations: AML, Acute myeloid leukemia; BM, Bone marrow; DBD, DNA binding domain; DHPLC, Denaturing high performance liquid chromatography; ET, Essential thrombocytopenia; FISH, Fluorescence in situ hybridization; Hb, Haemoglobin; I-FISH, Interphase-FISH; MCV, Mean corpuscular volume; Ph-MPN, Philadelphia negative myeloproliferative neoplasia; PMF, Primary myelofibrosis; PV, Polycythemia vera; qRT-PCR, Quantitative reverse transcription-polymerase chain reaction; RT-PCR, Reverse transcription-polymerase chain reaction; SNPa, Single nucleotide polymorphism array; TAD, Transcriptional-activating domain; WBC, White blood cell

* Correspondence: cristina.mecucci@unipg.it
†Equal contributors
Hematology and Bone Marrow Transplantation Unit, University of Perugia, C.R.E.O., Piazzale Menghini n.9, 06132 Perugia, Italy

Background

Ph-MPN are usually not aggressive malignancies. Evolution into Acute Myeloid Leukemia (AML) occurs in ~2 % of Polycythemia Vera (PV), 1 % of Essential Thrombocytopenia (ET), and 10–20 % of PMF, considering the first decade of disease. Although, transformation rates increase with genotoxic therapy, leukemic transformation is part of the natural history of these disorders as AML also occurs in treatment-naive patients [1, 2].

Genomic profiling of Ph-MPN is useful for understanding the pathobiology of leukemic transformation and improving prognostic stratification of patients and treatment. During leukemic transformation very few new mutations are acquired and the majority of somatic mutations are already present in the chronic phase. Two or more mutations affecting ASXL1, IDH1/2, SRSF2, and TP53, are considered high-risk events. Besides mutations, unfavourable (chromosome 3, 5 or 7 rearrangements), and very unfavourable (chromosome 17 abnormalities) karyotypic changes impact upon progno-sis [3, 4]. In any case, the molecular mechanisms under-lying the progression from Ph-MPN to AML are not yet completely understood [5–9].

Longitudinal genomic investigation into a unique case of $JAK2^{V617F}$ positive PMF with rapid leukemic evolution, detected a leukemia-specific complex rearrangement involving chromosomes 6, 9 and 22 which produced an aberrant EWSR1-MYB transcription factor. EWSR1-MYB ectopic expression, as well as high expression of MYB and its target BCL2, likely contributed to the leukemia phenotype. It is worth mentioning that, high level of MYB expression blocks differentiation and confers self-renewal properties to leukemic cells, whereas the ex-pression of the anti-apoptotic BCL2 protein inhibits leukemic cell death [10–12].

Case presentation

In January 2011, a 64-year-old man was referred to our Department with leukocytosis (WBC 20.100/uL with 71.8 % neutrophils), macrocytic anemia (Hb 11,5 g/dL; MCV 104 fl), splenomegaly, and hepatomegaly. Bone marrow (BM) biopsy revealed PMF with grade 1 fibrosis; karyotype was normal. The $JAK2^{V617F}$ mutation was found at 60 % allelic burden. After 4 months the patient developed an acute myeloid leukemia (AML; M2 morphology) and acquired an ins(6;22)(q23.3;q11) in the 20 metaphases analyzed (Fig. 1a). He was treated according to the FLAI protocol [13] and obtained hematologic and cytogenetic remission. Myeloproliferative features, including $JAK2^{V617F}$, persisted. Demethylating treatment with 5-azacytidine (5-AZA) was administered for 8 cycles, reducing anemia and splenomegaly, but treatment was discontinued because the patient developed a gastric adenocarcinoma. He died 30 months after PMF was diagnosed.

Methods

Molecular-cytogenetic and mutational analyses

All molecular and cytogenetic studies were carried out on BM samples. Multi-FISH (24XCyte Multi-colour probe kit, MetaSystems), whole chromosome paints for chromosomes 6, 9 and 22 (Cytocell, Milan, Italy), and metaphase FISH with DNA clones for MYB (G248P8686G9 and G248P89100B2), EWSR1 (G248P89991F7 and G248P80286D12), 9q33.1-q33.3, and 22q11-q12 regions, were done at leukemic transformation (Additional file 1 and Additional file 2: Tables S1, S2, S3). A EWSR1-MYB FISH assay (RP1-32B1 for MYB and RP11-367E7 for EWSR1) was performed at leukemic transformation, diagnosis and post-chemotherapy. The EWSR1-MYB assay was also applied to a cohort of 7 PMF and 3 leukemia groups (Additional file 1). Single Nucleo-tide Polymorphism array (SNPa) experiments were per-formed at initial PMF and at leukemic transformation; targeted mutational analysis of DNMT3A, SETBP1, EZH2, IDH1, IDH2, SRSF2, ASXL1, NRAS, TET2 and TERT pro-moter was done at diagnosis, leukemic transformation, and after chemotherapy by DHPLC and Sanger's Sequen-cing. For details of experiments see Additional file 1 and Additional file 2: Table S4.

Reverse transcription-polymerase chain reaction (RT-PCR) and cloning of EWSR1-MYB

cDNA from each patient sample was amplified using primers EWSR1_400F (5′-GCCCACTCAAGGATATGCA C-3′) and MYB_561R (5′-TGCTTGGCAATAACAGAC CA-3′), for the first amplification round; nested PCR was set up with primers EWSR1_515F (5′-CAGACCGCC TATGCAACTTC-3′) and MYB_433R (5′-GCACTGCAC ATCTGTTCGAT-3′). PCR products were cloned and se-quenced (Additional file 1).

Quantitative reverse transcription PCR (qRT-PCR) for MYB and BCL2

MYB expression was investigated in our patient, at all time points, and in 7 PMF cases (four at leukemic transformation and three in paired chronic phase/leukemic transformation) (TaqMan assay probe Hs00920556_m1; Applied Biosystems, Foster City, CA). Negative controls were four healthy BM samples. Positive controls were 12 acute leukemias with high MYB expression (4 RUNX1-RUNX1T1 AML, 4 AML with MLL translocations, and 4 BCR-ABL1-positive B-cell ALL) [14]. Expression of BCL2, a known MYB target, was also investigated in our case (TaqMan assay probe Hs00608023_m1, Applied Biosystems). Amplifications were normalized to the endogenous reference control ABL1 (Hs00245445_m1, Applied Biosystems) (Additional file 1).

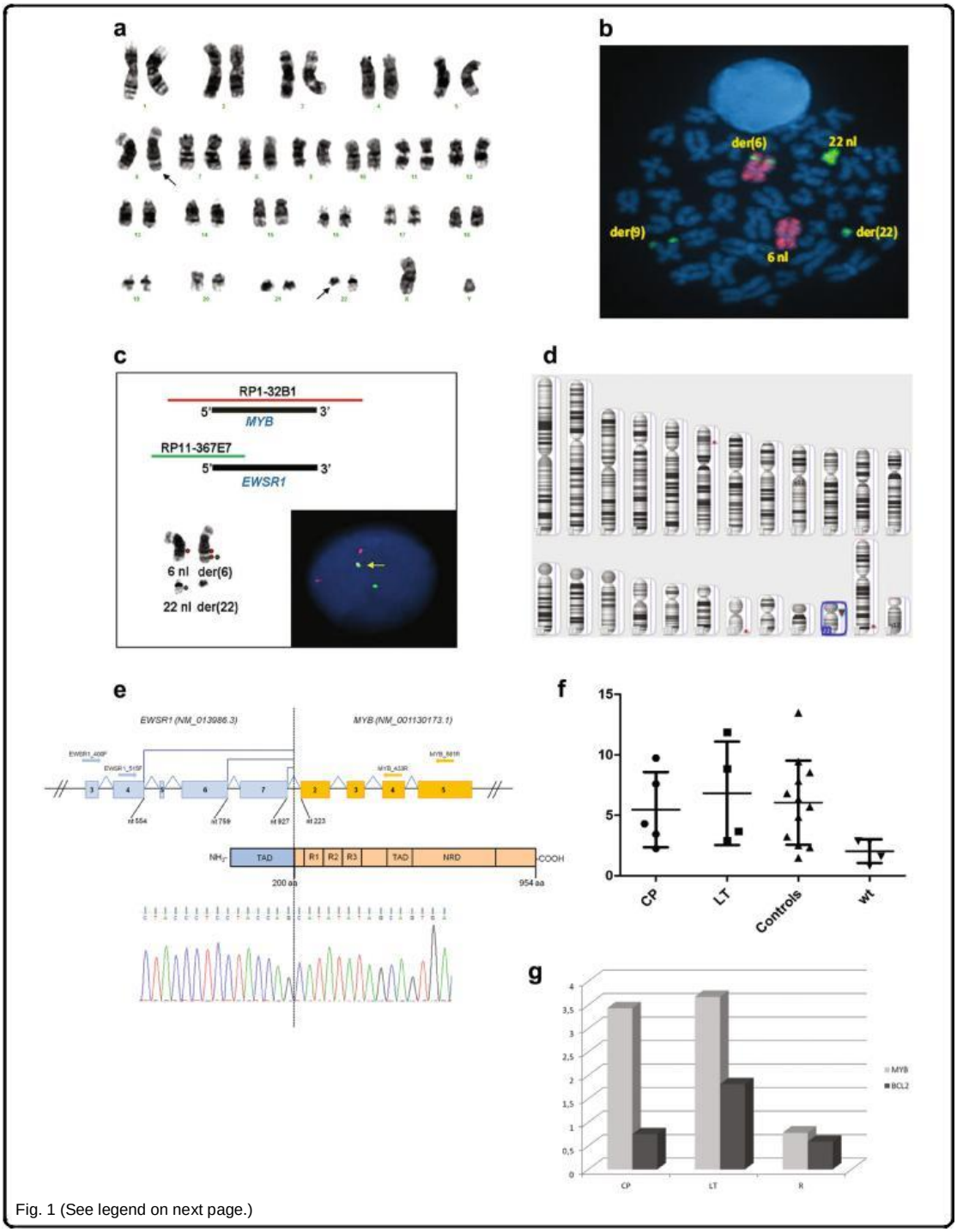

Fig. 1 (See legend on next page.)

(See figure on previous page.)
Fig. 1 a) G-banded karyotype bone marrow cells at leukemic transformation showed ins(6;22)(q23.3;q11) and der(22q) (black arrows). b) Metaphase FISH experiment with Whole Chromosome Paint (WCP) 6 (Texas Red) and WCP 22 (FITC). Genomic material of chromosome 22 was present on der(6) and der(9) long arms. c) Schema of clones RP1-32B1 (MYB) (Spectrum Orange) and RP11-367E7 (EWSR1) (Spectrum Green) and their mapping. Normal and derivative chromosomes 6 and 22 hybridization patterns; a green/orange fusion signal was present on der(6). A fusion signal was found in interphase nuclei (yellow arrow). d) SNPa analysis detected loss at 22q (red triangle) in BM sample at leukemic transformation. e) Schema of the EWSR1-MYB fusion gene and putative protein. f) MYB expression analysis in four combined cases at chronic phase and leukemic transformation and in a positive control group (4 RUNX1-RUNX1T1 AML, 4 MLL-positive AML, and 4 BCR-ABL1-positive B-cell ALL). g) Longitudinal expression of MYB and BCL2 in the index case. Data are reported for one representative of three independent experiments. Abbreviations: der, derivative chromosome; nl, normal; TAD, transcriptional-activating domain; R1, R2, R3, imperfect aminoacidic repeats; NRD, negative regulatory domain; CP, chronic phase; LT, leukemic transformation; wt, wild-type; R, relapse

Results

Molecular cytogenetic and mutational analyses

Multi-FISH and whole chromosome paints showed chromosome 22q11-q12 material inserted into chromosome 6q23 and revealed an additional rearrangement between der(22) and an apparently normal chromosome 9 (Fig. 1b) (Additional file 3: Figure S1). The breakpoint occurred at 6q23 within the MYB oncogene (Additional file 3: Figure S2). Fosmids for EWSR1 and the EWSR1-MYB assay showed that the 5′EWSR1 was inserted into the MYB locus (Fig.1c) (Additional file 3: Figure S2). The EWSR1-MYB rearrangement was not detected at chronic phase or in 3 consecutive samples analyzed after chemotherapy and during treatment with 5-AZA (Table 1).

SNPa detected a 96 Mb copy neutral loss of heterozygos-ity (cnLOH) at 12q11-12q24.33 at chronic phase and leukemic transformation. Lack of germinal material pre-cluded definition as a congenital or acquired event. Apply-ing a 50 Kb filter revealed a 99 kb loss at 22q11.1 (cytostart 17585764 - cytoend 17684472) only at leukemic transform-ation (Fig. 1d) (Additional file 3: Figure S3). SRSF2 (c.284C > A; p.P95H) and TET2 (c.3781C > T; p.R1261C) (c.2732_2733insC; p.A912Cfs*12) mutations were found, and confirmed, at all disease stages (Table 1).

RT-PCR and qRT-PCR

At leukemic transformation an in-frame fusion tran-script EWSR1-MYB with breakpoint in EWSR1 exon 7 (nt 927) (NM_013986.3) and MYB exon 2 (nt 223) (NM_001130173.1) was detected. The 954 aminoacids predicted fusion protein retained the EWSR1 transcriptional-activating domain (TAD) at the N-terminal and all MYB functional domains at the C-terminal (Fig. 1e). After chemotherapy, at hematological and cytogenetic remis-sion, the EWSR1-MYB fusion disappeared. At leukemic phase, MYB and BCL2 expression was respectively ≥4.7 and ≥2.8 fold higher than at remission. High MYB expres-sion was detected in 7 PMF and in the 3 groups of acute leukemia used as positive controls (Fig. 1f).

Discussion

This case of JAK2-positive PMF with very rapid evolution to AML had a specific mutational profile at diagnosis bearing mutations of JAK2, SRSF2 and TET2. A complex rearrangement involving chromosomes 6, 9, and 22, which produced a previously undescribed EWSR1-MYB fusion, underlies the leukemic transformation.

EWSR1 is a member of the TET (TLS, EWSR1, TAFII68) protein family which acts as multifunctional protein and

Table 1 Longitudinal cytogenetic and molecular studies in our patient with rapidly evolving PMF

	PMF diagnosis	Leukemic transformation	Post-consolidation therapy	*Monitoring +3 months	*Monitoring +14 months
Karyotype	46,XY [20]	46,XY,ins(6;22)(q23q11q12),del(22)(q11) [20]	46,XY [20]	46,XY [20]	46,XY [20]
JAK2 ^{V617F} allele burden	60 %	63 %	70 %	n.d.	36 %
TET2 c.2732_2733insC, p.A912Cfs*12; .c.3781C>T, p.R1261C	yes	yes	yes	n.d.	n.d.
SRSF2 c.284C>A p.P95H	yes	yes	yes	n.d.	n.d.
SNPa	cnLOH 12q11-12q24.33	cnLOH: 12q11-12q24.33	n.d.	n.d.	n.d.
		LOSS: 22q11.1			
I-FISH: EWSR1-MYB	negative	positive	negative	negative	negative
RT-PCR: EWSR1-MYB	negative	positive	negative	n.d.	n.d.

n.d. not done
*from leukemia transformation

regulates transcription and mRNA splicing to maintain cellular homeostasis. Although well known in soft tissue sarcoma, EWSR1 fusions have only occasionally been detected in leukemia [15–19]. Interestingly, all EWSR1 fusions retained the TAD portion at the N-terminal and the partner DNA Binding Domain (DBD) at the C-terminal. Since EWSR1-FLI1, the most frequent sarcoma-associated fusion, acted as an aberrant transcription factor, deregulating several targets [20], one might speculate that the EWSR1-MYB fusion in our patient also acted as an aberrant tran-scription factor, altering the MYB transcriptional program.

MYB is a leucin zipper transcription factor which plays a key role in cell proliferation and differentiation [21–23]. High level of MYB is common in AML associated with BCR-ABL1, RUNX1-RUNX1T1, MYST3-CREBBP, or MLL-rearrangements [11, 12, 24]. Chromosomal aberrations placing MYB under the promoter of a partner gene, such as TCRB-MYB in T-cell ALL [14, 25] or in close proximity of super-enhancer regions, such as MYB-NFIB in adenoid cystic carcinoma [26], caused MYB over-expression. It is worth noting, however, that besides promoting tumour growth through MYB over-expression, the MYB fusions might have their own oncogenic potential as demonstrated for the MYB-QKI in pediatric angiocentric glioma, which drives tumor development in vitro and in vivo models [27].

High MYB level confers self-renewal properties on leukemic cells and blocks differentiation, thus it has been regarded as a putative therapeutic target [11, 12]. Indeed, in vitro and in vivo studies showed that a slight MYB drop is enough to block leukemic cell proliferation without affecting normal haematopoiesis [28]. The present study confirmed two previous reports of high MYB expression in PMF [29, 30] as it was detected in all cases at chronic phase with a rising trend at leukemic transformation (Fig. 1f).

In determining whether and how the aberrant EWSR1-MYB transcription factor played a role in rapid disease progression, paired longitudinal studies showed that the EWSR1-MYB fusion was closely linked to leukemic trans-formation, as it was not detected at diagnosis and disap-peared after treatment. As a functional consequence of MYB deregulation we investigated BCL2 expression as it is a well-known MYB target which acts as an anti-apoptotic onco-suppressor. Recent findings in leukemia xenograft models showed that sustained MYB expression main-tained high BCL2 expression and consequently, inhib-ited leukemic cell death [10]. In line with these data, we found that MYB as well as BCL2 expression was higher at leukemic transformation than after treatment (Fig. 1g).

Our patient responded to treatment by regressing from AML to PMF maintaining JAK2, TET2 and SRSF2 mutations. Therefore, the JAK2-positive clone, showed a constant allele burden in all disease phases, marking the PMF stem line which persisted throughout disease, while the EWSR1-MYB fusion was the hallmark of the leukemic clone. Whether EWSR1-MYB affected a JAK2^{V617F} cell or developed as an independent clone, could not be established. Interestingly Engle E.K. et al. [31], identified MYB mutations in a complex PMF subclonal branching.

Conclusion

We report a unique case of JAK2^{V617F} PMF. Rapid leukemia transformation, due to complex cytogenetic rearrangement, produced a previously undescribed EWSR1-MYB fusion that appeared to act as an aberrant transcription factor de-regulating BCL2. Our study provided new insights to point to MYB as a good molecular target in patients pre-senting with high-risk PMF [11, 32].

Additional files

Additional file 1: Detailed materials/methods and results. (DOC 68 kb)

Additional file 2: Table S1. FISH clones for chromosome 6 long arm breakpoint characterization. Table S2. FISH clones for chromosome 22 long arm telomeric breakpoint characterization. Table S3. FISH clones for chromosome 9 long arm breakpoint characterization. Table S4. Genes, amplicons and primers for mutational analysis. (DOC 991 kb)

Additional file 3: Figure S1. Multi-FISH analysis showed a complex rearrangement between chromosomes 6, 9 and 22 (yellow arrows). Figure S2. A) Chromosome 6q23 breakpoint within MYB. B) Chromosome 22q11.2 breakpoint within EWSR1. Figure S3. A) SNPa findings at PMF diagnosis: no CNV with 100 and 50 Kb filters (left panel) but LOH at 12q (right panel, black arrow). B) SNPa findings at leukemic transformation: a genomic loss, at 22q11.2, was identified with a 50 Kb filter (left panel, red arrow); LOH at 12q (right panel, red arrow). (DOC 3447 kb)

Acknowledgements
The authors would like to thank Dr G A Boyd for assistance in preparing the manuscript.

Funding
This work was funded by Associazione Italiana per la Ricerca sul Cancro (AIRC, IG-15525), Fondo per gli Investimenti della Ricerca di Base (FIRB 2011 RBAP11TF7Z_005), Programmi di Ricerca scientifica di rilevante Interesse Nazionale (PRIN), Associazione Sergio Luciani, Fabriano, Italy and Fondazione Cassa di Risparmio di Perugia (2014.0265.021).

Availability of data and materials
Not applicable.

Authors' contributions
RLS and CM conceived and designed the study, analyzed the data, and wrote the manuscript; TP and DDG wrote the paper; TP and VP performed and analyzed FISH experiments; GB performed and analyzed SNP array; DDG and PG performed and analyzed RT-PCR and qRT-PCR; AGLF, FP, TI performed targeted mutational analysis and analyzed results; FF determined JAK2^{V617F} allelic burden. All Authors approved the manuscript.

Competing interests
Authors declare that they have no competing interests.

Consent for publication
Written informed consent was obtained from the patient's relatives for publication of this Case report and any accompanying images. A copy of the written consent is available for review by the Editor of this journal.

Received: 20 July 2016 Accepted: 22 August 2016
Published online: 01 September 2016

References

1. Kennedy JA, Atenafu EG, Messner HA, et al. Treatment outcomes following leukemic transformation in Philadelphia-negative myeloproliferative neoplasms. Blood. 2013;121(14):2725–33.
2. Finazzi G, Caruso V, Marchioli R, et al. Acute leukemia in polycythemia vera: an analysis of 1638 patients enrolled in a prospective observational study. Blood. 2005;105(7):2664–70.
3. Tam CS, Abruzzo LV, Lin KI, et al. The role of cytogenetic abnormalities as a prognostic marker in primary myelofibrosis: applicability at the time of diagnosis and later during disease course. Blood. 2009;113(18):4171–8.
4. Tefferi A, Pardanani A, Gangat N, et al. Leukemia risk models in primary myelofibrosis: an International Working Group study. Leukemia. 2012;26(6): 1439–41.
5. Abdel-Wahab O, Manshouri T, Patel J, et al. Genetic analysis of transforming events that convert chronic myeloproliferative neoplasms to leukemias. Cancer Res. 2010;70(2):447–52.
6. Harutyunyan A, Klampfl T, Cazzola M, Kralovics R. p53 lesions in leukemic transformation. N Engl J Med. 2011;364(5):488–90.
7. Klampfl T, Harutyunyan A, Berg T, et al. Genome integrity of myeloproliferative neoplasms in chronic phase and during disease progression. Blood. 2011; 118(1):167–76.
8. Lundberg P, Karow A, Nienhold R, et al. Clonal evolution and clinical correlates of somatic mutations in myeloproliferative neoplasms. Blood. 2014;123(14):2220–8.
9. Quintás-Cardama A, Kantarjian H, Pierce S, Cortes J, Verstovsek S. Prognostic model to identify patients with myelofibrosis at the highest risk of transformation to acute myeloid leukemia. Clin Lymphoma Myeloma Leuk. 2013;13(3):315–18.
10. Jing D, Bhadri VA, Beck D, et al. Opposing regulation of BIM and BCL2 controls glucocorticoid-induced apoptosis of pediatric acute lymphoblastic leukemia cells. Blood. 2015;125(2):273–83.
11. Uttarkar S, Dassé E, Coulibaly A, et al. Targeting acute myeloid leukemia with a small molecule inhibitor of the Myb/p300 interaction. Blood. 2016; 127(9):1173–82.
12. Lieu YK, Reddy EP. Conditional c-myb knockout in adult hematopoietic stem cells leads to loss of self-renewal due to impaired proliferation and accelerated differentiation. Proc Natl Acad Sci U S A. 2009;106(51):21689–94.
13. Russo D, Pricolo G, Michieli M, et al. Fludarabine, arabinosyl cytosine and idarubicin (FLAI) for remission induction in poor-risk acute myeloid leukemia. Leuk Lymphoma. 2001;40(3-4):335–43.
14. Lahortiga I, De Keersmaecker K, Van Vlierberghe P, et al. Duplication of the MYB oncogene in T cell acute lymphoblastic leukemia. Nat Genet. 2007; 39(5):593–5.
15. Schlaak M, Renner R, Treudler R, et al. CD30+ anaplastic lymphoma kinase-positive anaplastic large cell lymphoma with an unusual translocation t(11; 22). Br J Dermatol. 2008;159(1):240–2.
16. Martini A, La Starza R, Janssen H, et al. Recurrent rearrangement of the Ewing's sarcoma gene, EWSR1, or its homologue, TAF15, with the transcription factor CIZ/NMP4 in acute leukemia. Cancer Res. 2002;62(19): 5408–12.
17. Jakovljević G, Nakić M, Rogosić S, et al. Pre-B-cell acute lymphoblastic leukemia with bulk extramedullary disease and chromosome 22 (EWSR1) rearrangement masquerading as Ewing sarcoma. Pediatr Blood Cancer. 2010;54(4):606–9.
18. Hawkins JM, Craig JM, Secker-Walker LM, Prentice HG, Mehta AB. Ewing's sarcoma t(11;22) in a case of acute nonlymphocytic leukemia. Cancer Genet Cytogenet. 1991;55(2):157–62.
19. Cantile M, Marra L, Franco R, et al. Molecular detection and targeting of EWSR1 fusion transcripts in soft tissue tumors. Med Oncol. 2013;30(1):412.
20. Uren A, Toretsky JA. Ewing's sarcoma oncoprotein EWS-FLI1: the perfect target without a therapeutic agent. Future Oncol. 2005;1(4):521–8.
21. Sandberg ML, Sutton SE, Pletcher MT, et al. Myb and p300 regulate hematopoietic stem cell proliferation and differentiation. Dev Cell. 2005; 8(2):153–66.
22. Mucenski ML, McLain K, Kier AB, et al. A functional c-myb gene is required for normal murine fetal hepatic hematopoiesis. Cell. 1991;65(4):677–89.
23. Malaterre J, Carpinelli M, Ernst M, et al. Myb is required for progenitor cell homeostasis in colonic crypts. Proc Natl Acad Sci U S A. 2007;104(10):3829–34.
24. Pattabiraman DR, McGirr C, Shakhbazov K, et al. Interaction of c-Myb with p300 is required for the induction of acute myeloid leukemia (AML) by human AML oncogenes. Blood. 2014;123(17):2682–90.
25. Clappier E, Cuccuini W, Kalota A, et al. The C-MYB locus is involved in chromosomal translocation and genomic duplications in human T-cell acute leukemia (T-ALL), the translocation defining a new T-ALL subtype in very young children. Blood. 2007;110(4):1251–61.
26. Drier Y, Cotton MJ, Williamson KE, et al. An oncogenic MYB feedback loop drives alternate cell fates in adenoid cystic carcinoma. Nat Genet. 2016;48(3): 265–72.
27. Bandopadhayay P, Ramkissoon LA, Jain P, et al. MYB-QKI rearrangements in angiocentric glioma drive tumorigenicity through a tripartite mechanism. Nat Genet. 2016;48(3):273–82.
28. Zuber J, Rappaport AR, Luo W, et al. An integrated approach to dissecting oncogene addition implicates a Myb-coordinated self-renewal program as essential for leukemia maintenance. Genes Dev. 2011;25(15):1628–40.
29. Steensma DP, Pardanani A, Stevenson WS, et al. More on Myb in myelofibrosis: molecular analyses of MYB and EP300 in 55 patients with myeloproliferative disorders. Blood. 2006;107(4):1733–5.
30. Guglielmelli P, Tozzi L, Pancrazzi A, et al. MicroRNA expression profile in granulocytes from primary myelofibrosis patients. Exp Hematol. 2007;35(11): 1708–18.
31. Engle EK, Fisher DA, Miller CA, et al. Clonal evolution revealed by whole genome sequencing in a case of primary myelofibrosis transformed to secondary acute myeloid leukemia. Leukemia. 2015;29(4):869–76.
32. Amaru Calzada A, Todoerti K, Donadoni L, et al. The HDAC inhibitor Givinostat modulates the hematopoietic transcription factors NFE2 and C-MYB in JAK2(V617F) myeloproliferative neoplasm cells. Exp Hematol. 2012;40(8):634–45.

Genetic profile of T-cell acute lymphoblastic leukemias with MYC translocations.pdf

Brief Report

LYMPHOID NEOPLASIA

Genetic profile of T-cell acute lymphoblastic leukemias with MYC translocations

Roberta La Starza,[1] Chiara Borga,[2] Gianluca Barba,[1] Valentina Pierini,[1] Claire Schwab,[3] Caterina Matteucci,[1] Anair G. Lema Fernandez,[1] Anna Leszl,[2] Gianni Cazzaniga,[4] Sabina Chiaretti,[5] Giuseppe Basso,[2] Christine J. Harrison,[3] Geertruy te Kronnie,[2] and Cristina Mecucci[1]

[1]Hematology Unit, University of Perugia, Polo Unico S.M. Misericordia, Perugia, Italy; [2]Oncohematology, Department of Women's and Children's Health, University of Padova, Padova, Italy; [3]Leukaemia Research Cytogenetics Group, Northern Institute for Cancer Research, Newcastle University, Newcastle-upon-Tyne, United Kingdom; [4]Centro Ricerca Tettamanti, Pediatric Clinic University of Milano-Bicocca, Monza, Italy; and [5]Division of Hematology, "Sapienza" University of Rome, Rome, Italy

Key Points

- MYC translocations represent a genetic subgroup of NOTCH1-independent T-ALL clustered within the TAL/LMO category.
- MYC translocations are secondary abnormalities, which appear to be associated with induction failure and relapse.

MYC translocations represent a genetic subtype of T-lineage acute lymphoblastic leukemia (T-ALL), which occurs at an incidence of ~6%, assessed within a cohort of 196 T-ALL patients (64 adults and 132 children). The translocations were of 2 types; those rearranged with the T-cell receptor loci and those with other partners. MYC translocations were significantly associated with the TAL/LMO subtype of T-ALL (P 5.018) and trisomies 6 (P < .001) and 7 (P < .001). Within the TAL/LMO subtype, gene expression profiling identified 148 differentially expressed genes between patients with and without MYC translocations; specifically, 77 were upregulated and 71 downregulated in those with MYC translocations. The poor prognostic marker, CD44, was among the upregulated genes. MYC translocations occurred as secondary abnormalities, present in subclones in one-half of the cases. Longitudinal studies indicated an association with induction failure and relapse. (Blood. 2014;124(24):3577-3582)

Introduction

MYC is one of the main phosphatidylinositol 3-kinase (PI3K)/ AKT targets, thus rearrangements underlying PI3K/AKT activa-tion result in MYC overexpression. Deregulation of the PI3K/ AKT pathway plays a pivotal role in T-lineage acute lympho-blastic leukemia (T-ALL), being constitutively activated in cases with NOTCH1/FBXW7 (50%-60%) mutations, PTEN (10%-30%) inactivation and PTPN2 (6%) deletions.[1-4] These observations have identified MYC as a key T-ALL oncogene and an effective therapeutic target.[5] The potential role of MYC activation in initiating T-ALL tumorigenesis has been demonstrated in transgenic zebrafish and mouse models, where the induced over-expression of c-Myc lead to T-ALL development with high penetrance and short latency.[5-8] Moreover, in T-ALL murine models, c-Myc appeared to be critical for leukemia initiation, maintenance, and self-renewal, as its sup-pression, prevents leukemia development.[9-11]

We have characterized an emerging group of T-ALL with MYC translocations, identified as a specific subgroup of NOTCH1-independent TAL/LMO-positive leukemia, occurring in about 6% of adult and childhood T-ALL.

Study design

To assess the incidence of MYC translocations in T-ALL, we investigated 64 adults and 132 children (supplemental Methods, available on the Blood Web site). Combined interphase fluorescence in situ hybridization (CI-FISH) and/or Predictive Analysis of Microarrays[12] classified 80% of cases into groups according to distinct genetic features: TAL/LMO (57), HOXA (49), TLX3 (31), TLX1 (16), and NKX2-1 (5), whose distribution into age groups reflected previous studies (supplemental Table 1). Karyotyping, CI-FISH, single nucleotide polymorphism array, and mutational anal-ysis investigated concurrent genomic abnormalities (supplemental Methods).[12]

Results and discussion

Incidence and type of MYC translocations

MYC translocations were detected in 12 of 196 cases of T-ALL (6.1%) and were equally distributed between children and adults (Table 1). They involved T-cell receptor (TCR) loci in 6 cases and

Submitted June 3, 2014; accepted September 12, 2014. Prepublished online as Blood First Edition paper, September 30, 2014; DOI 10.1182/blood-2014-06-578856.

The microarray data reported in this article have been deposited in the Gene Expression Omnibus database (accession number GSE60733).

The online version of this article contains a data supplement.

The publication costs of this article were defrayed in part by page charge payment. Therefore, and solely to indicate this fact, this article is hereby marked "advertisement" in accordance with 18 USC section 1734.

Table 1. Clinical, hematologic, and molecular-cytogenetic features of T-ALL with MYC translocations

No.	Sex	Age, y	WBC mmc	Phenotype	Treatment	Relapse	Status	Follow-up, mo	Karyotype	FISH	Category*	PTEN	NOTCH1/ FBX7
Children													
1	M	14	235.600	Early	AIEOP, IR	No	Alive	107	46,XY,t(1;8)(q32;q24),del(4)(p15) [13]	MYC translocation (85%) del(4)(q25)/LEF1 del(9)(p21)/CDKN2A/B del(10)(q23)/PTEN	TAL/LMO	wt	wt/wt
2	F	12	43.800	Cortical	AIEOP, SR	Yes	Died	13	46,XX,t(8;14)(q24;q11)[3] 48,idem,16, 17[7]	TCRAD-MYC (60%) del(9)(p21)/CDKN2A.B Trisomy 6 Trisomy 7	TAL/LMO	mut	wt/wt
3	M	10	754.800	Mature	AIEOP, HR	Yes	Died	24	n.a.	SIL-TAL1 MYC translocation (70%)	TAL/LMO	mut	wt/wt
4†	M	5	112.100	Mature	AIEOP, HR	No	Alive	87	46,XY,del(6)(q16),t(7;8)(q22;q24), t(11;14)(p14;q11)[6] 46,XY[6]	SIL-TAL1 TCRAD-LMO2 MYC translocation (18%) del(6)(q16)/GRIK2 del(9)(p21)/CDKN2AB	TAL/LMO	wt	wt/wt
5†	M	8	168.000	n.a.	UKALL2003, regimen B	No	Alive	60	46,XY,t(8;14)(q24;q11)[2]/46,XY[6]	TCRB-TAL2 TCRAD-MYC (30%)	TAL/LMO	wt	wt/wt
6	F	9	618.000	n.a.	MRC.ALL97/99, regimen B	No	Alive	84	46,XX[14]	SIL-TAL1 TCRB-MYC (86%) del(10)(123)/PTEN del(9)(p21)/CDKN2AB	TAL/LMO	wt	wt/wt
7†	M	13	79.500	n.a.	MRC.ALL97/99, regimen C	No	Alive	83	46,XY,t(11;19)(q23;p13)[10]	MLL-ENL MYC translocation (28%) trisomy 6 trisomy 7	HOXA	mut	wt/wt
8†	F	3	650.000	n.a.	MRC.ALL97,SR	No	Alive	120	46,XX,t(8;14)(q24;q11)[6]/46,XX[4]	TCRAD-MYC (10%) bdel(9)(p21)/CDKN2AB	Unclassified	wt	wt/wt
Adults													
9	F	25	62.700	Cortical vs mature	GIMEMA LAL 2000	Yes	Died	30	n.a.	SIL-TAL1 TCRB-LM01 TCRB-MYC (62%) del(9)(p21)/CDKN2AB del(6q15)/CAS8AP2	TAL/LMO	mut	wt/wt
10	M	44	251.000	Cortical del(10)(q23)/PTEN del(9)(p21)/CDKN2AB Gain 10p13/AF10	NILG ALL 10/07	No	Alive	29	46,XY,t(8;14)(q24;q11)[13].46,XX[3]	SIL-TAL1 TCRA/D-YC (90%)	TAL/LMO	mut	wt/wt

AIEOP, Associazione Italiana Emato-Oncologia Pediatrica; CHOP, cyclophosphasmide, doxorubicin, vincristine, prednisone; F, female; GIMEMA, Gruppo Italiano Malattie Ematologiche Maligne dell'Adulto protocols; HR, high risk; hyperCVAD, cyclophosphasmide, doxorubicin, vincristine, prednisone, methotrexate, cytarabine; IR, intermediate risk; LAL, acute lymphoblastic leukemia; M, male; mmc, cubic millimeter; MRC, Medical Research Council protocols; mut, mutated; n.a., not available; NILG, Northen Italy Leukemia Group protocol; SR, standard risk; UKALL2003, United Kingdom acute lymphoblastic leukemia protocol; WBC, white blood cell; wt, wild type.

*The genetic category was defined by CI-FISH and/or gene expression profile.

†Cases with subclonal MYC translocations. Between brackets the percentage of cells with MYC translocation is indicated.

Table 1. (continued)

	WBC			Follow-up.			NOTCH1/No.SexAge.ymmcPhenotypeTreatmentRelapseStatusmoKaryotypeFISHCategory*PTENFBX7													
74011†	F	5684.	Cortical vs mature	CHOP,HyperCVAD	Yes	Died	8	n.a.								MYC translocation (50%) del(9)(p21)/CDKN2AB Gain 6q23/MYB Trisomy 7 Gain Xq28/MTCP1	TAL/LMO	wt	wt/wt
12†	M	48	20. Cortical	GIMEMA 0904	Yes	Died	18	n.a.	TCRAD-TLX1	TLX1	wt	mut/mut000				MYC translocation (8%) del(18)(q11)/PTPN2 del(9)(q21)/CDKN2AB 9del(12)(p13)/3ETV6 del(14)(q32)/BCL11B del(11)(p13)/WT1			

AIEOP, Associazione Italiana Emato-Oncologia Pediatrica; CHOP, cyclophosphamide, doxorubicin, vincristine, prednisone; F, female; GIMEMA, Gruppo Italiano Malattie Ematologiche Maligne dell'Adulto protocols; HR, high risk; hyperCVAD, cyclophosphamide, doxorubicin, vincristine, prednisone, methotrexate, cytarabine; IR, intermediate risk; LAL, acute lymphoblastic leukemia; M, male; mmc, cubic millimeter; MRC, Medical Research Council protocols; mut, mutated; n.a., not available; NILG, Northen Italy Leukemia Group protocol; SR, standard risk; UKALL2003, United Kingdom acute lymphoblastic leukemia protocol; WBC, white blood cell; wt, wild type.
*The genetic category was defined by CI-FISH and/or gene expression profile.
†Cases with subclonal MYC translocations. Between brackets the percentage of cells with MYC translocation is indicated.

new partners in the other 6. The 8q24 breakpoints clustered within the telomeric region of MYC in all TCR translocations, whereas in the non-TCR translocations the 8q24 breakpoints mapped both telomeric and centromeric to MYC (supplemental Figure 1) mirroring non-IGH MYC translocations in B-cell ALL.[13]

Here, non-TCR translocation partners were assessed in 4 cases. CDK6/7q21.2, rearranged in T-ALL with t(5;7)(q35;q21) and TLX3 overexpression,[14] was involved in cases 3 and 4. Hitherto-undescribed breakpoints involved 1q32.1, in case 1, within a long intergenic noncoding RNA, about 300 kb downstream of PTPRC and Xq25, in case 7, in a no-gene region 5 kb upstream of SH2D1 (supplemental Figure 2). Whatever the partner, MYC translo-cations resulted in MYC overexpression (Figure 1B). Remarkably, common to all cases was MYC relocation close to genes which are transcriptionally active in T lymphocytes (supplemental Figure 2).

In T-ALL, high MYC expression is mainly caused by molecular mechanisms acting at the transcriptional or posttranscriptional level.[15] In this study, we have shown that other genes/regions besides TCR may be involved in MYC translocations and that the incidence of MYC translocations in T-ALL is higher than previously reported.

Genetic profile of T-ALL with MYC translocations

Similar to other type B abnormalities, MYC translocations were not seen as isolated changes. In-depth molecular-cytogenetic character-ization revealed from 2 to 9 abnormalities per case (median, 3.7) (Table 1; supplemental Table 2). T-ALL with MYC translocations clustered within the TAL/LMO category (Pearson x^2, P 5 .018) (Figure 1C). Complete or partial trisomies of chromosomes 6 (3 of 12, 25%) (x^2, P , 0,001) and 7 (3 of 12, 25%) (x^2, P , .001) were significantly associated with MYC translocations and occurred together in all cases (2, 7, and 11 from Table 1). Other cooccurring abnormalities were CDKN2A/B deletions ($CDKN2AB^{del}$) (75%) and PTEN inactivation, resulting from deletion or mutation ($PTEN^{del/mut}$) (58%). Similar results were found in the MOLT-16 and SKW-3/KE-37 cell lines with t(8;14)(q24;q11)/TCRAD-MYC. In fact, they both carry SIL-TAL1 and/or LMO2 translocations as primary abnormalities, and $CDKN2AB^{del}$ and $PTEN^{del/mut}$ as addi-tional hits (supplemental Table 3). PTEN inactivation in primary samples as well as cell lines reflect results from experimental mouse models, which have shown that c-Myc rearrangements and $Pten^{del}$ exert a synergistic effect in the development of T-ALL, appearing to replace the function of Notch1.[8,16] Interestingly, $PTEN^{del/mut}$ and NOTCH1 mutations were mutually exclusive in our cases, confirming that they arise in different T-ALL subgroups.[17] In a unique TLX1-positive case (no. 12), the MYC translocation was associated with PTPN2 loss. The 2 PTEN- and PTPN2-negative regulators of PI3K/ AKT signaling[18] were inactive in ;65% of our cases, suggesting that constitutive PI3K/AKT pathway activation is a critical synergis-tic hit in this T-ALL subgroup.

MYC translocations identify a subgroup within the TAL/LMO category

Within the set of 51 pediatric patients with TAL/LMO-positive T-ALL, the 6 with MYC translocations belonged to the group with the highest MYC expression, defined as the fourth quartile (Q4) based on MYC expression. Supervised gene expression profiling analysis of the Q4 group showed that patients with and those without MYC translocations clustered separately (Figure 1D). A Shrinkage t test revealed 148 genes differently expressed between the 2 groups (supplemental Table 4). Namely, 77 were significantly upregulated and 71 genes downregulated (local false discovery rate ,0.05) in the

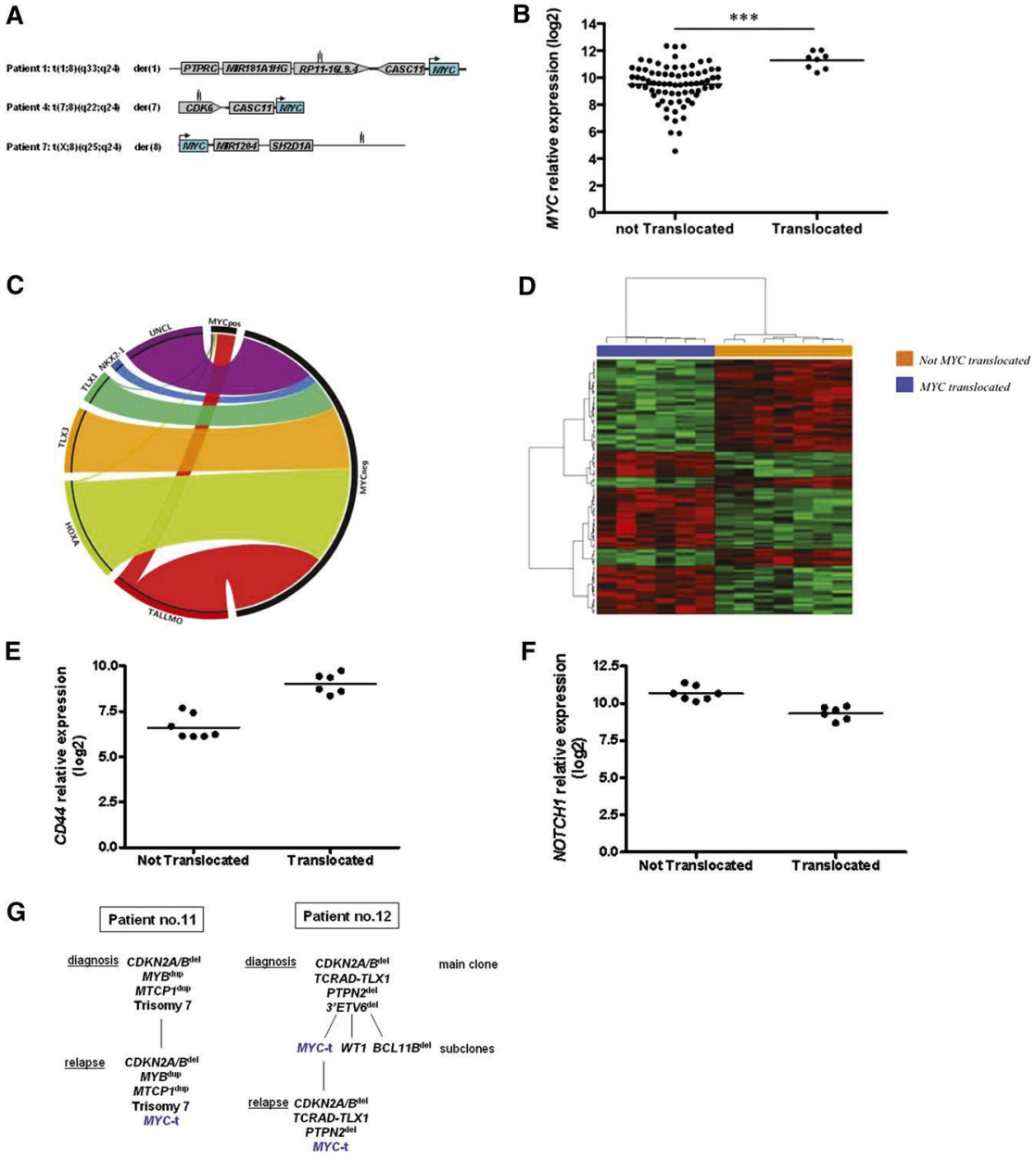

Figure 1. (A) Non-TCR partners of 3 cases of T-ALL (nos. 1, 4, and 7 from Table 1) with MYC translocations. Mapping of superenhancers at 1q32, 7q21, and Xq25 were indicated with 3 vertical thin bars. (B) MYC expression in 83 cases of pediatric T-ALL and in 8 MYC translocation–positive T-ALL (nos. 1-4, 9-12 from Table 1). Cases with translocations had a significantly higher MYC expression. (C) Circos plot shows distribution of MYC translocations according to genetic categories. MYC translocation–positive T-ALL clustered into the TAL/LMO category; (D) Supervised gene expression profiling analysis of 13 TAL/LMO-positive T-ALL with high MYC expression at diagnosis (Q4): 6 cases with MYC translocations (nos. 1-4, 9, 10; Table 1) clustered together and separated from the 7 cases without. (E) Q4 TAL/LMO-positive T-ALL: CD44 expression was higher in T-ALL cases with MYC translocation compared with cases without. (F) NOTCH1 expression was significantly lower in cases with MYC translocations compared with cases without. (G) Longitudinal FISH studies in 2 cases: in case no. 11 the clone with MYC translocation was not detected at diagnosis but only at relapse (left); in case no. 12, the small subclone (;8%) with the MYC translocation present at diagnosis was found in 100% of leukemic blasts at relapse. Q4, fourth quartile.

group with MYC translocations compared with the group without. Specifically, a .1.3-fold change in CD44 expression was observed in patients with MYC translocations, whereas NOTCH1 and genes associated with NOTCH1 activation (PTCRA, NOTCH3, HES4, and CR2) were significantly downregulated (Figure 1E-F). In support of these results, gene set enrichment analysis confirmed enrichment of genes in the NOTCH1 pathway in the group without MYC translocations (q value 5 0.06; NES, 1.71) (supplemental

Figures 3 and 4A). Gene set enrichment analysis further indicated significant enrichment of cell death and apoptosis pathway genes in patients harboring MYC translocations (supplemental Figure 4B-C).

MYC-positive subclones are associated with relapse/induction failure

In case 12 (Table 1), paired diagnostic and relapse bone marrow samples showed that the size of the subclone with MYC translocations increased at relapse, rising from 8% to 100%, whereas other abnormalities, which were present either in the main clone, that is, $ETV6^{del}$, or in diverse subclones, such as $WT1^{del}$ and $BCL11B^{del}$, disappeared at relapse (Figure 1G). These findings are in line with results from xenograft models[19] which showed that MYC confers a proliferative advantage and resistance to drug toxicity. It is noteworthy that in mice c-Myc plays a crucial role in maintenance and self-renewal of leukemia-initiating cells, which are thought to be resistant to chemotherapy and mediate relapse.[11] In case 11, the MYC translocation, present at relapse, was not detected at diagnosis, implicating that it was acquired during disease progression (Figure 1G). Taken together, these data suggest that identification and possible eradication of small MYC-positive subclones at diagnosis and/or during the early stages of treatment may assist in prevention of disease progression. Notably, MYC translocations were found in subclones of variable size (range, 8%-62%) in 4 additional cases (Table 1).

Clinical and hematologic characteristic of T-ALL with MYC translocations

MYC translocation–positive T-ALL is characterized by leukocytosis and cortical/mature differentiation arrest in the majority of cases. It was not possible to evaluate the prognostic implications of MYC translocations in this retrospective study including children and adults belonging to different treatment protocols. However, poor prognostic markers, such as high CD44 expres-sion and PTEN inactivation, appeared to be strongly associated with this leukemia subgroup.[20-23] Moreover, although determi-nation of minimal residual disease, the most powerful criteria used for risk stratification of pediatric ALL, classified case 2 into the standard-risk group, this patient failed induction therapy and died in disease. Similar to B-lineage ALL and acute myeloid leukemia,[24,25] in which disease relapse has been related to minor leukemic subclones rather than to the predominant clone at diagnosis, subclones with MYC translocations in T-ALL may be more resistant to therapy and thus sustain relapse.

Acknowledgments

The authors thank Drs Francesca Grillo and Maddalena Paganin for mutational analysis in selected patients belonging to the Associazione Italiana Emato-Oncologia Pediatrica (AIEOP) protocol, Dr Giovanni Roti for providing cell lines, and Drs Renato Bassan and Cristina Morerio for providing biological samples.

C. Mecucci is supported by Fondo per gli Investimenti della Ricerca di Base (FIRB 2011 RBAP11TF7Z_005), Associazione Italiana per la Ricerca sul Cancro (AIRC IG 11512), and Fondazione Cassa di Risparmio di Perugia (Cod. 2012.0108.021 Ricerca Scientifica e Tecnologica). G.t.K. is supported by Fondazione Cariparo Progetto d'Eccellenza.

Authorship

Contribution: R.L.S. and C. Mecucci conceived and designed the study; C.S., C.J.H., A.L., G.C., S.C., and G. Basso provided study materials or patient samples; C. Matteucci and A.G.L.F. provided mutational analyses; R.L.S., C.B., G. Barba, V.P., G.t.K., and C. Mecucci ana-lyzed and interpreted data; R.L.S. and C. Mecucci wrote the manuscript; and all authors gave final approval of the manuscript.

Conflict-of-interest disclosure: The authors declare no competing financial interests.

Correspondence: Cristina Mecucci, Hematology Unit, Univer-sity of Perugia, Ospedale S.M. della Misericordia, 06156 Perugia, Italy; e-mail: cristina.mecucci@unipg.it.

References

1. Kleppe M, Lahortiga I, El Chaar T, et al. Deletion of the protein tyrosine phosphatase gene PTPN2 in T-cell acute lymphoblastic leukemia. Nat Genet. 2010;42(6):530-535.
2. Silva A, Yunes JA, Cardoso BA, et al. PTEN posttranslational inactivation and hyperactivation of the PI3K/Akt pathway sustain primary T cell leukemia viability. J Clin Investig. 2008;118(11):3762-3774.
3. Zuurbier L, Homminga I, Calvert V, et al. NOTCH1 and/or FBXW7 mutations predict for initial good prednisone response but not for improved outcome in pediatric T-cell acute lymphoblastic leukemia patients treated on DCOG or COALL protocols. Leukemia. 2010;24(12):2014-2022.
4. Wong GW, Knowles GC, Mak TW, Ferrando AA, Zun¨¨iga-Pflucker¨ JC. HES1 opposes a PTEN-dependent check on survival, differentiation, and proliferation of TCRb-selected mouse thymocytes. Blood. 2012;120(7):1439-1448.
5. Guo W, Lasky JL, Chang CJ, et al. Multi-genetic events collaboratively contribute to Pten-null leukaemia stem-cell formation. Nature. 2008; 453(7194):529-533.
6. Langenau DM, Traver D, Ferrando AA, et al. Myc-induced T cell leukemia in transgenic zebrafish. Science. 2003;299(5608):887-890.
7. Gutierrez A, Grebliunaite R, Feng H, et al. Pten mediates Myc oncogene dependence in a conditional zebrafish model of T cell acute lymphoblastic leukemia. J Exp Med. 2011;208(8): 1595-1603.
8. Smith DP, Bath ML, Metcalf D, Harris AW, Cory S. MYC levels govern hematopoietic tumor type and latency in transgenic mice. Blood. 2006;108(2): 653-661.
9. Filippakopoulos P, Qi J, Picaud S, et al. Selective inhibition of BET bromodomains. Nature. 2010; 468(7327):1067-1073.
10. King B, Trimarchi T, Reavie L, et al. The ubiquitin ligase FBXW7 modulates leukemia-initiating cell activity by regulating MYC stability. Cell. 2013; 153(7):1552-1566.
11. Roderick JE, Tesell J, Shultz LD, et al. c-Myc inhibition prevents leukemia initiation in mice and impairs the growth of relapsed and induction failure pediatric T-ALL cells. Blood. 2014;123(7): 1040-1050.
12. La Starza R, Lettieri A, Pierini V, et al. Linking genomic lesions with minimal residual disease improves prognostic stratification in children with T-cell acute lymphoblastic leukaemia. Leuk Res. 2013;37(8):928-935.
13. Bertrand P, Bastard C, Maingonnat C, et al. Mapping of MYC breakpoints in 8q24 rearrangements involving non-immunoglobulin partners in B-cell lymphomas. Leukemia. 2007; 21(3):515-523.
14. Su XY, Busson M, Della Valle V, et al. Various types of rearrangements target TLX3 locus in T-cell acute lymphoblastic leukemia. Genes Chromosomes Cancer. 2004;41(3):243-249.
15. Bonnet M, Loosveld M, Montpellier B, et al. Posttranscriptional deregulation of MYC via PTEN constitutes a major alternative pathway of MYC activation in T-cell acute lymphoblastic leukemia. Blood. 2011;117(24):6650-6659.
16. Kaveri D, Kastner P, Dembel´e´ D, Nerlov C, Chan S, Kirstetter P. b-Catenin activation synergizes with Pten loss and Myc overexpression in Notch-independent T-ALL. Blood. 2013;122(5):694-704.
17. Zuurbier L, Petricoin EF III, Vuerhard MJ, et al. The significance of PTEN and AKT aberrations in pediatric T-cell acute lymphoblastic leukemia. Haematologica. 2012;97(9):1405-1413.
18. Omerovic J, Clague MJ, Prior IA. Phosphatome profiling reveals PTPN2, PTPRJ and PTEN as potent negative regulators of PKB/Akt activation

in Ras-mutated cancer cells. Biochem J. 2010; 426(1):65-72.

19. Clappier E, Gerby B, Sigaux F, et al. Clonal selection in xenografted human T cell acute lymphoblastic leukemia recapitulates gain of malignancy at relapse. J Exp Med. 2011;208(4): 653-661.

20. Vaskova M, Mejstrikova E, Kalina T, et al. Transfer of genomics information to flow cytometry: expression of CD27 and CD44 discriminates subtypes of acute lymphoblastic leukemia. Leukemia. 2005;19(5):876-878.

21. Cario G, Stanulla M, Fine BM, et al. Distinct gene expression profiles determine molecular treatment response in childhood acute lymphoblastic leukemia. Blood. 2005;105(2): 821-826.

22. Coustan-Smith E, Song G, Clark C, et al. New markers for minimal residual disease detection in acute lymphoblastic leukemia. Blood. 2011; 117(23):6267-6276.

23. Trinquand A, Tanguy-Schmidt A, Ben Abdelali R, et al. Toward a NOTCH1/FBXW7/RAS/ PTEN-based oncogenetic risk classification of adult T-cell acute lymphoblastic leukemia: a Group for Research in Adult Acute Lymphoblastic Leukemia study. J Clin Oncol. 2013;31(34):4333-4342.

24. Mullighan CG, Phillips LA, Su X, et al. Genomic analysis of the clonal origins of relapsed acute lymphoblastic leukemia. Science. 2008; 322(5906):1377-1380.

25. Ding L, Ley TJ, Larson DE, et al. Clonal evolution in relapsed acute myeloid leukaemia revealed by whole-genome sequencing. Nature. 2012; 481(7382):506-510.

blood
2014 124: 3577-3582
doi:10.1182/blood-2014-06-578856 originally published online September 30, 2014

Genetic profile of T-cell acute lymphoblastic leukemias with *MYC* translocations

Roberta La Starza, Chiara Borga, Gianluca Barba, Valentina Pierini, Claire Schwab, Caterina Matteucci, Anair G. Lema Fernandez, Anna Leszl, Gianni Cazzaniga, Sabina Chiaretti, Giuseppe Basso, Christine J. Harrison, Geertruy te Kronnie and Cristina Mecucci

Blood (print ISSN 0006-4971, online ISSN 1528-0020), is published weekly by the American Society of Hematology, 2021 L St, NW, Suite 900, Washington DC 20036.

Poster dic(1;7)PDF.pdf

Genetic and Epigenetic Landscape of dic(1;7)(q10;p10) in AML/MDS

Lema Fernandez AG[1], Crescenzi B[1], Pierini V[1], Barba G[1], Pellanera F[1], Di Giacomo D[1], Piazza R[2], Di Battista V[1], Adelman E[3], Figueroa ME[3], Mecucci C[1]

[1]Department of Medicine, Hematology and Bone Marrow Transplantation Unit, University of Perugia, Italy; [2]Hematology, School of Medicine and Surgery, University of Milano Bicocca, Italy; [3] Department of Pathology, University of Michigan School of Medicine, Ann Arbor, Michigan 48109, USA (Currently at Department of Human Genetics, University of Miami Miller School of Medicine, Miami, FL, USA).

BACKGROUND

Dic(1;7)(q10;p10) is an unbalanced translocation characterized by trisomy 1q and monosomy 7q, which has been related to secondary or therapy related MDS or AML in 50% of cases. It is classified as good risk karyotypic variant in the IPSS-R and recent studies argues that dic(1;7)(q10;p10) MDS has longer overall survival and a better response to bone marrow transplant compared to -7/del(7q). Cytogenetically the dic(1;7) may occur as isolated aberration or within complex karyotypes. Recurrent additional cytogenetic abnormalities are mostly trisomy 8 and del(20q). Due to the absence of genes within the centromeric region, no specific molecular targets have been identified.

MATERIALS AND METHODS

Table 1. Hematological and cytogenetic features of all patients from the three cohorts. Previously primary tumor indicated between brackets. M: males, F: Female, DIC: dicentric, CTL: control, t-MDS: Therapy-related Myelodysplastic Syndrome, AML: Acute Myeloid Leukemia, ET: Essential Thrombocythemia, sMDS: secondary Myelodysplastic Syndrome, RCMD: Refractory Cytopenia with Multilineage Dysplasia, NH-L: Non-Hodgkin Lymphoma, RAEB: Refractory Anemia with Excess Blasts. mERRBS was performed on all samples except on CTL 2, CTL 6, t-MDS 2 and t-MDS 6 due to quality control. RN A-seq analysis was not performed on CTL1 1.

We have analized 5 AML/MDS patients with dic(1;7)(q10;p10) at karyotype, against a cohort of 5 therapy-related MDS (t-MDS) to define their genetic and epigenetic landscape. As controls we used six cases with peripheral non-neoplastic cytopenia, normal bone marrow and normal karyotype(Table 1).

We performed i) karyotype and Fluorescent In Situ Hybridization (FISH), ii) Single Nucleotide Polymorphism-Array (SNPa) using CytoScan HD Affymetrix platform for inferring copy numbers and loss-of-heterozygosity, iii) Whole Exome sequencing (WES) to define mutational landscape iv) Gene expression profile and Differential Exon Usage using RNAseq, vi) and Multiplex Enhanced Reduced Representation Bisulfite Sequencing (mERRBS) in order to investigate methylation signature.

RESULTS

FISH and SNPa confirmed conventional cytogenetic results

Vysis D1Z5 and D7Z1 probes combined in double color FISH (Figure 1B-C) generated a fusion signal at the centromeric region of dic(1;7) in all five dicentric cases. Moreover, pE25.a (D1Z7) gave a signal on dic(1;7) weaker than normal chromosomes 1, confirming data published by Wang

L et al. (data not shown), who assigned the breakpoint between D1Z7 and D1S3445. Copy number alterations (CNAs) profiles confirmed 1q trisomy and 7q monosomy (Figure 1D). No cnLOH or karyotypically cryptic CNAs were found: 2/5 cases showed 1q gain and 7q loss as unique genetic imbalance, while the remaining three cases showed additional events as seen at conventional karyotype (Figure 1D).

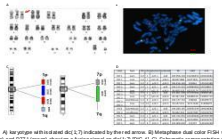

Figure 1. A) karyotype with isolated dic(1;7) indicated by the red arrow. B) Metaphase dual color FISH with D1Z5 (orange) and D7Z1 (green) showing a fusion signal on dic(1;7) [DIC 4]. C). Schematic representation with relative orientation of genomic FISH probes at centromere.D). Copy number alterations detected by SNP arrays in all five dicentric cases.

Mutational landscape of dic(1;7) identified private gene variations

In two cases WES on paired samples was performed, using DNA extracted from bone marrow derived fibroblasts as control. The somatic mutations on DIC 2 and 5 somatic mutations on DIC 5 (Table 2).

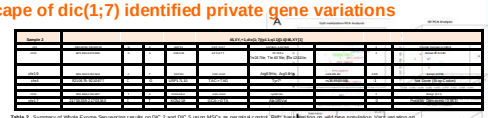

Table 2. Summary of Whole Exome Sequencing results on DIC 2 and DIC 5 using MSCs as germinal control. PMT: Base substitution. Var: Variation on our samples. Var Type= indicates variation type as single nucleotide Variation (SNV) or deletion. MAF= minor allele frequency.

dic(1;7) is characterized by a downregulated signature

PCA analysis of all filtered counts from RNAseq clearly separated the dicentrics from all other group of cases included in our analysis (Figure 2A). Gene expression profile, using RNAseq, defined a specific downregulation signature in dic(1;7) compared to both normal controls and t-MDS (Figure 2B). We performed Positional Gene Enrichment Analysis (PGE) to test if a given chromosomal region was enriched in the query set of DEG. With respect to the comparison DIC/CTL, among 138 PGE enriched regions we first examined the gene dosage effect due to chromosome 1q and 7q unbalances (Figure 2C).

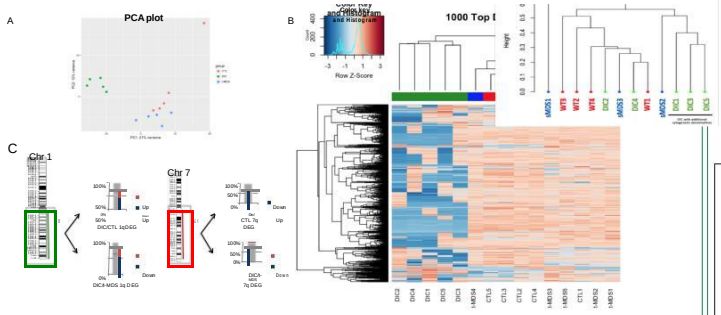

Figure 2. A) Principal Component Analysis (PCA) plot of all filtered counts from RNAseq using DESeq2. Observe that the DIC and all other samples are separated along dimension 2 (the y axis). B) Heatmap representing the top 1000 differentially expressed genes across all three groups of samples. The heatmap colors reflect values representing the degree of expression from low to high as blue to red, respectively, as shown on the scale at the top-left hand side of the figure. Reds- Control samples; Blues- t-MDS samples; Greens- Dicentric samples. C) Chromosome view of regions significantly enriched in genes differentially expressed using PGE on 1q (right). Percentage of DEG distribution within down- and up- regulated genes in DIC compare to controls (DIC/CTL, up-right) and to t-MDSs (DIC/t-MDS, bottom right). Chromosome view of regions significantly enriched in genes differentially expressed using PGE on 7q (right). Percentage of DEG distribution within down- and up- regulated genes in DIC compare to controls (DIC/CTL, up-right) and to t-MDSs (DIC/t-MDS, bottom right).

mERRBS: DMRs enriched in non-promoter regions

Unsupervised analysis of DNA methylation by mERRBS using hierarchical clustering, separated DIC_nonIso from DIC_Iso (Figure 3). When we looked at distribution within hyper- and hypo- methylated DMRs, DIC_isolated displayed prevalent hypomethylation and seemed more similar to normal controls (Figure 4 middle). Non-isolated dicentrics, with a prevalent hypermethylation, resembled t-MDS (Figure 4 bottom). Methylation changes on dicentric samples were enriched in non-promoter regions compared to both CTL and t-MDS (Figure 5).

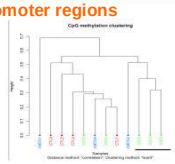

Figure 3. Unsupervised analysis of DNA methylation using hierarchical clustering shows a clustering dendrogram where samples that are most similar separated by larger numbers of branch points. Red= Control samples; Blue= t-MDS; Green= DIC.

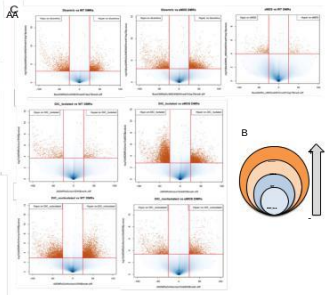

Figure 4. A)Volcano plots of all DMRs underlie the distribution of DMRs between each group. The plot shows the methylation difference on percentage (x-axis) with respect to the −log10 of the adjusted p-value for each DMR. Thresholds are shown as red lines: red vertical lines indicate methylation difference cut-off (-20% and + 20%), red horizontal line indicates statistical significant cut-off (q-value<= 0.1). Significantly different hypo- and hyper-DMRs are highlighted as red dots. **On the top:** DIC vs. CTL (left), vs. t-MDS (middle) and t-MDS/CTL (right). **On the middle:** DIC_isolated vs. CTL(left) and t-MDS (right); **on the bottom**: DIC_non-isolated vs. CTL (left) and t-MDS (right). **B)** Schematic representation of methylation gradient considering all comparisons.

Figure 5. A) Distribution of hypo- and hyper-methylated DMRs on promoter regions for each comparison. **B)** Distribution of annotated DMRs on genomic regions for each group. We used methylKit package on R to annotate to hg19 previously identified DMRs on methylSig. **C)** Statistical results for Binomial enrichment/depletion test conducts on R for annotated DMRs. For all tests , we used 95 percent confidence interval and percentage of background annotation for each category (promoters, exons, introns, intergenic) as true probability of success.

dic(1;7) Epigenetic Hallmark: Hypermethylation of Intronic Enhancers

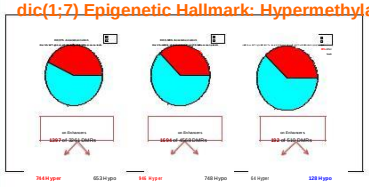

647 (46.3%) introns 780 (46%) introns 93 (48.4%) introns

Figure 6. Pie chart illustrates enrichment on DMRs on enhancer regions. If-left: final, enhancers; light blue: others, non-enhancers.

Hypermethylation of enhancer DMRs was the prevalent event on DIC samples. By contrast, comparing t-MDS against normal controls, the majority of differentially methylated enhancers were hypomethylated (Figure 6). Moreover, in all cases localized at intronic regions. Taken together, the results indicate that hypermethylation of intronic enhancers is an epigenetic hallmark

CONCLUSIONS

dic(1;7) in AML/MDS is correlated to a specific signature of downregulated genes associated to 27 pathways (data not shown).
Hypermethylation of intronic enhancers is an epigenetic hallmark of dicentrics, independently from additional aberrations at the karyotype.

Involvement of a member of the histone cluster 1 at 6p21 in NUP98-positive MDS:AML.pdf

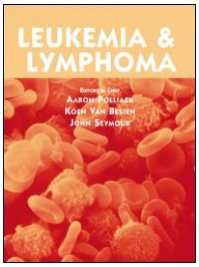

Leukemia & Lymphoma

ISSN: 1042-8194 (Print) 1029-2403 (Online) Journal homepage: http://www.tandfonline.com/loi/ilal20

Involvement of a member of the histone cluster 1 at 6p21 in NUP98-positive MDS/AML

Danika Di Giacomo, Valentina Pierini, Roberta La Starza, Erika Borlenghi, Fabrizia Pellanera, Anair Graciela Lema Fernandez, Daniela Bellotti, Cinzia Lamorgese, Giuseppe Rossi & Cristina Mecucci

To cite this article: Danika Di Giacomo, Valentina Pierini, Roberta La Starza, Erika Borlenghi, Fabrizia Pellanera, Anair Graciela Lema Fernandez, Daniela Bellotti, Cinzia Lamorgese, Giuseppe Rossi & Cristina Mecucci (2017): Involvement of a member of the histone cluster 1 at 6p21 in NUP98-positive MDS/AML, Leukemia & Lymphoma, DOI: 10.1080/10428194.2017.1312375

To link to this article: http://dx.doi.org/10.1080/10428194.2017.1312375

LEUKEMIA & LYMPHOMA, 2017
http://dx.doi.org/10.1080/10428194.2017.1312375

Taylor & Francis
Taylor & Francis Group

LETTER TO THE EDITOR

Involvement of a member of the histone cluster 1 at 6p21 in NUP98-positive MDS/AML

Danika Di Giacomo[a], Valentina Pierini[b], Roberta La Starza[a], Erika Borlenghi[b], Fabrizia Pellanera[a], Anair Graciela Lema Fernandez[a], Daniela Bellotti[b], Cinzia Lamorgese[b], Giuseppe Rossi[b] and Cristina Mecucci[a]

[a]Molecular Medicine Laboratory, Department of Medicine, CREO, University of Perugia, Perugia, Italy; [b]Department of Hematology, Spedali Civili, Brescia, Italy

ARTICLE HISTORY Received 17 December 2016; revised 7 February 2017; accepted 19 March 2017

HIST1H1T, one of the eleven members of the histone H1 gene family (H1A, H1B, H1C, H1D, H1E, H1T, H1F0, H1FNT, H1FOO, HILS1 and H1FX), is considered a germinal variant as it is specifically expressed in early meiotic spermato-cytes until late spermatids in mammals [1]. Information on the involvement of this family in malignancy are still scarce. Members of the histone cluster 1 have never been reported in myeloid malignancies, so far, though HIST1H1B, C, D and E mutations were observed in chronic lymphocytic leukemia (CLL), diffuse large B-cell lymphoma (DLBCL) and follicular lymphoma (FL) [2]. A deregulation of HIST1H1T was found in carcinomas of prostate, head and neck, bladder and endometrium [2]. In addition, a pathogenetic role has been attributed to the rs2051542 HIST1H1T polymorphism because of its association with lung carcinoma [3].

We here provide the first evidence of HIST1H1T gene involvement in human myeloid leukemia as a new partner of the promiscuous NUP98 gene.

In 2012, a 38-year-old Jamaican woman with adult T-cell leukaemia lymphoma (ATLL) $HTLV^b$ was treated with combination chemotherapy (VCAP-AMO-VECP, six cycles), obtaining complete remission. Maintenance ther-apy was a-interferon (3MU) and zidovudine (600 mg/day) for 10 months. Three years later, in April 2015, the patient developed secondary myelodysplastic syndrome (MDS), with trilinear cytopenia and macrocytosis (WBC 2.67 10^9/l, PMN 18%, Hb 93 g/l, PLT 80 10^9/l, MCV 121 fl). Bone marrow aspirate showed RAEB1 with trilin-ear dysplasia and 7% blasts. Karyotype was 46,XX,t(6;11)(p21;p15)[10]/46,XX[12] (Figure 1(A)). No ther-apy was administered. In August 2015, patient developed frank AML with 48% bone marrow blasts CD34 , $CD117^{\pm}$, $CD33^b$, $CD13^b$, CD14 , CD16 and $HLA\text{-}DR^{\pm}$. Karyotypic evolution was observed: 47,XX,t(6;11)(p21;p15),þ8[13]/46,XX,t(6;11)(p21;p15) [7]. Mutational analysis (primers in Supplementary Table 2) showed FLT3 mutation (D835H) at the AML diagnosis, but not at the MDS phase. No other mutations were found in ASXL1, RUNX1, SETBP1, SRSF2, TET2, EZH2, DNMT3A, IDH1-2, SF3B1, JAK2, HRAS, WT1, KIT, NRAS and KRAS genes. Induction therapy used idarubicin 12 mg/m^2/day, 3 days, cytosine arabinoside 100 mg/m^2/dayX2, 7 days, VP16 100 mg/m^2/day, 5 days. Consolidation therapy was idarubicin (10 mg/m^2/day, 2 days), cytosine arabinoside (100 mg/m^2/day 2, 7 days) followed by cytarabine (1 g/m^2/day 2, 4 days). Complete remission was obtained and in February 2016 the patient underwent successful syngeneic peripheral blood stem-cell transplantation from her HLA-identical twin after con-ditioning with busulphan and fludarabine.

To characterize the t(6;11)(p21;p15) chromosomal translocation, FISH was performed on bone marrow cells. At least 200 interphase nuclei and/or seven abnormal metaphases were analyzed in each experiment. A break-apart FISH assay with RP11-348A20 (NUP98 exons 1–27) and CTD-3234F16 (NUP98 exons 13–32) indicated the 11p15 breakpoint fell within NUP98 exons 1–13 in 75% of cells at AML diagnosis, with RP11-348A20 showing three hybridization signals: on normal 11, on derivative 11 and on derivative 6. Homebrew BAC and PAC clones (Supplementary Table 1) investigated the 6p breakpoint, which was identified within clone RP1-221C16 at 6p22.2. Figure 1(B) shows the reciprocal translocation in a double fusion experiment. RP1-221C16 clone encompasses the 3^0-end of the hemochromatosis gene (HFE) and H4C, H1T, H2BC, H2AC, H1E, H2BD, H2BE and H4D genes, members of histone gene cluster 1, on chromosome 6p21. The hybridization pattern indicated that the breakpoint local-ized to the most telomeric RP1-221C16 region, where two putative partner genes, HIST1H1T and HIST1H2BC, were mapped with appropriate centromere–telomere orientation. Total RNA was extracted by Trizol reagent

CONTACT Cristina Mecucci cristina.mecucci@unipg.it Department of Hematology, Laboratory of Molecular Medicine, CREO, University of Perugia, Piazza Menghini 9, 06132 Perugia, Italy

Supplementary material available online here

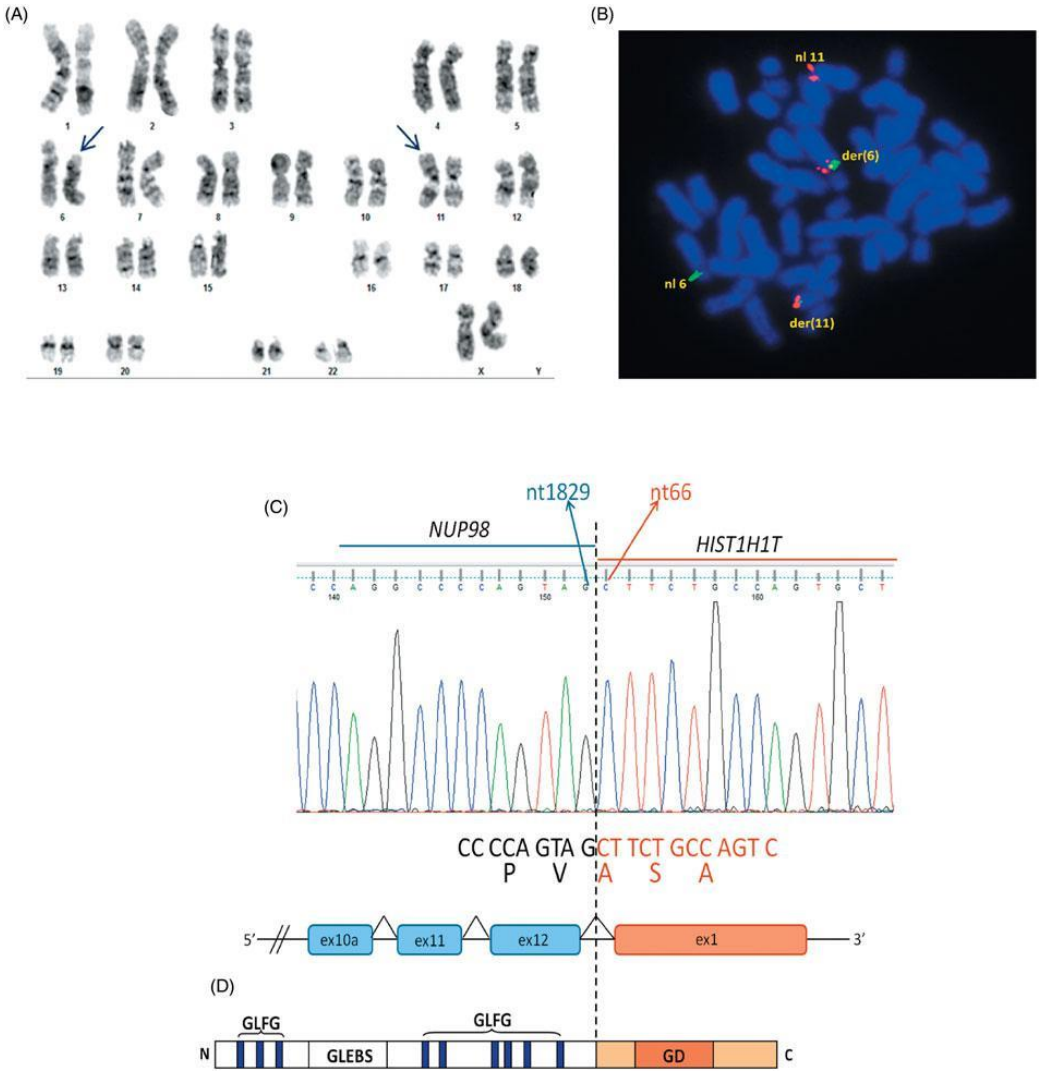

Figure 1. Molecular characterization of the new NUP98/HIST1H1T fusion. (A) A representative G-banded karyotype from the patient's bone marrow cells at MDS onset showing 46,XX,t(6;11)(p21;p15). Arrows indicate abnormal chromosomes 6p and 11p. (B) Double color double fusion FISH assay (RP11-348A20/11p15, Spectrum Orange and RP1-221C16/6p22, Spectrum Green, Vysis, Abbott Molecular, Illinois, U.S.A) showed two fusion signals on der(6) and der(11); nl ¼ normal. (C) Direct sequencing showed an in-frame NUP98/HIST1H1T fusion joining nucleotide 1829 of NUP98 (exon 12) to nucleotide 66 of HIST1H1T (exon 1). Sequence numbers refer to GenBank accession NM_00139131.3 for NUP98 and NM_005323.3 for HIST1H1T. nt, nucleotide; ex, exon. (D) The hypothetical fusion protein retained all NUP98 39 GLFG-repeats at the N-terminus and the HIST1H1T Globular Domain at the C-terminus. GLEBS, Gle2-binding sequence; GD, globular domain.

(Invitrogen, Carlsbad, CA) and retrotranscribed with Thermoscript (Invitrogen) according to the manufacturer's protocol. Nested-PCR was performed using primers NUP98_737F 5^0-AGTCACTAGAGGAACTTCG-3^0 and HIST1H1T_691R 5^0-CAAATTGGCCTCCCGGAAAG-3^0 in the first amplification, NUP98_1083F 5^0-GGTAATACCAGCAC CATAGGACAG-3^0 and HIST1H1T_551R 5^0-CCTTTCTCCCGC TCCTAACA-3^0 in the second (NUP98: NM_00139131.3, HIST1H1T: NM_005323.3). An amplification product of 988 bp was cloned into the pGEM-Teasy vector (Promega, Madison, WI) and sequenced by Sanger's method (ABI 3500 Genetic Analyzer, Applyed Biosystems, Foster City, CA). An in-frame fusion was detected between nt 1829 (exon 12) of NUP98 and nt 66 (into exon 1) of HIST1H1T (Figure 1(C)).

As in individual cases more than one transcript was originated from fusions between NUP98 and different genes belonging to the same homeobox cluster

(HOXA/7p15, HOXC/12q13 or HOXD/2q35), we tested the hypothesis that HIST1H2BC, the other putative partner of this non-homeobox cluster, was also involved. However, we did not identify any additional fusions by RT-PCR (data not shown) (primers listed in Supplementary Table 2).

Similar to other fusions, NUP98 here retained its N-terminal GLFG-repeats, which are essential for leukemic transformation [4]. The in-frame NUP98/HIST1H1T fusion hypothetically produced a protein retaining the NUP98 Gle2-binding sequence (GLEBS) and all the 39 GLFG-repeats (Figure 1(D)), as well as the HIST1H1T globular domain (GD) and the C-terminal region, which are both involved in DNA binding and nucleosome compaction [5]. Compared with somatic H1 variants, HIST1H1T is known to compact chromatin to a lesser extent and binds DNA with lower affinity, thus making chromatin prone to recombination and accessible to transcription factors [1]. Altogether these data suggest that NUP98/HIST1H1T pro-tein behaved as chromatin-modifying factor. Moreover, since HIST1H1T expression has never been reported in normal hematopoietic cells [6], HIST1H1T transcription in leukemic cells likely occurred under the control of the NUP98 promoter.

NUP98 positive acute myeloid leukemia originates from multiple chromosomal translocations involving homeobox and non-homeobox genes, and are typically associated with a poor clinical outcome [4]. Only nine cases of MDS, six in adults and three in pediatric age, have been described so far [7–9].

Here for the first time, we reported an isolated t(6;11)(p21;p15) chromosomal translocation involving NUP98 in a treatment-induced MDS case. Similar to previ-ously published cases with available follow-ups [9], dis-ease progressed to AML in <6 months, suggesting that NUP98 translocations are hallmarks of AML, despite presentation as MDS. Our patient highlights the poor prognosis of NUP98-positive AML and the role of bone marrow transplantation to cure this high-risk leukemias [10,11].

Acknowledgements

Authors thank Mrs. Pacchiarini Angela, Dr. Silvio Canino for morphological analyzes and Dr G.A. Boyd for English editing.

D.D.G. performed molecular analysis, analyzed the data and wrote the article; V.P. and R.L.S. performed FISH experi-ments; E.B. and G.R. provided clinical–hematological data; F.P. and A.G.L.F. performed mutational analysis; D.B. and C.L. performed cytogenetic studies; and C.M. supervised the study, analyzed the data and wrote the article. All authors approved the final article.

Ethical approval has been obtained for the protocol “In-depth genomic characterization of leukemia to provide new tools for personalized diagnosis and disease monitoring” (AIRC 2011–2014) from the University Bioethics Committee of the University of Perugia (Prot. 1.X.2011).

Potential conflict of interest: Disclosure forms provided by the authors are available with the full text of this article online at http://dx.doi.org/10.1080/10428194.2017.1312375.

Funding

This work was supported by Associazione Italiana per la Ricerca sul Cancro (AIRC IG-15525), Sergio Luciani Association, Fabriano, Italy, Fondazione Cassa di Risparmio Perugia (2016.0113.021 Ricerca Scientifica e Tecnologica).

References

[1] Perez-Montero S, Carbonell A, Azorın F. Germline-specific H1 variants: the “sexy” linker histones. Chromosoma. 2016;125:1–13.

[2] Scaffidi P. Histone H1 alterations in cancer. Biochim Biophys Acta. 2016;1859:533–539.

[3] Kim YI, Lee J, Choi YJ, et al. Proteogenomic study beyond chromosome 9: new insight into expressed variant proteome and transcriptome in human lung adenocarcinoma tissues. J Proteome Res. 2015;14:5007–5016.

[4] Gough SM, Slape CI, Aplan PD. NUP98 gene fusions and hematopoietic malignancies: common themes and new bio-logic insights. Blood. 2011;118:6247–6257.

[5] Bednar J, Hamiche A, Dimitrov S. H1-nucleosome interactions and their functional implications. Biochim Biophys Acta. 2016;1859:436–443.

[6] NCBI Unigene EST Profile. [cited 2017 Apr 10]. http://www.ncbi.nlm.nih.gov/UniGene/ESTProfileViewer.cgi?uglist¼Hs.533293

[7] Romana SP, Radford-Weiss I, Ben Abdelali R, et al. NUP98 rearrangements in hematopoietic malignancies: a study of the Groupe Francophone de Cytogenetique Hematologique. Leukemia. 2006;20:696–706.

[8] Soler G, Kaltenbach S, Dobbelstein S, et al. Identification of GSX2 and AF10 as NUP98 partner genes in myeloid malig-nancies. Blood Cancer J. 2013;3:e124.

[9] Crescenzi B, Nofrini V, Barba G, et al. NUP98/11p15 transloca-tions affect CD34þ cells in myeloid and T lymphoid leuke-mias. Leuk Res. 2015;39:769–772.

[10] Akiki S, Dyer SA, Grimwade D, et al. NUP98-NSD1 fusion in association with FLT3-ITD mutation identifies a prognostically relevant subgroup of pediatric acute myeloid leukemia patients suitable for monitoring by real time quantitative PCR. Genes Chromosomes Cancer. 2013;52:1053–1064.

[11] Ostronoff F, Othus M, Gerbing RB, et al. NUP98/NSD1 and FLT3/ITD coexpression is more prevalent in younger AML patients and leads to induction failure: a COG and SWOG report. Blood. 2014;124:2400–2407.

Hamilton_Certificate.pdf

HAMILTON LIFE SCIENCE ROBOTICS

HAMILTON Italia
Via Tadino, 52 • 20124 Milano • Italy
Phone +39 02 29533722 • Fax +39 02 29401778

HAMILTON THE MEASURE OF EXCELLENCE SM

Certificato di Partecipazione

Si certifica che

La Dr.ssa Lema Anair

Ha partecipato al Training introduttivo del software Venus 3 appartenente alla linea MicroLab STAR della Hamilton Robotics .

HAMILTON Life Scienze Robotics

Perugia, lì 24 Febbraio 2016

Application Specialist
Daniele Maldini

MiSeq_Certificate.pdf

illumina

Certificate of Completion

This certifies that:

Anair Lema

has successfully completed the training for:

MiSeq System

provided by Illumina, Inc.

Date: 17.03.2016 - 18.03.2016

Signed: Simone Cani

Simone Cani
FAS
Illumina, Inc.

GRC_Certificate.pdf

Gordon Research Conferences
frontiers of science

visit us on the web at http://www.grc.org

Certificate of Participation

04/29/2017

Anair Graciela Lema Fernandez
Universita degli Studi di Perugia
Centro Ricerche Emato-Oncologiche, Piazzale G. Menghini 9
Perugia, PG 06129
Italy

This is a certificate of participation for:
Conference: Cancer Genetics & Epigenetics
Dates: 04/23/2017 - 04/28/2017
Location: Renaissance Tuscany Il Ciocco in Lucca (Barga) Italy

This letter certifies your participation as a Poster Presenter at the Gordon Research Conference on Cancer Genetics & Epigenetics held 04/23/2017 - 04/28/2017 at Renaissance Tuscany Il Ciocco in Lucca (Barga) Italy.

Presented poster titled: Genetic and Epigenetic Landscape of Centromere Collision in dic(1;7)(q10;p10) in AML/MDS

Dr. Nancy Ryan Gray, President and Chief Executive Officer
Gordon Research Conferences

Corso di Citogenetica.pdf

ACCADEMIA NAZIONALE DI MEDICINA

Genova, 5 giugno 2017
Prot. N° 259/SL/ep

Gent. Dott.ssa
Anair Lema Fernandez
Perugia

Oggetto: Lettera di incarico ECM
Corso avanzato di citogenetica costituzionale e acquisita. VIII edizione
Roma, 14-15 settembre 2017
Responsabili Scientifici: Paola Grammatico, Orsetta Zuffardi

Gentile Dottoressa,

la ringraziamo per aver accettato l'invito delle proff. Paola Grammatico e Orsetta Zuffardi e le confermiamo l'incarico di relatore all'evento formativo in oggetto.

La preghiamo di prendere visione dei seguenti allegati e di inviarci la documentazione richiesta al più presto:

All_A_Programma preliminare
All_B_Scheda indicazioni normativa ECM, con modello autocertificazione conflitto d'interesse
All_C_Scheda autorizzazione utilizzo diapositive

Desideriamo informarla che sarà cura di Elida Pagni (tel. 010 83794225, pagni@accmed.org) contattarla successivamente per gli aspetti di gestione dell'evento formativo mentre la Segreteria Organizzativa di Forum Service la contatterà per l'organizzazione del suo viaggio e soggiorno.

Ringraziandola ancora per la collaborazione, restiamo a sua disposizione per qualsiasi informazione e con l'occasione porgiamo i nostri più cordiali saluti.

Stefania Ledda
Direttore Generale

All. n. 3

Firma leggibile per accettazione

_____

Riconoscimento personalità giuridica M.I.U.R. – D.M. 6 dicembre 1995 | Membro Federazione Europea delle Accademie di Medicina

GENOVA *(sede legale)* Via Martin Piaggio 17, 16122 | Tel. +39.010.837.94.1 | Fax +39.010.837.94.260
BOLOGNA Galleria Ugo Bassi 2, 40121 | Tel. +39.051.636.00.80 | Fax +39.051.0569.162
ROMA Viale Regina Elena 295, 00161 | Tel. +39.366.393.2004

www.accmed.org | info.anm@accmed.org | CF/PIVA IT04208241002 | REA GE – 482138

Università degli Studi di Perugia

Ce.Se.R.P. e OPBA

Si certifica che la Dott.ssa

ANAIR GRACIELA LEMAFERNANDEZ

Ha partecipato al Corso di Formazione per Attività Sperimentale in Vivo:
"CORRETTO APPROCCIO ALLA SPERIMENTAZIONE ANIMALE"
ed ha superato la verifica finale.

Perugia, 12-13-14 giugno 2017

Perugia, 20 giugno 2017

Il Responsabile del Corso
DIRETTORE del CENTRO SERVIZI per la RICERCA PRECLINICA
Dott. Paolo Mosci

CIB.pdf

CONSORZIO INTERUNIVERSITARIO BIOTECNOLOGIE

Direzione c/o Dip. di Scienze Biomediche – Sezione Chimica Biologica – Via Campi 287 – 41100 Modena Segreteria c/o Dip. di Biochimica e Biologia Molecolare – Via Corsari 46 – 44100 Ferrara Amministrazione c/o Area Science Park – Loc. Padriciano 99 – 34012 Trieste – Italy tel. 040 398979 – fax. 040 398990 – cib@lncib.it

---

Gent.ma Dott.ssa Lema Fernandez Anair Graciela
siamo lieti di comunicarLe che il Consorzio Interuniversitario Biotecnologie ha accolto la Sua richiesta di contributo per lo svolgimento di attività di formazione presso laboratori nazionali o stranieri.

Il contributo verra' erogato nella forma di rimborso delle spese effettuate. La Sua assegnazione prevede un rimborso delle spese fino a un massimo di
€ 1500 (vedi allegati)

E' previsto l'anticipo del 50% del contributo, inviando al recapito indicato il modello a1 che trovera' allegato alla presente.
L'ottenimento del saldo (fino a corresponsione dell'ammontare a Lei assegnato) e' vincolato all'invio di:

- modello a2 debitamente compilato e corredato delle giustificative di spesa in originale - sintetica descrizione delle attivita' svolte
- dichiarazione firmata dal responsabile scientifico del laboratorio ospite che certifichi la Sua effettiva permanenza.

Le ricordo che qualora il totale delle spese presentate non copra interamente l'importo assegnatoLe, l'erogazione sara' comunque corrispondente all'importo complessivo delle spese, NON al totale del contributo.

Qualora il totale delle spese inviate non sia sufficiente a coprire il 50% erogato in via anticipata, il CIB richiedera' la restituzione di quanto versato in eccedenza.

Il CIB puo' rimborsare le seguenti tipologie di spesa: viaggio, trasporti urbani ed extraurbani, alloggio, pasti.

NON verranno rimborsate spese di viaggio sostenute con auto propria ne' relativi rimborsi chilometrici.

Qualora le spese siano state sostenute in valuta straniera, il CIB utilizzera' il valore di cambio della giornata in cui verra' processata la pratica di liquidazione del rimborso.

La documentazione andra' inviata a:
Amministrazione CIB
Area Science Park
Localita' Padriciano 99 - 34149 Trieste

Le ricordo che le spese devono essere effettivamente sostenute e verranno rimborsate solamente con l'allegata giustificativa (ricevuta, scontrino, fattura o quant'altro) da inviare IN ORIGINALE. Qualora la spesa sia stata anticipata dal Suo Dipartimento di afferenza o da altra struttura, La prego di compilare due volte il modello allegato, la prima per le spese da rimborsare a Lei direttamente, la seconda per le spese da rimborsare all'Ente che ha effettuato l'anticipo (indicandone descrizione, intestazione e dati bancari completi). Nel ribadire la necessita' dell'originale della giustificativa, qualora necessario il CIB puo' rilasciare specifica certificazione di possesso del documento originale all'amministrazione richiedente.

Si raccomanda inoltre una chiara e completa compilazione dei moduli.

Per qualsiasi ulteriore chiarimento necessario, La prego di non esitare a contattare l' Amministrazione nelle persone di:
Vanessa Florit e-mail: cib@lncib.it
tel. 040 398979 fax. 040 398990

SI PREGA DI INVIARE UNA MAIL CON LA CONFERMA DELL'ACCETTAZIONE DEL CONTRIBUTO

Cordiali saluti.

Consorzio Interuniversitario Biotecnologie
(C.I.B.)

FigueroaME_Letter.pdf

María E. Figueroa M.D.
Associate Professor of Human Genetics,
Co-Leader, Cancer Epigenetics Program
Sylvester Comprehensive Cancer Center.
University of Miami Miller School of Medicine,
1501 NW 10th Avenue, BRB 723,
Miami, FL 33136-1000

11/9/17

To whom it may concern,

It is a pleasure to write this letter to confirm that I have hosted Doctor Anair Graciela Lema Fernandez during her fellowship in my laboratory, while I was still Assistant Professor at the Department of Pathology of the University of Michigan, Ann Arbor. During this time, I provided Dr. Lema Fernandez training in the application of technologies for epigenomic and bioinformatic studies in human leukemias.

Our group has extensive experience in both local and genome-wide DNA methylation studies as well as in the necessary computational biology approaches for the analysis of next-generation sequencing.

Doctor Lema Fernandez acquired skills for an independent bioinformatic analysis data through the use of: Python, R statistical software, IGV, Bioconductor, alignments tools (TopHat, STAR, HTseq), RNA-seq and differential exon usage analysis tools (DESeq2, DEXSeq, EdgeR), DNA-methylation analysis (Bowtie, Bismark, MethylKit, MethylSig) and pathways/DNA motif analysis tools (GO, DAVID, Chip-Enrich, RNA-enrich, Hypergeometric Optimization of Motif EnRichment).

We continue to collaborate with Dr. Lema Fernandez and Dr. Mecucci's team of investigators, and we are currently working on the first co-authored publication, in which Dr. Lema Fernandez has been exclusively responsible for leading the analysis. I have every confidence that Dr. Lema Fernandez is capable of producing high quality analyses and will be capable of completing the studies delineated in this proposal.

Kind regards,

Maria E Figueroa, M.D.
Associate Professor,
Dept. of Human Genetics,
University of Miami,
Miller School of Medicine

A distinct epigenetic program.pdf

Leukemia
https://doi.org/10.1038/s41375-019-0433-9

ARTICLE

Myelodysplastic syndrome

A distinct epigenetic program underlies the 1;7 translocation in myelodysplastic syndromes

Anair Graciela Lema Fernandez[1] . Barbara Crescenzi[1] . Valentina Pierini[1] . Valeria Di Battista[1] . Gianluca Barba[1] . Fabrizia Pellanera[1] . Danika Di Giacomo[1] . Giovanni Roti[2] . Rocco Piazza[3] . Emmalee R. Adelman[4] . Maria E. Figueroa[4] . Cristina Mecucci[1]

Received: 26 October 2018 / Revised: 23 December 2018 / Accepted: 8 February 2019

Abstract

The unbalanced translocation dic(1;7)(q10;p10) in myelodysplastic syndromes (MDS) is originated by centromeric juxtaposition resulting into 1q trisomy and 7q monosomy. More than half of cases arise after chemo/radio-therapy. To date, given the absence of genes within the centromeric regions, no specific molecular events have been identified in this cytogenetic subgroup. We performed the first comprehensive genetic and epigenetic analysis of MDS with dic(1;7)(q10;p10) compared to normal controls and therapy-related myeloid neoplasms (t-MNs). RNA-seq showed a unique downregulated signature in dic(1;7) cases, affecting more than 80% of differentially expressed genes. As revealed by pathway and gene ontology analyses, downregulation of ATP-binding cassette (ABC) transporters and lipid-related genes and upregulation of p53 signaling were the most relevant biological features of dic(1;7). Epigenetic supervised analysis revealed hypermethylation at intronic enhancers in the dicentric subgroup, in which low expression levels of enhancer putative target genes accounted for around 35% of the downregulated signature. Enrichment of Krüppel-like transcription factor binding sites emerged at enhancers. Furthermore, a specific hypermethylated pattern on 1q was found to underlie the hypo-expression of more than 50% of 1q-deregulated genes, despite trisomy. In summary, dic(1;7) in MDS establishes a specific transcriptional program driven by a unique epigenomic signature.

Introduction

The dic(1;7)(q10;p10) is a rare cytogenetic alteration found in 1.5–6% of myelodysplastic syndromes (MDS), and less frequently in acute myeloid leukemia (AML) and myeloproliferative neoplasms [1]. Of note, dic(1;7)-associated MDS/AML are frequent after chemo/radio-therapy exposure. Interestingly, in both de novo and treatment-induced disorders, this abnormality usually occurs as isolated or associated with one additional cytogenetic change [2].

Dic(1;7) differs from other typical chromosome translocations that act as leukemia drivers by originating fusion genes and chimeric transcripts, as it derives from the translocation of whole arms of chromosomes 1 and 7 with juxtaposition at centromeric regions, without production of abnormal fusion genes.

Human centromeres are made by chromosome-specific no-gene DNA encompassing transposable elements and repetitive alpha-satellite (α-sat) sequences. Their function is under the control of epigenetic marks that promote binding of protein complexes directing segregation during cellular divisions (Fig. 1a). Aberrant recombinations of chromosomes 1, 9 and 16 at centromeric level, characterize a rare autosomal recessive disease with a constitutional methylation defect, immunodeficiency and facial anomalies (Online

Supplementary information The online version of this article (https://doi.org/10.1038/s41375-019-0433-9) contains supplementary material, which is available to authorized users.

* Cristina Mecucci
cristina.mecucci@unipg.it

1 Department of Medicine, Hematology and Bone Marrow Transplantation Unit, University of Perugia, Perugia, Italy

2 Hematology, University of Parma, Parma, Italy

3 Hematology, School of Medicine and Surgery, University of Milano Bicocca, Milano, Italy

4 Sylvester Comprehensive Cancer Center and Department of Human Genetics, University of Miami Miller School of Medicine, Miami, FL, USA

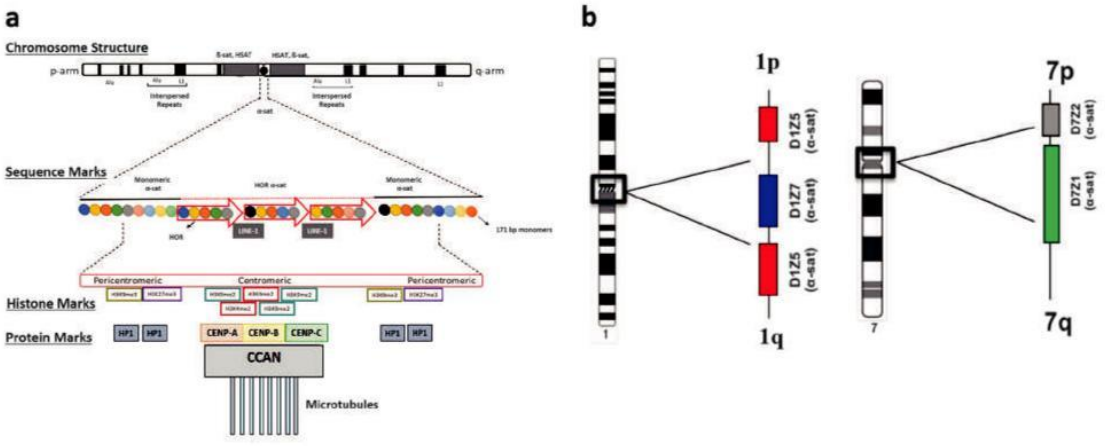

case	type	CN	chr	cytostart	cytoend	kb	start	end
DIC1	Gain	3.0	1	q21.1	q44	103.958.229	145266455	249224684
	Loss	1.0	7	q11.21	q36.3	96.647.886	62471821	159119707
	Gain	3.0	9	p24.3	q34.3	140.816.528	203861	141020389
DIC2	Gain	3.0	1	q21.1	q44	104.314.552	144884265	249198817
	Loss	1.0	7	q11.21	q36.3	96.600.533	62519174	159119707
DIC3	Gain	3.0	1	q21.2	q44	101.861.538	147225943	249087481
	Loss	1.0	7	q11.21	q36.3	94.387.294	64680416	159067710
	GainMosaic	2,4	8	p23.3	q24.3	146.137.723	158048	146295771
	Loss	1.0	13	q13.1	q31.3	59.187.041	32711638	91898679
DIC4	GainMosaic	2,4	1	q21.1	q44	104.289.145	144935539	249224684
	LossMosaic	1,5	7	q11.21	q36.3	96.682.318	62437389	159119707
DIC5	Gain	3.0	1	q21.1	q44	103.744.952	145436646	249181598
	Loss	1.0	7	q11.21	q36.3	95.865.811	63253896	159119707
	Gain	3.0	8	p23.3	q24.3	145.908.002	212297	146120299

Fig. 1 Cytogenetics, fluorescent in situ hybridization (FISH) and single-nucleotide polymorphism array (SNPa) result summary. a Human centromeric regions. Top: representative chromosome structure with position of repetitive sequences. Upper middle: small different colored circles represent monomers of alpha-satellite DNA at centromeres; large red arrows indicate high-order repeat (HOR) units that form centromeric chromatin. Lower middle: specific histone modifications promote binding of centromeric (CENP-A, CENPB, CENP-C) and pericentromeric (HP-1) proteins. Bottom: the con-stitutive 16 proteins, centromere-associated network (CCAN), interact with centromeric proteins and promote microtubule attachment to the centromere. b Schematic representation with relative orientation of genomic FISH probes at centromere 1 (D1Z5 SpectrumOrange) and centromere 7 (D7Z1 SpectrumGreen). c Metaphase dual-color FISH with D1Z5 (orange) and D7Z1 (green) showing a fusion signal on dic (1;7), indicated by a yellow arrow (DIC 4 case). d Copy number alterations (CNAs) detected by SNP-arrays in all five dicentric cases. CN copy number, chr chromosome, cytostart cytogenetic band start, cytoend cytogenetic band end

Mendelian Inheritance in Man (OMIM) #614069, OMIM #616910, OMIM #616911) [3]. In multiple myeloma, cytogenetic instability of 1q originating jumping translocations prevalently involves pericentromeric heterochromatin decondensation rather than α-sat [4].

Due to an absence of genes within the centromeric regions, specific molecular consequences have not been identified in dic(1;7) cases and detailed genomic information is still lacking. Using a comprehensive genetic and epigenetic approach we delineated the specific (epi)genomic features underlying the typical 1;7 centromere–centromere recombination in MDS.

Materials and methods

Samples

Cases were retrospectively collected from the files of the Laboratory of Cytogenetics and Molecular Genetics at the Hematology Department of the University of Perugia, Italy. All patients gave their written informed consent to sample collection and biological analyses in accordance with the Declaration of Helsinki. The study was approved by the Institutional Bioethics Committee (Prot.1.X.2011). Hematological and cytogenetic features of patients are listed in

Table 1 Hematological and cytogenetic features of all patients analyzed

Patient	Sex	Age	Diagnosis	Karyotype	mERRBS	RNA-seq	Mutations[a]
dic(1;7) cohort							
DIC 1	M	67	MDS (ET, JAK2+)	47,XY,+1,dic(1;7)(p10;q10),+9[15]	Yes	Yes	Not available
DIC 2	M	75	t-MDS (lung cancer)	46,XY,+1,dic(1;7)(p11;q11)[14]/46,XY[1]	Yes	Yes	GGPS1 (R74H); ANKS1B (T247I)
DIC 3	F	79	t-MDS (NHL)	46,XX,+1,dic(1;7)(p11;q11),del(13)(q13q31)[2]/47,idem,+8[8]/46,XX[2]	Yes	Yes	Not available
DIC 4	M	42	t-MDS (melanoma)	46,XY,+1,dic(1;7)(q10;p10)[7]/46,XY[8]	Yes	Yes	Not available
DIC 5	M	45	MDS	47,XY,+1,dic(1;7)(q10;p10),+8[20]	Yes	Yes	CCDC8 (R429K); PSMF1 (P168L)
Control cohort							
CTL 1	F	43	Wild type	46,XX[20]	Yes	NA	Not found
CTL 2	M	39	Wild type	46,XY[20]	Yes	Yes	Not found
CTL 3	F	46	Wild type	46,XX[20]	Yes	Yes	Not found
CTL 4	M	46	Wild type	46,XY[20]	Yes	Yes	Not found
CTL 5	F	63	Wild type	46,XX[20]	NA	Yes	Not found
t-MN cohort							
t-MN 1	F	77	t-MDS (lymphoma)	46,XX[20]	Yes	Yes	TET2 (P1115L*2); SF3B1 (K700E)
t-MN 2	F	46	t-MDS (NHL)	51,XXX,del(4)(q13),−5,+6,+8,+11,−17,−18,+19,+22,+2mar[11]/46,XX[7]	Yes	Yes	TP53 (R273H)
t-MN 3	M	70	t-MDS (bowel carcinoma)	46,X,-Y,t(1;10)(q21;q21),−5,der(7)(?),del(7q)(q11),+8,+19,−22+mar[15]	NA	Yes	TP53 (C135L*4)
t-MN 4	F	80	t-MDS (ovarian cancer)	47,XX,+8[7]/46,XX[8]	Yes	Yes	Not found
t-MN 5	M	77	t-MDS (bladder cancer)	43–45,XY,−5,del(7q)(q21q36),−9,add(12p)(p11),−13,+16,add(17)(p11),+19,del(21)(q?),+22[7]	NA	Yes	TP53 (M246R)

Previously primary tumor is indicated between brackets

mERRBS was performed on all samples except on CTL 5, t-MN 3 and t-MN 5; RNA-sequencing (RNA-seq) analysis was performed on all samples except on CTL 1, due to quality control

M male, F female, mERRBS multiplex enhanced reduced representation bisulfite sequencing, DIC dic(1;7), CTL control, t-MN therapy-related myeloid neoplasm, t-MDS therapy-related myelodysplastic syndrome, AML acute myeloid leukemia, ET essential thrombocythemia, JAK2+ Val617Phe detected at diagnosis of ET, NHL non-Hodgkin lymphoma, NA not available due to quality control

[a]Mutations: mutational results indicate whole exome sequencing (WES) for DIC cohort and denaturing high-performance liquid chromatography (DHPLC)/Sanger screening of MDS-related genes for CTL and t-MN cohorts (detailed gene list and results are reported in Supplementary Table 1)

Table 1. dic(1;7)(q10;p10) cases were compared with a series of controls and therapy-related myeloid neoplasms (t-MNs). As controls we used bone marrow samples from non-neoplastic cytopenias, normal bone marrow morphology and normal karyotype. Mutational diagnostic screening of 14 MDS-related genes was performed on both controls and t-MNs (Supplementary Table 1).

Karyotype, fluorescent in situ hybridization (FISH), denaturing high-performance liquid chromatography (DHPLC) and Sanger

Cytogenetic analysis was performed following standard procedure and G-banded karyotypes. FISH experiments on metaphase chromosomes were performed using the following probes: Vysis CEP 1 (D1Z5, SpectrumOrange Probe, Abbott) for alphoid sequences of chromosome 1 and Vysis CEP 7 (D7Z1, SpectrumGreen Probe, Abbott) for chromosome 7 α-sat DNA (Fig. 1b). Analyses were carried out using a fluorescence microscope Olympus BX61 equipped with a highly sensitive camera JAI and driven by CytoVision 4.5.4 software. At least seven abnormal metaphases were analyzed in each experiment.

Nucleic acids were extracted from unsorted bone marrow cells of patients using All Prep DNA/RNA Mini Kit (Qiagen), quantified with Qubit fluorimeter using Quant-i-T dsDNA HS Assay Kit and RNA HS Assay Kit (Invitrogen) respectively and samples quality was evaluated using Tapestation visualization (Agilent 2100 Bioanalyzer). Mutational diagnostic screening of 14 MDS-related genes

was performed using DHPLC (Wavemaker software, Wave System, MD Transgenomic Inc., USA) and Sanger sequencing (3500 Genetic Analyzer, Applied Biosystems) (Table 1; Supplementary Table 1).

Single-nucleotide polymorphism array (SNPa)

SNPa was performed on CytoScan HD Affymetrix platform (Affymetrix, Santa Clara, CA, USA) following the manufacturer's instructions. A total of 250 ng of high-quality genomic DNA obtained from bone marrow cells was used to study copy number alterations (CNAs) and copy neutral loss of heterozygosity (cnLOH). The protocol was supported by Affymetrix GeneChip Command Console (AGCC) software and analyzed through Affymetrix Chromosome Analysis 3.1 (ChAS) software with filters set at 100 Kb dimension for CNAs and 10 Mb dimensions for cnLOH. Our data refer to NetAffx Build 32.3 (hg19) database. Polymorphic copy number variations were excluded from the analysis.

Whole exome sequencing (WES)

WES was performed in dic(1;7) (DIC) 2 and DIC 5 (Table 1) using germline DNA extracted from bone marrow fibroblasts with normal karyotype. All variations identified by WES were confirmed as somatic on matched tumor/normal samples and tested on the remaining three DIC cases by Sanger sequencing. Illumina paired-end libraries were generated according to the manufacturer's protocol (Illu-mina, San Diego, CA). Image processing and basecall were performed using the Illumina Real Time Analysis Software. Paired whole-exome fastq data were aligned to the human reference genome (GRCh38/hg38) with the BWA-MEM algorithm [5]. Duplicates were marked using Samblaster. Quality of the aligned reads, somatic variant calling and copy number analysis were performed through CEQer2 tool, as previously described [6]. Variants were annotated using dbSNP142. Variants with minor allele frequency <0.01 or carrying a 'Clinical' single-nucleotide poly-morphism database (dbSNP) flag were further processed; the other variants were discarded from subsequent analyses. Filtered variants were exported as vcf files and used as input for Annovar [7] analysis/annotation.

RNA-seq and quantitative real-time PCR (qRT-PCR)

All samples used for RNA-sequencing (RNA-seq) had RNA integrity number of 6 or above. Ribosomal RNA depletion and library preparation were obtained following the manufacturer's instructions using RiboGone Mammalian Kit (Clontech Laboratories Inc.) and NEBNext® Ultra™ RNA Library Prep Kit for Illumina (New England Biolabs, NEB), respectively. Reads were aligned against hg19 build of the human genome using TopHat [8], counts were generated using HTseq [9] and DESeq2 was used for differential expression analysis (false discovery rate (FDR) <0.1 and log2 fold change ≥I1I) [10]. To validate RNA-seq results, 1 µg RNA was retrotranscribed using 100 U of Superscript II and esarandom primers (Invitrogen, Carlsbad, CA, USA) and qRT-PCR was performed on ZMAT3 and NR1H2 using TaqMan assay probes Hs00536976_m1 and Hs01027215_g1 (Applied Biosystems, Life Technologies, Carlsbad, USA) respectively with endogenous ABL1 (Hs00245445 m1, Applied Biosystems, Life Technologies, Carlsbad, USA) and Universal Human Reference RNA (Stratagene, Cedar Creek, TX, USA) as reference controls. Real-time reactions were performed in triplicate using the Roche Light Cycler 480; fluorescence data were analyzed with the software version 1.5 and second derivative maximum method; gene expression was expressed as Cp (crossing point) values. Statistical significance was tested by Mann–Whitney test (*p < 0.05).

Multiplex enhanced reduced representation bisulfite sequencing (mERRBS)

mERRBS libraries were prepared with modified size selection fragments for multiplex application, as previously described [11]. Only genomic regions with coverage ran-ging from 10 to 450 times were used for the downstream analysis. Reads were aligned against a bisulfite-converted human genome (hg19) using Bismark with Bowtie2 [12]. Downstream analysis was performed with the MethylKit [13] and MethylSig [14] packages. We investigated cyto-sine methylation using beta-binomial regression (FDR ≤0.1) with a minimum cut-off of 25% methylation difference to identify differential methylated cytosines. Unsupervised clustering analysis with principal component analysis was conducted using only high-variance CpG tiles across all samples. Unsupervised analysis of DNA methylation using hierarchical clustering (distance = 1-Pearson Correlation, Ward's agglomeration method) was performed using MethylKit. Differentially methylated regions (DMRs) were identified by first summarizing the methylation status of the genomic regions into 25 bp tiles and then identifying regions with an absolute methylation difference ≥25% and an FDR ≤0.1. DMRs were annotated to the RefSeq genes (National Center for Biotechnology Information (NCBI)) using the following criteria: (a) DMRs overlapping with a gene were annotated to that gene; (b) intergenic DMRs were annotated to all neighboring genes within a 50 kb window; and (c) if no gene was detected within a 50 kb window, the DMR was annotated to the nearest transcription start site [15]. For Chip-Enrich annotation we used the option locus. def = "nearest_tss" [16]. Enhancer annotation was

performed using chromatin immunoprecipitation sequencing (ChIP-seq) data sets generated in human-mobilized $CD34^+$ cells. Enhancers were defined as regions with H3K4me1 and H3K27ac, with absence of the promoter marker H3K4me3 [17]. Moreover, we used data sets generated in human-adult $CD34^+$ cells based on histone repressive marks (H3K27me3 and H3K9me3) and histone active marks (H3K36me3, H3K4me1 and H3K4me3) to investigate if aberrant DNA methylation in dic(1;7) was associated with a particular chromatin and/or structural microenvironment modification [17].

Sequencing

All amplified libraries for RNA-seq and mERRBS underwent quality control steps as described for DNA and RNA extraction and were sequenced on Illumina HiSeq2500 using the manufacturer's recommendations (Illumina San Diego, CA). The data were deposited in NCBI Gene Expression Omnibus (GEO) under the accession number GSE118648.

Integrative functional analysis

To analyze the functional pathway and Gene Ontology (GO) enrichment of the identified gene list, we used the Database for Annotation, Visualization, and Integrated Discovery 6.8 (DAVID) [18] and RNA-Enrich [19]. Known and de novo DNA motif enrichment were identified with Hypergeometric Optimization of Motif EnRichment (HOMER) [20] using all tiled CpGs from our sequencing as background in the case of mERRBS analysis. In order to analyze the potential recruitment of transcriptional repressors that could be responsible for gene silencing, we intersected DMRs and extracted promoter position from the identified downregulated genes between dic(1;7) and controls with ChIP-seq data generated in $CD34^+$ cells for CTCF [21], one of the most well-characterized transcriptional repressor, and for seven well-known hematopoietic transcription factors [22].

Results

The dic(1;7) breakpoints fell within α-sat DNA

Double-color FISH with Vysis D1Z5 and D7Z1 probes generated a fusion signal between centromeric regions in all our five dic(1;7) cases (Fig. 1c). Three cases bore one or two additional events as seen at both conventional karyotypes and SNPa, in particular, trisomy 8, trisomy 9 and del(13q) (Table 1 and Fig. 1d). In DIC 3, trisomy 8 characterized a subclone of a main line including dic(1;7) and del(13q) (Fig. 1d). No CNAs or cnLOH, with reduplication of a chromosomal allele alongside with loss of its respective homologous region, were detected by SNPa.

dic(1;7) bore no common somatic mutations

WES on DIC 2 (Table 1) identified a mutation in the ankyrin 7 domain of ANKS1B/EB1 gene (12q23.1), a pro-miscuous gene originating multiple fusion transcripts in solid tumors [23] and overexpressed in a subset of B-cell acute lymphoblastic leukemia (B-ALL) [24]. The same case harbored a variation in the polyprenyl synthetase domain of GGPS1 (1q42.3), a gene transcribing for a long non-coding RNA which is overexpressed in lung cancer and mutated in adult T-cell lymphoma cases [25, 26]. In DIC 5 we iden-tified two mutations, the first one within the alanine-rich domain of CCDC8 gene (19q13), involved in maintaining microtubule integrity and mutated in the genetic 3 M growth retardation syndrome (OMIM #614205) [27]. The second mutation occurred in the proline-rich domain of PSMF1 gene (20p13), a proteasome regulator previously described as mutated in a case of ALL [28]. In silico analysis with three different software predicted the GGPS1 mutation to be disease causing, while the other three mutations showed conflicting results (Supplementary Figure 1). None of these variations were identified by Sanger sequencing in the other three patients (DIC 1, DIC 3 and DIC 4, Table 1).

dic(1;7) has a distinct expression signature

To characterize the transcriptomic differences between dic(1;7) cases and the other two groups, controls and t-MNs, we analyzed their gene expression profile. Unsupervised analysis using principal component analysis of transformed RNA-Seq count data separated cases bearing dic(1;7) from controls and t-MNs along the first principal component (Fig. 2a, b). We identified a total of 4860 differentially expressed genes (DEGs) between dic(1;7) and controls, and 4317 between dic(1;7) and t-MNs (Fig. 2c). Gene expression analysis showed a prevalent downregulation within the signature of dic(1;7) cases, affecting more than 80% of DEGs (Fig. 2c, d; Supplementary Figure 2). By analyzing promoters of downregulated genes for the presence of hematopoietic transcription factors binding sites, we found a low percentage of overlap, ranging from 0.58% of LYL to 10.8% of FLI (Supplementary Figure 3). Interestingly, the CTCF analysis at the level of promoters of silenced genes revealed that 920 out of 3971 downregulated genes between dic(1;7) and controls (23%) were CTCF targets, suggesting a potential contribution of transcriptional repressors in mediating the observed downregulated gene expression profile (Supplementary Table 2 and Supplementary Figure 3).

To capture biological differences, we analyzed functional pathways within DEGs. Dicentric cases showed 18 and 30 significantly enriched pathways when analyzed against controls and t-MNs, respectively (FDR ≤0.1) (Supplemen-tary Table 2 and 3). The t-MN cohort compared to controls showed 102 enriched pathways (Supplementary Table 4). When compared to controls, the two neoplastic subgroups included in this study, i.e., dic(1;7) and t-MNs, showed aberrant downregulation of biologically relevant pathways, specifically: mitogen-activated protein kinase (MAPK) signaling, spliceosome, ribosome, gonadotropin-releasing hormone (GnRH) signaling, IL12/Stat4 (interleukin-12/ signal transducer and activator of transcription 4)-dependent signaling and tumor necrosis factor (TNF)/stress-related signaling (Supplementary Tables 2-4). In addition, six pathways emerged as specifically deregulated (4 down-regulated and 2 upregulated) in dic(1;7) cases (Supple-mentary Tables 2-4). Notably, the signaling of ATP-binding cassette (ABC) transporters, a superfamily of proteins involved in the transport of metabolic products and drugs across biological membranes, emerged as specifically downregulated (Supplementary Tables 2-5). Of the ABC genes detected as enriched by our RNA pathway analysis, seven were found to be significantly deregulated in dic(1;7) compared to the other two subgroups (Supplementary Table 5). In particular, 5/7 were downregulated: ABCA6 and ABCA10, known as phospholipid and cholesterol transporters; ABCB4 and ABCG2 involved in phosphati-dylcholine and drug transport; and ABCB6, which plays a crucial role in heme synthesis by mediating porphyrin uptake into mitochondria [29]. Two other ABC genes, the phospholipid and drug transporters ABCA3 and ABCC3, were upregulated (Supplementary Table 5). Moreover, the cholesterol transporter ABCA9 was significantly down-regulated in dic(1;7) only when compared to t-MNs, while the peptide transporter ABCB2 was significantly upregu-lated only against controls (Supplementary Table 5).

GO analysis of differentially expressed genes showed significantly enrichment in lipid metabolism terms invol-ving 12 genes, 10 of which were downregulated only in dic (1;7) (Supplementary Tables 2-5). Among them, we found one group of lipid metabolism genes related to oxidative/ inflammatory response: the apolipoprotein APOM and the cholesterol esterifying enzyme LCAT that have been reported to decrease upon oxidative and/or inflammatory response [30, 31]; the cytidine deaminase APOBEC2, found to be regulated by the inflammatory transforming growth factor-beta signaling [32] and the nuclear receptor NR1H2 that was involved in lipid homeostasis and inflammation [33]. A second group of genes is encoding for lipids related to cancer: LPL, lipoprotein lipase hypo-expression that was shown to predict evolution in chronic lymphocytic leukemia patients [34]; PLA2G7, a phospholipase which expression in the peripheral blood was predictive of survival in mela-noma patients [35]; apolipoprotein APOC1 that was asso-ciated with poor prognosis in pancreas cancer patients; moreover, when inhibited, it induced apoptosis in pan-creatic cancer cell lines [36].

Only two specifically upregulated pathways emerged in dic(1;7), the most important of which was the TP53 signaling pathway, which included 9 of the DEGs (Supplementary Tables 2-5). In particular, the four TP53 target genes upregulated in dicentrics, compared to both t-MNs and controls, were: ZMAT3, STAT1, SUMO1 and CCNG1 (Supplementary Table 5). Moreover, SHISA5 and MYC were upregulated only against controls and SER-PINE1, FAS and ATR only against t-MNs. By contrast, t-MNs versus controls showed TP53 signaling down-regulation (Supplementary Table 4). The TP53 gene by itself was not significantly deregulated in any subgroups, although there was a trend towards RNA hyper-expression in dic(1, 7) and hypo-expression in t-MNs (data not shown). We validated the upregulation of the TP53 target gene ZMAT3 and the downregulation of NR1H2 gene, involved in lipid homeostasis and inflammation, by qRT-PCR (Fig. 2e).

Both gene dosage effect and DNA methylation profile contributed to the dic(1;7) signature

We investigated gene dosage effect of 1q trisomy and 7q monosomy from RNA-seq. Compared with controls and t-MNs, 97.5% (117/120) and 95.9% (118/123), respectively, of 7q DEGs were downregulated in dic(1;7), in keeping with 7q loss (Fig. 3a). Interestingly, downregulation also involved EZH2 and MLL3, previously identified as hap-loinsufficient putative suppressor genes on chromosome 7. Surprisingly, among 198 1q DEGs included in the signature of dicentrics against controls, 90 were upregulated and 108 downregulated (Fig. 3b). Also, when dic(1;7) was compared to t-MNs, the 157 1q DEGs resulted to be 52 up- and 105 down-regulated (Fig. 3b). These findings showed that, despite of trisomy, more than 50% of 1q genes were always hypo-expressed in the dic(1;7). Consistent with this, 85/119 1q DMRs were hypermethylated in dicentrics compared with controls (67/109 compared with t-MNs) (Fig. 3c) and they were annotated to 83 genes, 31 of which were down-regulated. Interestingly, 61/85 hypermethylated 1q DMRs (71.8%) were annotated to enhancers, thus linking 1q hypermethylation to functional DNA region (Supplemen-tary Table 6).

Global DNA methylation profiling captured 3.2 M CpGs across the genome. Principal component analysis of high-variance CpGs identified dic(1;7) and t-MN cases from controls (Fig. 4a, b). Unsupervised analysis using hier-archical clustering segregated dicentrics with additional

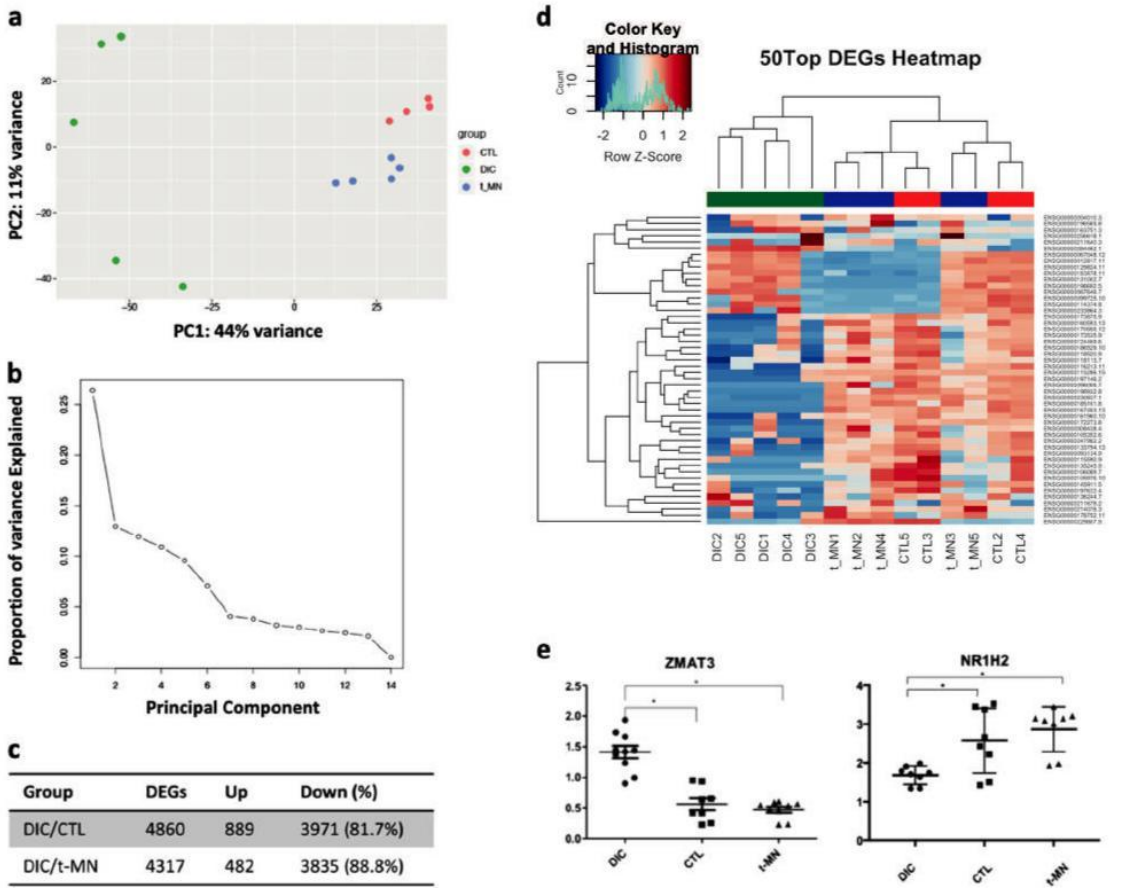

Group	DEGs	Up	Down (%)
DIC/CTL	4860	889	3971 (81.7%)
DIC/t-MN	4317	482	3835 (88.8%)

Fig. 2 Summary of RNA-sequencing (RNA-seq) results. a Scatter plot showing results of a principal component analysis (PCA) of transformed count data from RNA-seq using DESeq2 (varianceStabilizingtransformation). Samples are colored according to their disease status, observe that the DIC are separated from all other samples along dimension 1 (the x-axis). b The scree plot line indicates the amount of the total variance preserved by a principal component. c Table summary of RNA-seq result analysis. Up refers to upregulated genes, down refers to downregulated genes. d Heatmap representing the top 50 differentially expressed genes (DEGs) across all three groups of samples. The heatmap colors reflect values representing the degree of expression from low to high as blue to red, respectively, as shown on the scale at the top-left hand side of the figure. Red indicates control (CTL), blue therapy-related myeloid neoplasm (t-MN) and green dic (1;7). e Significance for ZMAT3 and NR1H2 expression were tested by Mann–Whitney test (*$p < 0.05$); values are expressed as means ± SEM

anomalies in a separate cluster with the t-MN cases with complex karyotype (Fig. 4c; Table 1). Supervised analysis showed both global hyper- and hypo-methylation in dic (1;7), compared with the other subgroups, while t-MNs showed global hypomethylation (Fig. 4b, c). We identified a total of 3261 DMRs between dic(1;7) and controls, and 4568 DMRs between dicentric cases and t-MNs (Fig. 5a). Genome-wide distribution of DMRs and annotation to genomic regions showed that, compared to controls, dicentrics were significantly depleted at promoter regions (15% vs. background 30%, binomial test $p < 2.2e^{-16}$) and significantly enriched in non-promoter regions (Fig. 5a, b).

These results were also maintained in the comparison against the t-MN group. Moreover, in comparing dicentrics to controls, 33% of DMRs had CTCF binding sites (Supplementary Figure 3). By contrast, the analysis of hematopoietic transcription factors revealed that less than 1% of DMRs had binding sites for the specific transcription factor (TF) motifs analyzed (Supplementary Figure 3).

Focusing on promoter regions, t-MNs showed gene-specific promoter hypermethylation (Fig. 5), confirming previous studies [37]. dic(1;7) cases compared with controls showed hypermethylation of 356/502 (68%) promoters (Fig. 5c). However, promoter hypermethylation correlated

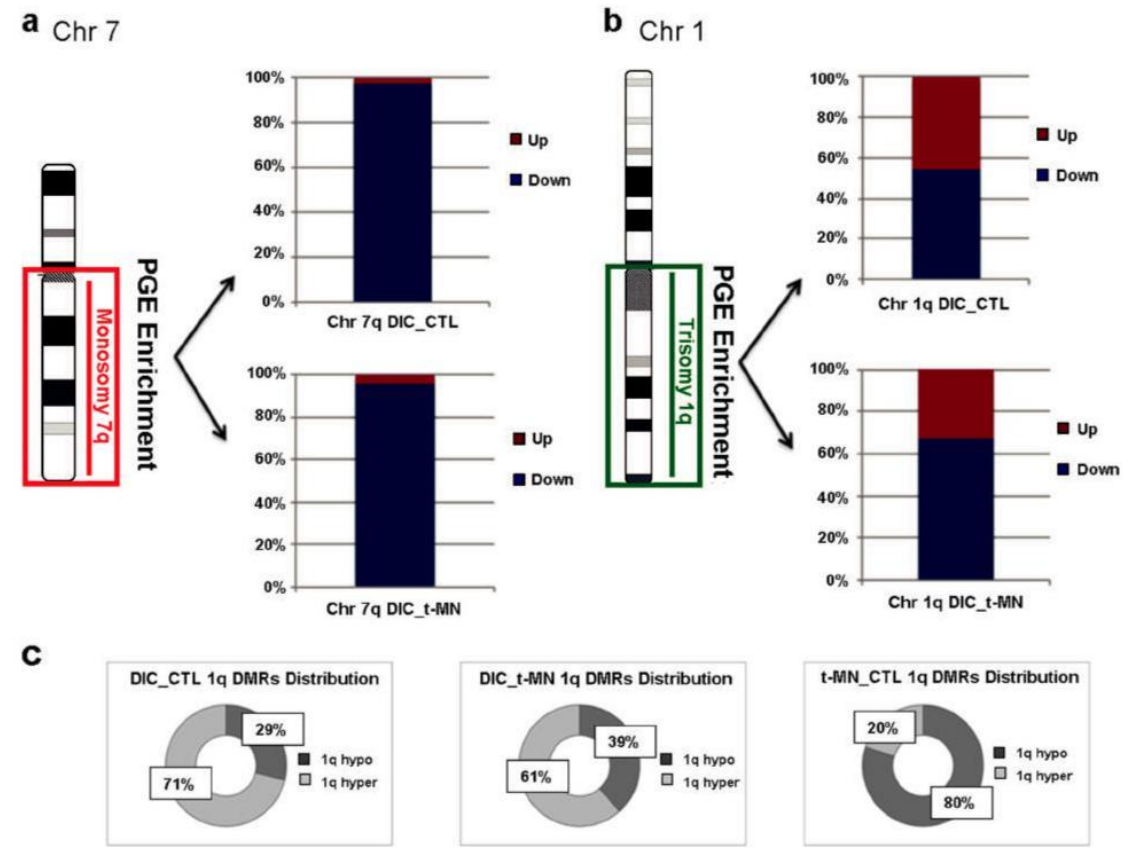

Fig. 3 Gene dosage effect and DNA methylation pattern on 7q and 1q regions of dic(1;7). a Chromosome view of regions significantly enriched in genes differentially expressed using PGE (Positional Gene Enrichment) on 7q (left). Percentage of differentially expressed gene (DEG) distribution within down- and up-regulated genes in dic(1;7) compared to controls (up-right) and to therapy-related myeloid neoplasms (t-MNs; bottom right). Compared to controls, 117/120 of 7q DEGs were downregulated in dic(1;7), while compared to t-MNs, 118/123 7q DEGs were downregulated. b Chromosome view of regions significantly enriched in genes differentially expressed using PGE on 1q (left). Percentage of DEG distribution within down- and up-regulated genes in dic(1;7) compared to controls (up-right) and to t-MNs (bottom right). The signature of dic(1;7) contained 90 up- and 108 (54.5%) down-regulated genes on 1q compared to controls; 52 up-and 105 (66.8%) down-regulated genes on 1q compared to t-MNs. c Differentially methylated region (DMR) distribution along chromo-some 1q involved in the translocation. Dicentric cases showed hypermethylation of DMRs on 1q compared to both controls (left) and t-MN (middle). By contrast, t-MNs showed a prevalent hypomethy-lated pattern on 1q (right)

with significant changes in expression level only for 31 genes, suggesting that its contribution to dic(1;7) expression profile was limited (Fig. 5d).

Enhancer hypermethylation enriched on TF binding sites emerged in dic(1;7)

Analysis of the non-promoter regions showed that 43% of the dic(1;7) DMRs were enriched for enhancers (background 34%, binomial test $p < 2.2e^{-16}$) when compared with controls, while t-MNs had 38% enrichment (background 34%, binomial test $p = 0.046$) (Fig. 6a). In silico analysis using ChIP-seq data sets for histone repressive marks (H3K27me3 and H3K9me3) and histone active marks (H3K36me3, H3K4me1 and H3K4me3) from $CD34^+$ primary cells [17] confirmed that aberrant DNA methylation in dic(1;7) is mainly associated with regions marked by active histone marks specifically linked to enhancers (72% of DMRs overlap with H3K4me1, background 68.6%; binomial test $p = 3.255e^{-07}$). Using the Hnisz D data set of 234 super-enhancers identified in $CD34^+$ adult cells [38], in our series we found 5 super-enhancers out of the 744 hypermethylated enhancers (Supplementary Table 6).

In both dicentric and t-MNs, enhancer DMRs were predominantly found in intronic regions. A direct enriched test

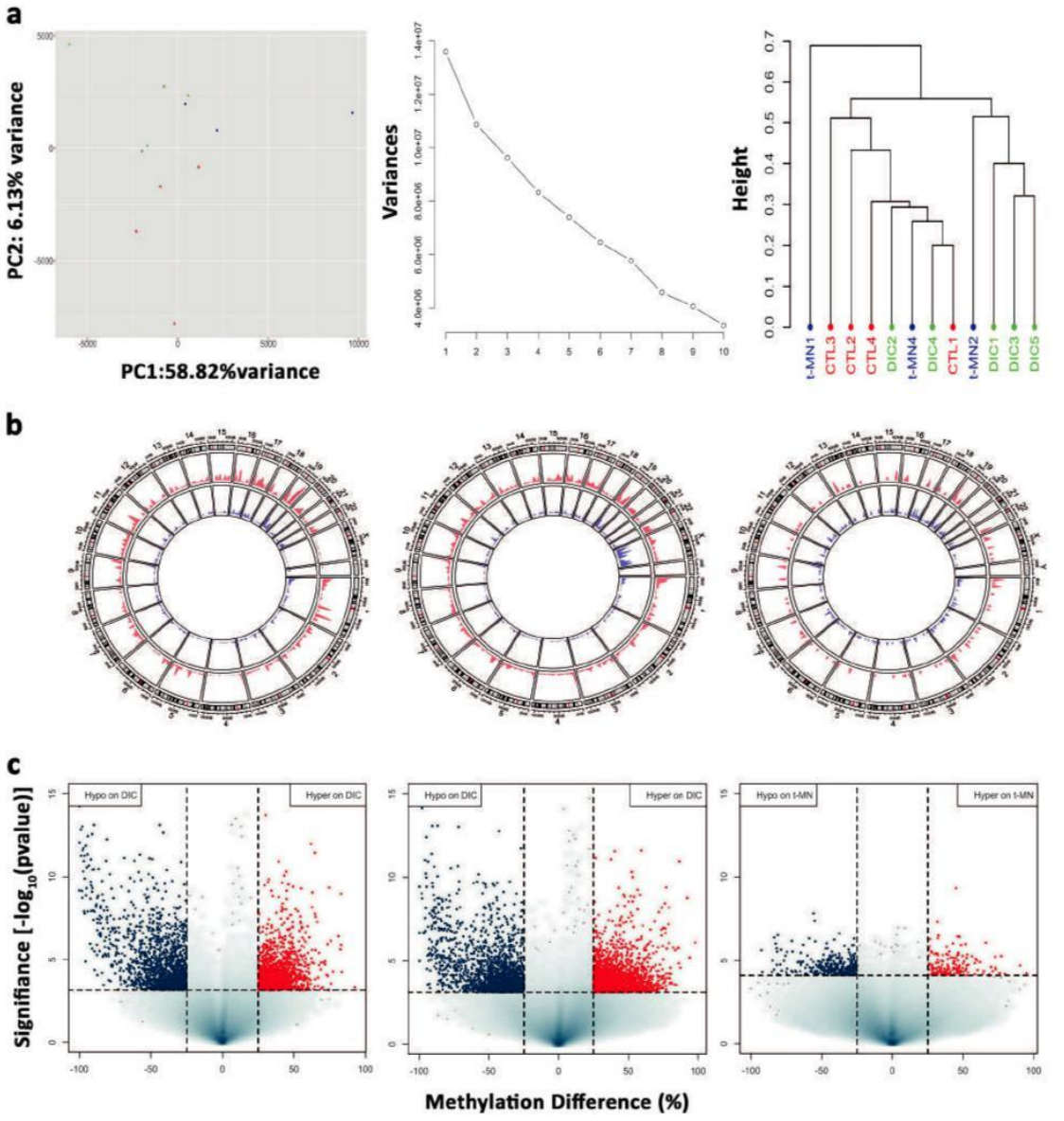

Fig. 4 Summary of multiplex enhanced reduced representation bisul-fite sequencing (mERRBS) analysis. a Unsupervised multivariate analysis using principal component analysis (PCA) was able to sepa-rate controls from all tumor samples. The scree plot line indicates the amount of the total variance preserved by a principal component (middle). Unsupervised analysis of DNA methylation using hier-archical clustering (left). Red indicates control (CTL), blue indicatestherapy-related myeloid neoplasms (t-MNs) and green dic (1;7) (DIC). b Circos plot showing the hyper- and hypomethylated differentially methylated regions (DMRs) found for each group com-parison: DIC/CTL (left), DIC/t-MN (middle) and t-MN/CTL (right). The outer circle indicates the G-banded human chromosomes, red and blue colors refers to hyper- and hypomethylated DMR distribution, respectively. c Volcano plots of all DMR distributions between each group. The plot shows the DNA methylation difference on percentage (x-axis) with respect to the $-\log_{10}$ of the adjusted p value for each DMR. Thresholds are shown as red lines: dot vertical lines indicate DNA methylation difference cut-off (−25% and +25%), dot hor-izontal line indicates statistically significant cut-off (q-value ≤0.1). Significantly different hypo- and hyper-DMRs are highlighted as blue and red dots, respectively. DIC vs. CTL (left), DIC vs. t-MN (middle) and t-MN vs. CTL (right)

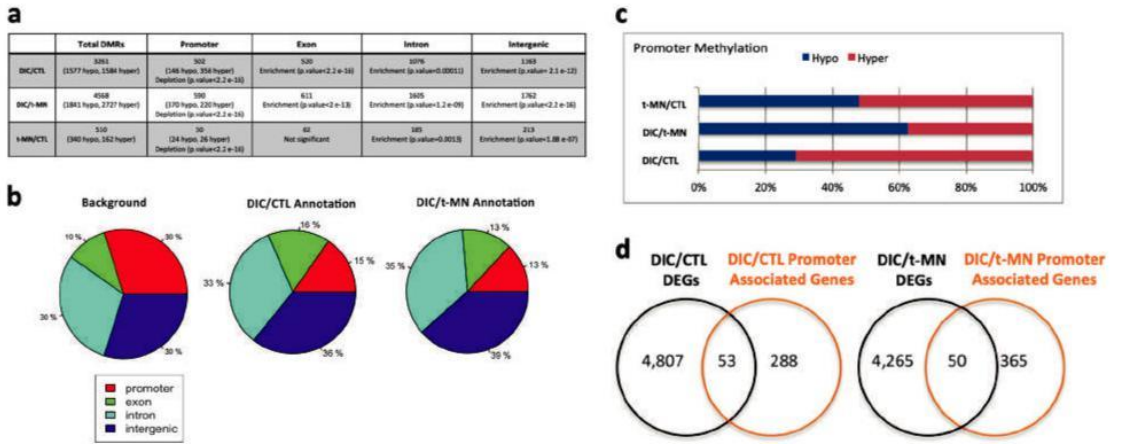

Fig. 5 Summary of annotation analysis. a Table summarizing the distribution of annotated differentially methylated regions (DMRs) on genomic regions for each group. We used Methylkit package on R to annotate previously identified DMRs on Methylsig to hg19. Statistical results for binomial enrichment/depletion test were conduct on R. For all tests, we used 95% confidence interval and percentage of back-ground annotation for each category (promoters, exons, introns, intergenic) as true probability of success. b Pie charts illustrate DMRs annotated to promoter (red), exonic (green), intronic (blue) and intergenic regions (purple) in dic(1;7) (DIC) vs. control (CTL; left) and vs. therapy-related myeloid neoplasm (t-MN; right). As background, we used total identified DMRs without filters (top left). c Distribution of hypo- and hypermethylated DMRs on promoter regions for each comparison (top) and relative number of hypo- and hyper-promoter DMRs for each group (bottom). d Venn diagram showed the overlap between genes annotated to promoter DMRs and all differentially expressed genes (DEGs) identified on RNA-sequencing (RNA-seq) analysis in DIC vs. CTL (i) and vs. t-MN (ii)

confirmed that the enrichment at enhancers was stronger in dicentric cases than in t-MNs, with a prevalent hypermethylation (Fig. 6a). Since DNA methylation negatively correlates with enhancer activity and transcription of target genes [39], we used the Predicting Enhancer Target by modules tool to identify putative enhancer-target genes [40]. Indeed, compared to controls, dic(1;7) RNA-seq revealed that 1747 out of 4860 DEGs were target genes of hypermethylated enhancers (Fig. 6b). Moreover, 1377/1747 DEGs had decreased gene expression, suggesting that enhancer hypermethylation directly accounts for 34.7% of the downregulated signature in dicentric cases (Fig. 6b). These results were maintained by dic(1;7) against t-MNs, with enhancer hypermethylation accounting for 40% of the downregulated profile (Fig. 6b). By contrast, the t-MN group showed 128 out of 192 enhancer DMRs (66%) to be hypomethylated (Fig. 6a). Since DNA methylation has been shown to prevent binding of TFs to their target sites [41], we analyzed DMRs with HOMER. This analysis revealed that DMRs were enriched for TF binding sites (Supplementary Figures 4-7), with those regions differentially methylated in dic(1;7) compared to t-MNs showing enrichment for the key hematopoietic TF factors, GATA1 (p-value = $1e^{-4}$), GATA2 (p-value = $1e^{-3}$), GATA3 (p value = $1e^{-2}$), ETV1 (p value = $1e^{-2}$), STAT3 (p value = $1e^{-2}$) and RUNX1 (p value = $1e^{-2}$) (Supplementary Figure 5). Specifically, GATA and RUNX1 transcription factors binding sites were hypermethylated while ETV1 and STAT3 binding sites were hypomethylated. With respect to hypermethylated enhancers, dic(1;7) showed enrichment of 28 and 27 TFs, compared to controls and t-MNs, respectively (Supplementary Figures 6 and 7). Interestingly, dic(1;7) hypermethylated enhancers were strongly enriched in motifs for Krüppel-like factor (KLFs) protein family transcription factors. Specifically, KLF5, KLF6 and KLF4 were included among the top enriched transcription factors in the analysis against controls (Supplementary Table 6), while KLF3, KLF5 and KLF4 emerged in the analysis against t-MNs (Supplementary Table 7). By contrast, none of these KLF transcription factors emerged as enriched in t-MNs enhancers when compared to controls (Supplementary Figures 8).

Discussion

This is the first in-depth genetic and epigenetic characterization of dic(1;7) which provided us with new insights into the biological features of a recurrent leukemic chromosome rearrangement involving repetitive DNA at centromeric regions.

In our patients, breakpoints of dic(1;7) fell within α-satellite DNA at chromosome 1 and chromosome 7, in agreement with previously reported data [42]. As a result, the affected cells had genomic imbalances involving both euchromatic regions, due to entire 1q trisomy and 7q

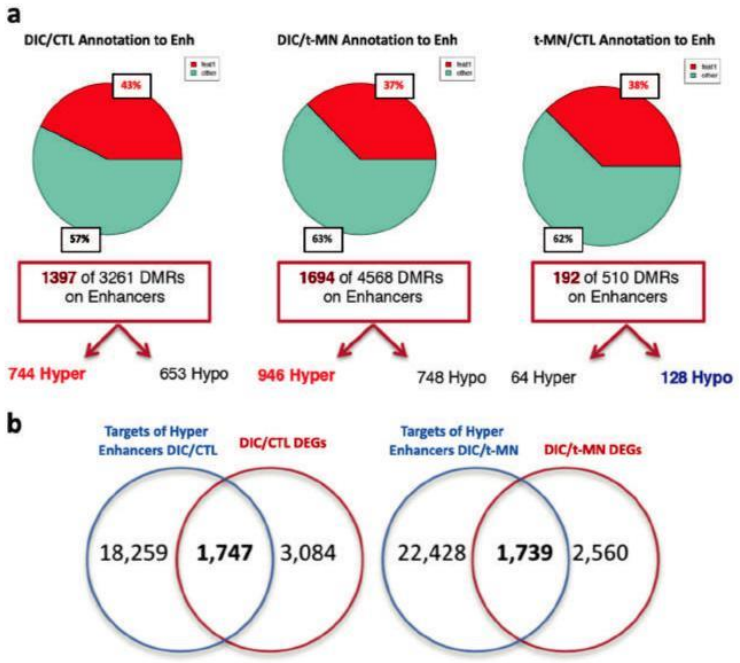

Fig. 6 Summary of enhancers analysis. a Pie chart illustrates differentially methylated region (DMR) enrichment on enhancer regions. Red indicates feat1, enhancers; and light blue indicates others, non-enhancers. Compared with controls (CTL), dic(1;7) (DIC) DMRs showed an enrichment on enhancers with p value < $2.2e^{-16}$ (left), compared with therapy-related myeloid neoplasms (t-MNs) that showed an enrichment on enhancers with p value of $6.617e^{-06}$ (middle) and t-MNs compared with controls that showed an enrichment on enhancers with p = 0.046 (right). For statistical analysis, we used binomial test with 95% confidence interval and percentage of background annotation as true probability of success. b Venn diagrams illustrate the overlap between hypermethylated enhancer target genes and downregulated signature on DIC/CTL (left) and DIC/t-MN (right) groups

monosomy, and heterochromatic regions, with an excess of α-satellite and pericentromeric sequences of chromosome 1. Interestingly, centromeric juxtaposition in dic(1;7) did not alter centromere action on chromosome segregation and the der(1;7) behaved as a stable clonal marker along mitotic divisions of many cell generations, even during long-lasting cytogenetic monitoring, for up to 5 years (data not shown). Moreover, the dic(1;7) chromosome behaved as a cyto-genetically primary abnormality since additional karyotypic changes, when present, were individually different, in both de novo and therapy-induced MDS. Accordingly, data from 258 cases of dic(1;7) collected from Mitelman database showed 82.5% of cases with the dic(1;7) as sole cytogenetic aberration or plus only one/two additional abnormalities [2]. In addition, here we excluded the presence of cytogeneti-cally cryptic changes by using SNP-arrays. Altogether, these data highlight dic(1;7) as the cytogenetic hallmark of a biological entity including both de novo and t-MDS strik-ingly different from other t-MNs typically associated with complex karyotypes [43].

Common somatic mutations did not emerge in our cases with dic(1;7) in which we found only private variations affecting GGPS1; CCDC8; and PSMF1 genes, still not reported in MDS/AML, and ANKS1B/EB1 gene, recently annotated in two AML cases [44].

Interestingly, when compared to both controls and t-MNs, the dic(1;7) subgroup was characterized by a signature with prevalence of gene downregulation that was supported by a specific epigenetic program. Notably, promoter hypermethylation contributed to downregulation to a lower extent than hypermethylation at the level of non-promoter regions, particularly at intronic enhancers which target genes represented at around 35% of the entire downregulated expression profile. Both enhancers and super-enhancers aberrant DNA methylation have been identified in malignancies [45, 46]. Interestingly, in multiple myeloma, Agirre et al. [47] found hypermethylated intronic enhancers to be associated with binding sites for transcription factors related to B-cell differentiation. Similarly, the hypermethylated enhancers in dic(1;7) included binding sites for important transcription factors in normal hematopoiesis, such as GATA1, GATA2, GATA3 and RUNX1. In addition, in dic(1;7) the KLF protein family specifically emerged with four top enriched

members involved in the regulation of: stem/progenitor proliferation and localization in the bone marrow (KLF5) [48], erythroid differentiation (KLF5, KLF6, KLF3) [49], stem cell pluripotency (KLF4) [50] and tumor suppression (KLF4) [51]. Intriguingly, a checkpoint role following DNA damage was attributed to KLF4 loss of function in a murine model, in which its inactivation was associated with high level of apoptosis and genetic aberrations, including dicentric chromosomes [52]. Altogether, these data first emphasize a pathogenetic role of the KLF family in a distinct cytogenetic subgroup of MDS/AML. Future studies are required to investigate potentialities of their modulation for new therapeutic strategies.

Dosage effect due to chromosome number variations is a well-known mechanism altering gene expression in leukemic cells with a strong relationship between gene hypo-expression and chromosome loss [53]. Accordingly, in the dicentric signature we found the expected gene dosage effect due to 7q monosomy, as more than 95% of differentially expressed genes belonging to the long arm of chromosome 7 were downregulated. Among them, EZH2 and MLL3 downregulation might have an impact on global gene expression.

In contrast, a gene dosage effect by 1q trisomy acted only partially, given that more than 50% of 1q differentially expressed genes were downregulated in the cases with dicentric chromosome. Indeed, DNA methylation profile clarified that discrepancies between 1q trisomy and gene hypo-expression were related to high level of 1q hyper-methylation in dic(1;7), compared to both controls and t-MNs. Whether gain of the 1q heterochromatin is related to this epigenetic effect is still unknown.

Pathway analysis of the signature showed that ABC transporters were significantly downregulated in dic(1;7) when compared to both controls and t-MNs. ABC transporters, a large family of proteins with localization at mitochondria, endoplasmic reticulum, Golgi, endosomes and cytoplasmic membranes, are involved in multiple cellular functions, including protection against genetic damage caused by xenobiotic and chemotherapeutical compounds, and transmembrane transport of amino acids, ions, polysaccharides and lipids [54]. In particular, ABCB1, alias MDR1/p-glycoprotein, and ABCG2, alias BCRP/MXR, have been extensively studied in drug resistance in AML [55]. The ABC transporters specifi-cally involved in the dic(1, 7) signature are known to play a role in the transport of phospholipids, cholesterol and phosphatidylcholine. Accordingly, only in the dic(1;7) subgroup, our GO analysis showed a significant enrichment for genes regulating the lipid metabolism involved in stress and inflammatory responses [37, 58]. Among them the downregulated gene NR1H2 is.an ubiquitous isoform of the liver X receptor (LXR), a targetable candidate in leukemic cells with deregulation of cholesterol homeostasis [56, 57]. Whether the ABC involvement impacts the chemo-resistance/sensitivity of dic(1;7)-affected cells remains to be elucidated.

The p53 signaling pathway emerged as a specifically upregulated pathway in dic(1;7) versus both controls and t-MNs. In the last subgroup, loss-of-function p53 mutations accompanied complex karyotypes, as expected [58]. Interestingly, upregulation of p53 target genes has been previously found in AML with wild-type p53 gene, suggesting that, in tumor cells, downstream targets may mediate p53 dysfunction regardless of gene mutations [59]. In line with this hypothesis, both our series of dicentrics and the published AML series [59], sharing wild-type p53, showed upregulation of ZMAT3, a p53 target gene encoding for an RNA-binding zinc-finger protein regulating cell cycle arrest [60]. Altogether, these data suggest that dic(1;7) MDS belong to a subgroup of myeloid malignancies in which, in the absence of mutations at the gene, p53 is involved through deregulation of its targets.

In conclusion, in this study we showed that MDS with dic(1;7) are a distinct cytogenetic–epigenetic entity characterized by a downregulated expression profile closely connected to gene dosage effect and site-specific hypermethylation, mostly at intronic enhancers enriched for hematopoietic transcription factors. Downregulation of pathways and genes involved in lipid homeostasis and upregulation of TP53 signaling emerged as specific biological features, and separated dic(1;7)-positive MDS from t-MN.

Acknowledgements This work was supported by AIRC 5 × 1000 call “Metastatic disease: the key unmet need in oncology” to MYNERVA project, #21267 (MYeloid NEoplasms Research Venture Airc). A detailed description of the MYNERVA project is available at http://www.progettoagimm.it; Sergio Luciani Association, Fabriano, Italy; Fondazione Cassa di Risparmio Perugia (2016.0113.021 Ricerca Scientifica e Tecnologica).

Author contributions AGLF performed methylation and expression experiments, the analysis and wrote the article; BC and VP performed cytogenetic studies and FISH experiments; GB performed SNPa experiments and analysis; GR and VDB provided clinical–hematological data; DDG and VDB performed mutational analysis; RP and FP performed and analyzed whole exome sequencing; ERA contributed to methylation and expression analysis; MEF supervised all epigenetic experiments and contributed to data interpretation and writing; CM conceived and designed the study, contributed to data interpretation and wrote the article. All authors approved the final article.

Compliance with ethical standards

Conflict of interest The authors declare that they have no conflict of interest.

Publisher’s note: Springer Nature remains neutral with regard to jurisdictional claims in published maps and institutional affiliations.

References

1. Huret JL, Dessen P, Bernheim A. Atlas of genetics and cytogenetics in oncology and haematology, year 2003. Nucleic Acids Res. 2003;31:272–4.
2. Mitelman F, Johansson B, Mertens F. Mitelman database of chromosome aberrations and gene fusions in cancer. 2014. http:// cgap.nci.nih.gov/Chromosomes/Mitelman
3. Miniou P, Jeanpierre M, Bourc'his D, Coutinho Barbosa AC, Blanquet V, Viegas-Pequignot E. alpha-satellite DNA methylation in normal individuals and in ICF patients: heterogeneous methy-lation of constitutive heterochromatin in adult and fetal tissues. Hum Genet. 1997;99:738–45.
4. Sawyer JR, Tricot G, Mattox S, Jagannath S, Barlogie B. Jumping translocations of chromosome 1q in multiple myeloma: evidence for a mechanism involving decondensation of pericentromeric heterochromatin. Blood. 1998;91:1732–41.
5. Li H, Durbin R. Fast and accurate long-read alignment with Burrows-Wheeler transform. Bioinformatics. 2010;26:589–95.
6. Gambacorti-Passerini CB, Donadoni C, Parmiani A, Pirola A, Redaelli S, Signore G, et al. Recurrent ETNK1 mutations in atypical chronic myeloid leukemia. Blood. 2015;125:499–503.
7. Wang K, Li M, Hakonarson H. ANNOVAR: functional annotation of genetic variants from high-throughput sequencing data. Nucleic Acids Res. 2010;38:e164.
8. Trapnell C, Pachter L, Salzberg SL. TopHat: discovering splice junctions with RNA-Seq. Bioinformatics. 2009;25:1105–11.
9. Anders S, Pyl PT, Huber W. HTSeq--a Python framework to work with high-throughput sequencing data. Bioinformatics. 2015;31:166–9.
10. Love MI, Huber W, Anders S. Moderated estimation of fold change and dispersion for RNA-seq data with DESeq2. Genome Biol. 2014;15:550.
11. Garrett-Bakelman FE, Sheridan CK, Kacmarczyk TJ, Ishii J, Betel D, Alonso A, et al. Enhanced reduced representation bisulfite sequencing for assessment of DNA methylation at base pair resolution. J Vis Exp. 2015;96:e52246.
12. Krueger F, Andrews SR. Bismark: a flexible aligner and methylation caller for Bisulfite-Seq applications. Bioinformatics. 2011;27:1571–2.
13. Akalin A, Kormaksson M, Li S, Garrett-Bakelman FE, Figueroa ME, Melnick A, et al. methylKit: a comprehensive R package for the analysis of genome-wide DNA methylation profiles. Genome Biol. 2012;13:R87.
14. Park Y, Figueroa ME, Rozek LS, Sartor MA. MethylSig: a whole genome DNA methylation analysis pipeline. Bioinformatics. 2014;30:2414–22.
15. Meldi K, Qin T, Buchi F, Droin N, Sotzen J, Micol JB, et al. Specific molecular signatures predict decitabine response in chronic myelomonocytic leukemia. J Clin Invest. 2015;125:1857–72.
16. Welch RP, Lee C, Imbriano PM, Patil S, Weymouth TE, Smith RA, et al. ChIP-Enrich: gene set enrichment testing for ChIP-seq data. Nucleic Acids Res. 2014;42:e105.
17. Kundaje A, Meuleman W, Ernst J, Bilenky M, Yen A, Heravi-Moussavi A, et al. Integrative analysis of 111 reference human epigenomes. Nature. 2015;518:317–30.
18. Huang dW, Sherman BT, Lempicki RA. Systematic and integrative analysis of large gene lists using DAVID bioinformatics resources. Nat Protoc. 2009;4:44–57.
19. Lee C, Patil S, Sartor MA. RNA-Enrich: a cut-off free functional enrichment testing method for RNA-seq with improved detection power. Bioinformatics. 2016;32:1100–2.
20. Heinz S, Benner C, Spann N, Bertolino E, Lin YC, Laslo P, et al. Simple combinations of lineage-determining transcription factors prime cis-regulatory elements required for macrophage and B cell identities. Mol Cell. 2010;38:576–89.
21. Steiner LA, Schulz V, Makismova Y, Lezon-Geyda K, Gallagher PG. CTCF and cohesin SA-1 mark active promoters and bound-aries of repressive chromatin domains in primary human erythroid cells. PLoS ONE. 2016;11:e0155378.
22. Beck D, Thoms JA, Perera D, Schutte J, Unnikrishnan A, Kne-zevic K, et al. Genome-wide analysis of transcriptional regulators in human HSPCs reveals a densely interconnected network of coding and noncoding genes. Blood. 2013;122:e12–22.
23. Huret JL, Ahmad M, Arsaban M, Bernheim A, Cigna J, Desangles F, et al. Atlas of genetics and cytogenetics in oncology and hae-matology in 2013. Nucleic Acids Res. 2013;41(Database issue): D920–4.
24. Fu X, McGrath S, Pasillas M, Nakazawa S, Kamps MP. EB-1, a tyrosine kinase signal transduction gene, is transcriptionally acti-vated in the t(1;19) subset of pre-B ALL, which express onco-protein E2a-Pbx1. Oncogene. 1999;18:4920–9.
25. Li J, Bi L, Shi Z, Sun Y, Lin Y, Shao H, et al. RNA-Seq analysis of non-small cell lung cancer in female never-smokers reveals candidate cancer-associated long non-coding RNAs. Pathol Res Pract. 2016;212:549–54.
26. Kataoka K, Nagata Y, Kitanaka A, Shiraishi Y, Shimamura T, Yasunaga J, et al. Integrated molecular analysis of adult T cell leukemia/lymphoma. Nat Genet. 2015;47:1304–15.
27. Hanson D, Murray PG, O'Sullivan J, Urquhart J, Daly S, Bhaskar SS, et al. Exome sequencing identifies CCDC8 mutations in 3-M syndrome, suggesting that CCDC8 contributes in a pathway with CUL7 and OBSL1 to control human growth. Am J Hum Genet. 2011;89:148–53.
28. Chen C, Bartenhagen C, Gombert M, Okpanyi V, Binder V, Rottgers S, et al. Next-generation-sequencing of recurrent child-hood high hyperdiploid acute lymphoblastic leukemia reveals mutations typically associated with high risk patients. Leuk Res. 2015;39:990–1001.
29. Aye IL, Singh AT, Keelan JA. Transport of lipids by ABC proteins: interactions and implications for cellular toxicity, viability and function. Chem Biol Interact. 2009;180:327–39.
30. Xu N, Hurtig M, Zhang XY, Ye Q, Nilsson-Ehle P. Transforming growth factor-beta down-regulates apolipoprotein M in HepG2 cells. Biochim Biophys Acta. 2004;1683:33–7.
31. Petropoulou PI, Berbee JF, Theodoropoulos V, Hatziri A, Stamou P, Karavia EA, et al. Lack of LCAT reduces the LPS-neutralizing capacity of HDL and enhances LPS-induced inflammation in mice. Biochim Biophys Acta. 2015;1852(10 Pt A):2106–15.
32. Vonica A, Rosa A, Arduini BL, Brivanlou AH. APOBEC2, a selective inhibitor of TGFbeta signaling, regulates left-right axis specification during early embryogenesis. Dev Biol. 2011;350:13– 23.
33. Fessler MB. Liver X receptor: crosstalk node for the signaling of lipid metabolism, carbohydrate metabolism, and innate immunity. Curr Signal Transduct Ther. 2008;3:75–81.

34. Kristensen L, Kristensen T, Abildgaard N, Royo C, Frederiksen M, Mourits-Andersen T, et al. LPL gene expression is associated with poor prognosis in CLL and closely related to NOTCH1 mutations. Eur J Haematol. 2016;97:175–82.
35. Saenger Y, Magidson J, Liaw B, de Moll E, Harcharik S, Fu Y, et al. Blood mRNA expression profiling predicts survival in patients treated with tremelimumab. Clin Cancer Res. 2014;20:3310–8.
36. Takano S, Yoshitomi H, Togawa A, Sogawa K, Shida T, Kimura F, et al. Apolipoprotein C-1 maintains cell survival by preventing from apoptosis in pancreatic cancer cells. Oncogene. 2008; 27:2810–22.
37. Uehara E, Takeuchi S, Tasaka T, Matsuhashi Y, Yang Y, Fujita M, et al. Aberrant methylation in promoter-associated CpG islands of multiple genes in therapy-related leukemia. Int J Oncol. 2003;23:693–6.
38. Hnisz D, Abraham BJ, Lee TI, Lau A, Saint-Andre V, Sigova AA, et al. Super-enhancers in the control of cell identity and disease. Cell. 2013;155:934–47.
39. Aran D, Sabato S, Hellman A. DNA methylation of distal regulatory sites characterizes dysregulation of cancer genes. Genome Biol. 2013;14:R21.
40. Zhao C, Li X, Hu H. PETModule: a motif module based approach for enhancer target gene prediction. Sci Rep. 2016;6:30043.
41. Tate PH, Bird AP. Effects of DNA methylation on DNA-binding proteins and gene expression. Curr Opin Genet Dev. 1993;3:226–31.
42. Wang L, Ogawa S, Hangaishi A, Qiao Y, Hosoya N, Nanya Y, et al. Molecular characterization of the recurrent unbalanced translocation der(1;7)(q10; p10). Blood. 2003;102:2597–604.
43. Olney HJ, Le Beau MM. The cytogenetics of myelodysplastic syndromes. Best Pract Res Clin Haematol. 2001;14:479–95.
44. Cancer Genome Atlas Research N, Weinstein JN, Collisson EA, Mills GB, Shaw KR, Ozenberger BA, et al. The Cancer Genome Atlas Pan-Cancer analysis project. Nat Genet. 2013;45:1113–20.
45. Heyn H, Vidal E, Ferreira HJ, Vizoso M, Sayols S, Gomez A, et al. Epigenomic analysis detects aberrant super-enhancer DNA methylation in human cancer. Genome Biol. 2016;17:11.
46. Vidal E, Sayols S, Moran S, Guillaumet-Adkins A, Schroeder MP, Royo R, et al. A DNA methylation map of human cancer at single base-pair resolution. Oncogene. 2017;36:5648–57.
47. Agirre X, Castellano G, Pascual M, Heath S, Kulis M, Segura V, et al. Whole-epigenome analysis in multiple myeloma reveals DNA hypermethylation of B cell-specific enhancers. Genome Res. 2015;25:478–87.
48. Shahrin NH, Diakiw S, Dent LA, Brown AL, D'Andrea RJ. Conditional knockout mice demonstrate function of Klf5 as a myeloid transcription factor. Blood. 2016;128:55–9.
49. Humbert M, Halter V, Shan D, Laedrach J, Leibundgut EO, Baerlocher GM, et al. Deregulated expression of Kruppel-like factors in acute myeloid leukemia. Leuk Res. 2011;35:909–13.
50. Takahashi K, Yamanaka S. Induction of pluripotent stem cells from mouse embryonic and adult fibroblast cultures by defined factors. Cell. 2006;126:663–76.
51. Shen Y, Chen TJ, Lacorazza HD. Novel tumor-suppressor function of KLF4 in pediatric T-cell acute lymphoblastic leukemia. Exp Hematol. 2017;53:16–25.
52. Hagos EG, Ghaleb AM, Dalton WB, Bialkowska AB, Yang VW. Mouse embryonic fibroblasts null for the Kruppel-like factor 4 gene are genetically unstable. Oncogene. 2009;28:1197–205.
53. Schoch C, Kohlmann A, Dugas M, Kern W, Hiddemann W, Schnittger S, et al. Genomic gains and losses influence expression levels of genes located within the affected regions: a study on acute myeloid leukemias with trisomy 8, 11, or 13, monosomy 7, or deletion 5q. Leukemia. 2005;19:1224–8.
54. Raaijmakers MH. ATP-binding-cassette transporters in hematopoietic stem cells and their utility as therapeutical targets in acute and chronic myeloid leukemia. Leukemia. 2007;21:2094–102.
55. Fukuda Y, Lian S, Schuetz JD. Leukemia and ABC transporters. Adv Cancer Res. 2015;125:171–96.
56. Ceroi A, Masson D, Roggy A, Roumier C, Chague C, Gauthier T, et al. LXR agonist treatment of blastic plasmacytoid dendritic cell neoplasm restores cholesterol efflux and triggers apoptosis. Blood. 2016;128:2694–707.
57. Sanchez PV, Glantz ST, Scotland S, Kasner MT, Carroll M. Induced differentiation of acute myeloid leukemia cells by activation of retinoid X and liver X receptors. Leukemia. 2014;28:749–60.
58. Wong TN, Ramsingh G, Young AL, Miller CA, Touma W, Welch JS, et al. Role of TP53 mutations in the origin and evolution of therapy-related acute myeloid leukaemia. Nature. 2015;518: 552–5.
59. Parikh N, Hilsenbeck S, Creighton CJ, Dayaram T, Shuck R, Shinbrot E, et al. Effects of TP53 mutational status on gene expression patterns across 10 human cancer types. J Pathol. 2014;232:522–33.
60. Bersani C, Xu LD, Vilborg A, Lui WO, Wiman KG. Wig-1 regulates cell cycle arrest and cell death through the p53 targets FAS and 14-3-3sigma. Oncogene. 2014;33:4407–17.